UNIVERSITAT DE BARCELONA

Source localization of deviance detection and regularity encoding in the auditory brain

Marc Recasens Fusté

Source localization of deviance detection and regularity encoding in the auditory brain

PhD Thesis, 2014

Marc Recasens Fusté

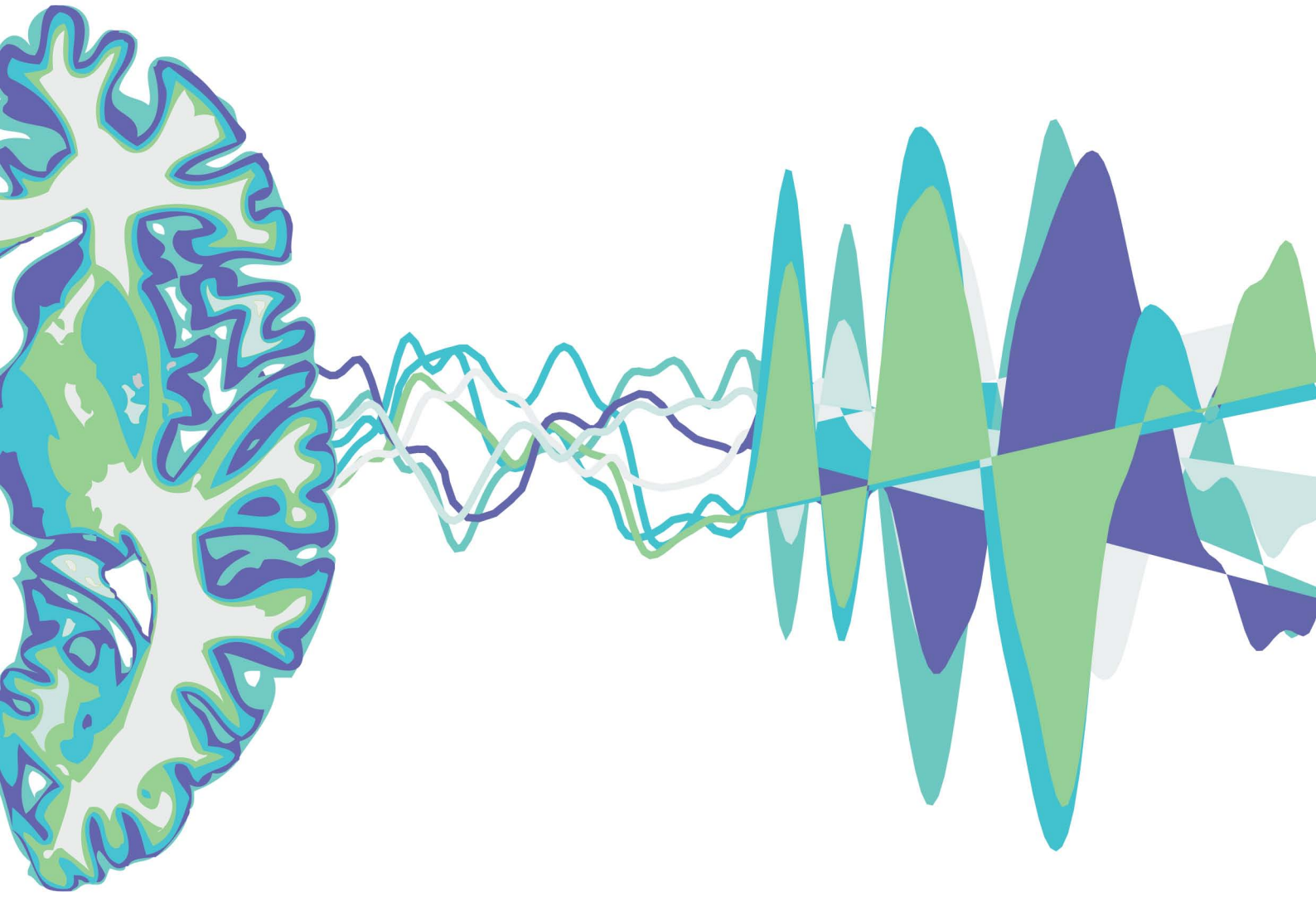

Departament de Psiquiatria i Psicobiologia Clínica
Facultat de Medicina
Universitat de Barcelona

Source localization of deviance detection and regularity encoding in the auditory brain

Thesis presented by
Marc Recasens Fusté

to obtain the
Grau de Doctor per la Universitat de Barcelona
in accordance with the requirements for the
European PhD Diploma

Programa de Doctorat en Biomedicina
Supervised by: Dr. Carles Escera

Barcelona, September 2014

Universitat de Barcelona
Brainlab
cognitive neuroscience research group
grup de recerca en neurociència cognitiva

A la mare i al pare,
pel vostre suport constant i incondicional.

I a la Irene,
per aguantar-me, que ja és molt.

AGRAÏMENTS – AGRADECIMIENTOS – ACKNOWLEDGEMENTS

Sense cap mena de dubte, els meus agraïments més sentits van dirigits al meu pare i a la meva mare. Si no fos pel vostre suport no estaria escrivint aquesta tesi doctoral. Al meu pare, que de petit sempre em deia que "la paciència és la mare de la ciència", i al final he entès el que volia dir. I a la meva mare, de qui he après que no tot es soluciona amb paciència, sinó treballant com una formigueta. Vull donar les gràcies a la meva família extensa. A l'àvia, al padrí i la padrina, a les tietes i tiet, i als meus cosins. Heu contribuït molt més del que us penseu en aquesta tesi. Amb vosaltres he après a explicar el que faig amb paraules divertides i planeres. Això també és un repte pendent de la ciència.

Els agraïments amb l'*effect size* més significatiu sens dubte se l'emporten els meus companys, ex-companys, col·legues i amics del Grup de Neurociència Cognitiva de la Universitat de Barcelona, "el Brainlab", que en són uns quants. En primer lloc, al meu mentor i "*sherpa* de lo científic", en Carles Escera. Sempre t'agrairé que confiessis en mi des de que era un alumne de pràcticum i em demostressis que l'esforç té recompensa. Mil gràcies per donar-me la oportunitat de la meva vida. Aquesta tesi és tant teva com meva.

A la Sabine. Thanks for being Brainlab's second in command, for helping me and everyone else with ... with everything! Nothing can pay all your patience and kindness to me. I will always look up to you. Milions de gràcies també a la resta de doctors que han compartit aquests anys amb mi al laboratori. Al Raffaele, amb els seus rinxols i el seu anàlisi amb SPM! I had a wonderful time with you in Seattle. Thanks and sorry for annoying you with my constant smoking-trips to the terrace. A la Lavinia, you taught me so much when I knew absolutely nothing! Thanks for your patience, and for sharing your knowledge, frustrations, success, and cigarettes with me. A la Sumie, because you brought the Australian sun to our office! I enjoyed our time in the MEG unit a lot!

A la Iria, Manu i Judith. Vaig compartir amb vosaltres els meus primers passos com a estudiant de doctorat i vosaltres, juntament amb en Jordi, m'heu fet veure que hi ha llum al final del doctorat. Gràcies per l'empremta que vau deixar al Grup. Manu, no me olvido del congreso en Quebec, del *road-trip*, la estancia en tu piso y la noche en que casi duermo en *Central Park*. Gracias. I Jordi, per tu necessitaria pàgina i

mitja. Gràcies per tot, tant a casa com al "curro". Gràcies per baixar les escales corrent de matinada i explicar-me que has trobat els efectes esperats en el teu estudi.

Vull fer una menció especial als meus companys d'oficina i als altres *PhD students*: Heike *und* Mareike, gracias por vuestra compañía durante los primeros años de tesis. No he llegado a aprender alemán como prometí, *sorry*, pero algo de vuestra puntualidad alemana sí que se me ha pegado. Heike, ha sido un placer trabajar y vivir contigo. Molestarte cuando estabas concentrada y ocupar tu mesa con todos mis *mess* de papers. Lenka-*superwoman,* ets una crack en tot el que fas. Encara no entenc d'on treus el temps per fer tantes coses. Míriam, si amb algú he compartit l'experiència "vital" de fer un doctorat és amb tu. Mil gràcies per ser la millor companya d'oficina i proveir-me dels millors productes andorrans. Kasia, I am grateful that I could share a tiny piece of your PhD adventure with you; but stop asking me about non-parametric statistics, you already know more than me! Amb tots vosaltres he viscuts moments inesborrables durant les nostres presentacions de pòsters als diferents congressos on hem anat (gràcies per això també, Carles), hem compartit i creat coneixement de forma conjunta, hem afrontat *deadlines* estressant, i hem viscut experiències enriquidores que van molt més enllà de l'àmbit professional. Part d'aquests agraïments també van dirigits a tots els estudiants de pràcticum, estudiants de màster i futurs *PhD students* que han passat pel laboratori. Entre ells la Natàlia, l'Almu, a l'Amalia, i molt especialment al Carles Costa, per ajudar-me en algun dels experiments que vaig portar a terme. A tots vosaltres, us desitjo molta sort en la vostra futura carrera investigadora o professional.

No només de ciència i *abstracts* viu l'estudiant de doctorat i, per sort, he tingut l'oportunitat de conviure amb el "PAS" que m'ha fet la vida molt més fàcil. Paco, "illo", gracias por reírte de mis primeros *scripts* de Matlab, por intentar ayudarme a entender lo que es un filtro espacial y explicarme con palabras sencillas todo eso oculto bajo fórmulas incomprensibles para mi. Marta, gràcies per la alegria constant que sempre ens transmets, per solucionar-nos totes les traves burocràtiques i per ser la mà dreta, no només del "jefe", sinó la de tots nosaltres. Irene, mi polola del laboratorio ¡qué bonito fue tenerte cerca! Jose, Laura i Enric, mil gràcies. Comer con todos vosotros era la mejor terapia contra la rutina diaria.

Aquesta tesi doctoral també va dedicada a la MJ, per ser la primera professora, i després col·lega, que em va donar a conèixer el meravellós món de la neurociència cognitiva. Gràcies. A ella, i a la resta de membres del departament de Psiquiatria i Psicobiologia Clínica de la facultat de Psicologia, que m'han donat l'oportunitat de desenvolupar tasques docents. Gràcies a la Imma, a la Ma. Àngels, a la Dolo, al Marc, a la Maria, a la Roser, i un llarg etcètera. Gràcies també al Jorge, a la Marina, a la Isabel, i a la Idoia, amb qui he compartit no només doctorat sinó també màster. Un agraïment molt gran també a la família Nowak-Giménez. Tant amb tu Rafal, com amb tu Sandra, he tingut un bon rotllo que va més enllà de les paraules. Simplement, crec que oscil·lem en bandes de freqüència semblants. Gràcies per compartir amb mi el congrés de Milà. Gràcies al Jaume Guilera i a tots als que m'heu empès a arribar fins aquí.

Si la ciència i el coneixement no tenen fronteres, els meus agraïments tampoc. So, thanks to all the members of the *Institut für Biomagnetismus & Biosignalanalyse* (IBB). Especially to Dr. Christo Pantev, for accepting me to work with you. Thanks for finding a place for me near the best MEG technician, Andreas; and for introducing me to Max and all the crew in Münster. Thanks for making possible the second study of this thesis.

I finalment, gràcies a la institució que representa la Universitat de Barcelona. I un gràcies més petit a la institució que ha finançat aquesta tesi doctoral. El desaparegut "Ministerio de ciencia e innovación", que va canviar la ciència per la economia y la innovació per la competitivitat en una declaració palpable d'intencions.

No vull deixar de fer menció a molts dels meus amics. Tots vosaltres heu col·laborat activament perquè deixi l'escriptura d'aquesta tesi pel final. Heu endarrerit moltes de les meves entregues. Heu aconseguit que molts dilluns treballi a mig gas, i que els divendres se'm facin eterns. Això no és una crítica, sinó l'agraïment més sincer i fraternal que us puguin fer. Sergi, Roger, Xevi, gràcies per fer-me matinar els caps de setmana. Escalar amb vosaltres em donava l'energia necessària per treballar. Als tots els meus companys de pis: Pablo, Carles, Jordi, Lis, Heike, Nena, Laia, Sergi i Jordi... Gràcies per suportar-me en els meus alts-i-baixos. Borja, Gerard, Jordi, Jota, Omar, Laura, Carles, Dani, Unai, Albert, Jandro, Tomeu... i tots els altres que formeu part d'aquest extens grup d'amics, moltes gràcies.

I finalment a tu, Irene. Has patit aquesta tesi doctoral tant o més que jo. Has compartit amb mi els èxits de les publicacions i la felicitat transitòria dels efectes estadísticament significatius que acaben per desaparèixer. M'has sentit parlar de coses estranyes, amb paraules malsonants com *deviant*, *mismatch negativity* i *potencial evocat*. I crec que alguna cosa "se t'ha quedat". Estaré eternament agraït amb tu per la teva paciència. Gràcies.

Gràcies també a tots els participants i subjectes que han participat en els meus experiments. Molts de vosaltres amics i coneguts. Gràcies per activar les vostres neurones al ritme de la estimulació auditiva. Gràcies per "deixar-me" el vostre cervell.

SUMMARY

Our auditory environment is wealth of continuously flowing information. From the whole set of acoustic inputs entering our sensory system we must create trustworthy mental representations of our world. In order to do so, our auditory system encodes regular acoustic features, stores them in sensory memory as auditory objects, and continuously compares such regularities with the incoming sensory input. Since mismatching events might carry extremely relevant information for the accomplishment of our goals, novel sounds or acoustic changes must be detected fast in an automatic and unconscious fashion, thus allowing for the reallocation of attentional resources and the proper adjustment of our behavior. Sudden deviations in our acoustic environment evoke the mismatch-negativity (MMN), an auditory evoked potential (AEP) generated between 100 and 250 ms after change onset in supratemporal and prefrontal cortices. Experimentally, the MMN can be elicited in an "oddball" paradigm, where novel or infrequent stimuli (deviants) are interspersed in a regular sequence of repetitive sounds (standards) characterized by a particular acoustic feature (frequency, intensity, location, pace), or by more complex auditory regularities like patterns, abstract rules or feature combinations. Operationally, the MMN is obtained by subtracting the evoked activity to standards from that of the deviant sounds. However, recent studies challenged the notion that human deviance detection is solely indexed by the MMN. Simple auditory deviations in the early time range of the middle-latency responses (MLR), evoked between 20 and 50 ms after sound onset, produce amplitude modulations that are thought to reflect a very early mechanism of regularity encoding and deviance detection.

The objective of the present PhD thesis is to examine the neuronal sources underlying auditory regularity encoding, and the subsequent detection of regularity-violating events in early (MLR) and late (MMN) time ranges. Specifically, in study I aimed to show a separation between deviance-related MLR and MMN source generators. Using an oddball paradigm, frequency changes elicited enhanced responses in both the MLR and MMN time ranges. Our magnetoencephalographic (MEG) source modeling revealed that deviance-relate MLR sources were generated in primary auditory areas, whereas MMN generators

were located in secondary regions. In study II, the goal was to probe that MLR and the later MMN deviance detection mechanism are devoted to the processing of different levels of acoustic regularity. Using a sophisticated oddball design with both local and global changes, it was observed that complex regularities are encoded in the time range of the MMN only, with neuronal generators located in secondary auditory regions. Early deviance detection mechanisms did not show enhanced responses to complex regularity violations, thus suggesting that early and late mechanisms are devoted to different levels of regularity encoding and deviance detection. Finally, the third study aimed to show the neuronal sources involved in the encoding of acoustic features. A roving-standard paradigm was employed were trains of repeated tones are presented. Results indicated that both repetition suppression and repetition enhancement underlie auditory memory trace formation, and source generators are located in both typically auditory and non-auditory high-order regions.

In conclusion, results presented in the current thesis indicate that early mechanisms of deviance detection exist in time intervals preceding the MMN and are generated in the primary auditory cortex, thus paralleling previous animal findings showing stimulus-specific adaptation of neurons located in primary regions. Moreover, results suggest that regularity encoding is not only a pervasive phenomenon, but is organized hierarchically with lower mechanisms devoted to the encoding of simple features and high-order regions engaged in complex regularity processing. In support for a hierarchical organization of regularity encoding, results suggest that high-order non-auditory regions of the human brain participate in the formation of new echoic memory traces. Such findings are in line with the notion that auditory perception is based on hierarchically organized sensory systems whose goal is to predict future events on the basis of previously encoded regularities. To do so, error and predictive signals are passed through organized processing stages in the brain.

LIST OF ORIGINAL PUBLICATIONS

STUDY I

Recasens, M., Grimm, S., Capilla, A., Nowak, R., Escera, C. (2014). Two sequential processes of change detection in hierarchically ordered areas of the human auditory cortex. *Cerebral Cortex*, 24(1), 143-153.

STUDY II

Recasens, M., Grimm, S., Wollbrink, A., Pantev, C., Escera, C. (2014). Encoding of nested levels of acoustic regularity in hierarchically organized areas of the human auditory cortex. *Human Brain Mapping*, (in press), doi: 10.1002/hbm.22582

STUDY III

Recasens, M., Leung, S., Grimm, S., Nowak, R., Escera, C. (2014). Repetition suppression and repetition enhancement index acoustic memory-trace formation in the human brain: an MEG study. (*in preparation*).

This word has been carried out at the Cognitive Neuroscience Research Group (Center of Excellence established by the Generalitat de Catalunya: 2009GR11; 2014SGR177) at the Department of Psychiatry and Clinical Psychobiology, Faculty of Psychology, Universitat de Barcelona (UB; Barcelona, Catalonia, Spain), lead by Dr. Prof. Carles Escera, and partly at the Institut für Biomagnetismus & Biosignalanalyse (IBB), Medizinische Fakultät, Westfälische Wilhelms-Universität Münster (WWU, Münster, Germany) lead by Dr. Prof. Christo Pantev.

This work has been supported by the Spanish Ministry of Economy and Competitiveness (pre-doctoral fellowship FPI: BES-2010-030160), the National Program for Fundamental Research (PSI2009-08063; PSI2012-37174), the program Consolider Ingenio 2010 (CDS2007-00012), the (EUI2009-04086) ERANET-NEURON PANS project, and the ICREA Academia Distinguished Professorship awarded to Carles Escera.

ABBREVIATIONS

ABR	Auditory Brainstem Response
ERP / F	Event-Related Potential / Field
EEG	Electroencephalography
FFR	Frequency Following Response
fMRI	functional Magnetic Resonance Imaging
HG	Heschl's Gyrus
MEG	Magnetoencephalography
MLR	Middle-Latency Response
MMN / m	Mismatch Negativity / magnetic
PAC	Primary Auditory Cortex
PT	Planum Temporale
RP	Repetition Positivity
SSA	Stimulus-Specific Adaptation
STG	Superior Temporal Gyrus

CONTENTS

Introduction

INTRODUCTION

Countless sound stimuli reach our ears incessantly. Some of them might be extremely relevant in terms of nowadays survival, like voices or the sound of our morning alarm clock. Others might be definitively irrelevant, like the humming noise of our laptop. In any case, air vibrations will reach our eardrums and a cascade of neural activity will convey that information to our central sensory systems. Information will be processed and transformed along the auditory pathway and just a few of those stimuli, if sufficiently relevant, will reach our conscious perception. How does our brain process such an enormous amount of information and parses it automatically and unconsciously? This PhD thesis contains three studies and revises some literature that focus on the unconscious processing of sound stimuli, intending to shed some light on the understanding of this highly complex mechanism.

REGULARITY ENCODING, AUDITORY OBJECTS, AND PREDICTIONS

In order to interact with the overwhelming amount on information arriving to our ears our auditory system must create trustworthy mental representations of our acoustic environment. To do so, the mammalian brain encodes the whole-range of details of the auditory input, or statistical regularities, and extracts the relevant information (Nelken, 2008). In other words, "An important part of building a representation is to decide which parts of the sensory stimulation are telling us about the same environmental object or event" (Bregman, 1990). Accordingly, invariances are used to organize the sound input and create auditory objects, that is, perceptual or experiential entities defined in frequency and time (Griffiths and Warren, 2004). Prevailing theories of perception argue that auditory objects are not static representations of invariances, stored in long- or short-term memory buffers (Bregman, 1990; Näätänen and Winkler, 1999), but rather dynamic and "online" cognitive models with an inherently predictive nature that provide continuity to perception and allow us to generate predictions and expectations about future events (Winkler et al., 2009). Predictive coding theories state that "perceptual system's primary objective is to minimize the discrepancy between predictions from its internal generative models of the environment and the actual

sensory input" (Winkler and Czigler, 2012). Therefore, perception goes beyond a "standard model" extrapolation by creating predictions about forthcoming events. Bendixen and colleagues (2012) defined this idea in a three-stage recursive model: First, acoustic regularities among sounds are extracted and represented. Next, a mental representation of the extracted invariances is compared with the incoming sensory input. Finally, a predictive model is formed on the basis of the previous comparison. Both predictive coding theories (Friston, 2005) and the model adjustment hypothesis proposed by Winkler et al. (1996) assume that when the incoming acoustic input differs from the predictive model an error, or mismatch, signal is generated. In this way, our internal models of the world are iteratively updated. In neurophysiological terms, predictive coding theories state that predictive and error signals are passed up and down through hierarchically organized sensory systems. That is, several stages of signal processing receive and send bottom-up and top-down projections that modulate connection strengths via synaptic changes (Baldeweg, 2007). Similarly, this PhD thesis is rooted on the idea that several stages of regularity encoding and subsequent deviance detection are organized hierarchically throughout the auditory pathway.

DEVIANCE DETECTION AND THE MISMATCH NEGATIVITY

In 1978, Näätänen, Gaillard, and Mäntysalo discovered the mismatch negativity (MMN) event-related potential (ERP). Since then, Näätänen's research has been cited more than 43.000 times, and circa two thousand research articles in different research fields have been published addressing the topic or using the MMN as a tool to study human brain function (N = 1893, PubMed search date August 2014: "mismatch negativity"). It is then not surprising that the MMN has been considered a breakthrough in normative and pathological cognitive neuroscience (Light and Näätänen, 2013; Sussman and Shafer, 2014). The MMN is an ERP, or auditory evoked potential (AEP), first obtained in electroencephalographic (EEG) recordings that is elicited by rare, oddball, or infrequent sounds (deviants), in a context of otherwise constant, repetitive or frequent sounds (standards). This situation is experimentally implemented in "oddball" paradigms, where a regular sequence of events containing some invariant feature is infrequently mottled with deviants differing in one or more of the features defined by the repetitive standard

stimuli. Importantly, regularity violations indexed by the MMN are processed passively or "pre-attentively", that is, without overt attention. Therefore, the MMN is a negative deflection of the human ERP elicited between 100 and 250 ms from deviance onset by changes in simple acoustic features like frequency, intensity, duration; or more complex violations of phonetic contrasts, patterns, and even abstract rules (for a recent review see: Näätänen et al., 2011; Paavilainen, 2013).

But how is MMN, a change detection index, related to regularity encoding and hence to memory-trace formation? One of the dominant interpretations for the MMN is the "sensory-memory" hypothesis (Näätänen, 1992; Näätänen et al., 2005). Rather than a simple change-detection mechanism, according to this account "the MMN is elicited by a mismatch between the auditory input and the predictions formed on the basis of the trends or rules that are automatically detected in the recent auditory stimulation" (Näätänen et al., 2011). Indeed, pharmacological studies have shown that administration of N-methyl-D-aspartate (NMDA) receptor antagonists diminish or abolish the MMN (Javitt et al., 1996; Umbricht et al., 2000; Tikhonravov et al., 2008), thus linking the MMN to the NMDA-receptor system, and hence to memory formation. Even though the memory-trace explanation of the MMN has received great empirical support, an alternative explanation states that the MMN, as obtained by subtracting deviant activity from that of the standard, can be fully explained by the N1 difference between deviant and standard (Jääskeläinen et al., 2004; May and Tiitinen, 2010). The N1 is an electrically recorded negative AEP peaking about 100 ms after stimulus onset, originated by multiple subcomponents in multiple regions of the supratemporal cortex (Woods, 1995; Loveless et al., 1996; Jääskeläinen et al., 2004). The N1, or N100, is elicited by sudden changes in sound energy (Näätänen and Picton, 1987), is extremely sensitive to stimulation rate, and its amplitude is attenuated with stimulus repetition (Budd et al., 1998). This has led to the alternative "adaptation hypothesis", stating that the MMN is actually the result of the activation of fresh neuronal populations not habituated by preceding standard stimulation. According to this neurophysiological interpretation, different states of refractoriness of the different populations generating N1 to different sound features are sufficient to account for a bottom-up "transient-detector system" (May and Tiitinen, 2010). This interpretation implies that afferent feature-specific N1 neurons, rather than

specific MMN neurons, trigger attentional switching to novel stimuli, and thus obviates the involvement of higher-order, memory-related mechanisms in MMN generation (Näätänen et al., 2005). Nevertheless, a bulk of empirical evidence indicates that the MMN reflects a more complex mechanism than just an N1 suppressed and delayed response by stimulus-specific adaptation. A detailed review of studies arguing in favor of a memory-based interpretation of the MMN can be found elsewhere (Näätänen et al., 2005, 2011; Näätänen and Winkler, 2007). For the sake of brevity only a few examples will be reviewed here. A paradigmatic example is the use of improbable omissions during an oddball design, which do not evoke an obligatory N1 component. Yabe et al. (1997) showed that MMN was elicited when omitting a stimulus in a regular sequence of tones presented at 150 ms stimulus-onset-asynchrony (SOA), or below. This finding has been corroborated by subsequent studies using sound and speech omissions, in both simple and complex oddball paradigms (Yabe et al., 1998; Wacongne et al., 2011; Bendixen et al., 2014). Separability of N1 and MMN mechanisms is also evidenced by the use of complex designs where high-level regularities are established across temporally separated sounds (Tervaniemi et al., 1994; Horváth et al., 2001; Paavilainen et al., 2007; Bendixen et al., 2008) or even defined in abstract rules, not apparent to subjects (Schröger et al., 2007). In a series of experiments, Sussman et al. (1998) and Sussman and Gumenyuk (2005) observed that the MMN was not elicited when sequences of AAAAB tones were presented at a regular and fast pace. Instead, in the control condition, where A and B tones were presented randomly with the same probability as in the previous condition, an MMN component was evoked. Sussman's absence of MMN indicates that the MMN response reflects the representation of inter-sound regularities based on feature- and temporally integrated sensory stimulus information (Näätänen and Winkler, 1999), and suggests that explanations based solely on refractoriness cannot account for the absence of MMN in the regular condition. Similarly, the second study of the present PhD thesis describes the elicitation of an MMN response to an unexpected tone repetition. Such a result cannot be accommodated by adaptation mechanisms solely, as will be discussed later. Even though memory-based interpretations prevail over adaptation in the MMN literature, the MMN obtained in the classic oddball protocol (where deviant activity is subtracted from standard

activity) poses the problem that refractory effects are indeed larger for standards than for less probable deviant stimuli. Thus, the classic MMN might reflect a combination of differential states of refractoriness, as predicted by the "adaptation hypothesis", and "genuine" memory-based comparison process. In order to overcome this issue, control conditions have been designed to elicit pure memory-based comparisons, or "genuine MMN". Schröger and Wolff (1996) designed a control condition with several randomly occurring equiprobable sounds. Responses from infrequent deviant stimuli in the oddball block were compared to physically identical sounds in the control condition, both with the same probability of occurrence. In this way, MMN elicited in the deviant minus control comparison cannot be explained by differences in stimulus probability and associated differences in the state of refractoriness of neural populations, and hence, only memory-based mechanism can account for it (Schröger and Wolff, 1996; Jacobsen and Schröger, 2001; Jacobsen et al., 2003). An example of such a control condition for frequency oddball designs is implemented in the first study of the present work.

BRAIN SOURCES OF THE MMN

First evoked magnetic field recordings of the MMN (Hari et al., 1984; Sams et al., 1985) confirmed that the magnetic counterpart of the MMN, termed "magnetic mismatch field" (MMF) or MMNm, was generated in the supratemporal plane, bilaterally. Pioneering magnetoencephalographic (MEG) studies employing equivalent current dipole (ECD) as inverse solution defined the sources of frequency-MMNm approximately 1 cm anterior to the N1m sources (Hari et al., 1984; Sams et al., 1985; Csépe et al., 1992; Tiitinen et al., 1993). Such findings were replicated in animals (Javitt et al., 1992; Pincze et al., 2001), and by using optical-imaging human data (Rinne et al., 1999b). The separability of the MMN and N1 components at the anatomical level is in consonance with the notion that N1-adaptation and memory-based MMN index different sensory mechanisms (Näätänen et al., 2011). In spite of the general agreement that supratemporal regions allocate MMN sources, the exact location of the neuronal generators might be slightly different depending on of the feature (frequency, intensity, duration, feature-combination), or features, that are used to elicit the MMN (Paavilainen et

al., 1991; Alho et al., 1995, 1996; Giard et al., 1995; Molholm et al., 2005; but see: Sams et al., 1991). A clear example regarding the different localization is the case of lexical stimuli. Several studies indicate that MMN activity is generally stronger in the right hemisphere (Giard et al., 1990; Paavilainen et al., 1991; Levänen et al., 1996; Grimm et al., 2006), especially for pitch (Mathiak et al., 2002; Doeller et al., 2003). However lexical and speech stimuli elicit stronger activation in left auditory regions (Näätänen et al., 1997; Rinne et al., 1999a; Shtyrov et al., 2008). Such hemispheric asymmetry is in line with the different degrees of sensitivity to spectral and temporal cues shown in the right and left hemispheres, respectively (Zatorre and Belin, 2001; Zatorre et al., 2002). Functional resonance imaging (fMRI) and positron emission tomography (PET) studies, allowing for a high spatial resolution, reported MMN source generators in the superior temporal gyrus (STG), and Heschl's gyrus (HG), structures of the temporal lobe (Downar et al., 2001, 2002; Müller et al., 2002; Opitz et al., 2002, 2005; Doeller et al., 2003; Schall et al., 2003; Rinne et al., 2005, 2007; Schönwiesner et al., 2007; Szycik et al., 2013). Such results have been confirmed in studies employing high temporal resolution techniques like EEG (Giard et al., 1990; Rinne et al., 2000), MEG (Alho et al., 1998; Maess et al., 2007), and intracranial recordings (Kropotov et al., 1995). However deviance detection generators are not localized in auditory areas solely. A number of experiments have revealed the involvement of frontal generators, suggested to underlie attention shifts towards attention-capturing deviant events (Giard et al., 1990; Rinne et al., 2000, 2005; Yago et al., 2001; Opitz et al., 2002; Deouell, 2007) as opposed to the temporal subcomponent, suggested to reflect perceptual change detection. Even larger change-detection networks encompassing distributed temporo-frontal and temporo-parietal connections have been described during novelty processing and subsequent attention switch to relevant and distracting events (Rinne et al., 2007).

Besides of methodological differences, the traditional pitch-MMN is suggested to reflect both a "sensory" and a "cognitive" mechanism, as mentioned in the previous section. In other words, the traditional MMN (deviant minus standard) reflects both a release from adaptation of the frequency-specific afferent neurons, and a "true" mismatch detection process based on sensory-memory. Opitz and colleagues (2005) addressed this issue in an fMRI experiment where deviance-

detection generators were activated using both the traditional and the controlled (deviant minus control) oddball protocol. The authors observed that primary auditory cortex (PAC) activity, in medial loci of the HG, was associated with the sensory mechanism. The cognitive mechanism, reflecting a memory-based comparison process, activated non-primary auditory regions surrounding the HG. Similar findings have been reported in subsequent fMRI studies (Szycik et al., 2013), and using combined EEG-fMRI combined recordings (Schönwiesner et al., 2007). Similar attempts to elucidate a purely memory-based comparison process in MEG have failed to reveal a spatial separation between the sensory and cognitive mechanisms, but revealed that the early interval of the traditional MMN is mainly due to sensorial mechanisms, while the later can be attributed to cognitive mechanisms (Maess et al., 2007). Supporting the adaptation hypothesis, Jääskelainen and colleagues (2004) observed that an anterior N1-source activity, displaying narrower frequency tuning, showed a larger N1-amplitude difference between deviant and standard than a posterior N1-source, showing a wide frequency tuning. Thus, deviants would elicit larger activity in anterior regions of the STG, whereas only large frequency variations would elicit large activity in posterior sources. Under this assumption, the authors concluded that the MMN is in fact the result from differential adaptation dynamics of different N1 subcomponents, but not a separate mechanism. Still, Jääskeläinen et al. (2004) interpreted enhanced N1 feature-specific responses to deviants as signaling sensory-memory and novelty detection, in line with previous animal studies (Ulanovsky et al., 2003) summarized below.

EARLIER CORRELATES OF DEVIANCE DETECTION

Deviance detection, and hence, regularity encoding has traditionally been investigated using the MMN. In 2003, a seminal paper by Ulanovsky and colleagues reported for the first time direct evidence of the encoding of acoustic regularities at the neuronal level, by recording single-neuron and multi-unit electrophysiological activity in the PAC of anesthetized cats during an oddball paradigm. The authors used the term stimulus-specific adaptation (SSA) to refer to a specific decrease in the response of neuronal assemblies to repeated tone presentation. Notably, this form of adaptation could not be regarded as mere

neuronal fatigue, since neuronal excitability of the adapted populations was recovered when a new low-probability feature (i.e., a new frequency tone) was presented. SSA described in the animal auditory cortex shares many characteristics with the human MMN: SSA has very high stimulus specificity and spans during long inter-stimulus gaps (> 1700 ms), both the magnitude of MMN and SSA is positively correlated with the frequency-difference between standards and deviants, and negatively correlated with the deviant probability. SSA is also sensitive to parametric changes in the inter-stimulus interval of the presented sounds. These similarities with the MMN have led to the suggestion that SSA might be a neuronal correlate of the scalp-recorded MMN (Nelken and Ulanovsky, 2007). However, some striking differences suggest that MMN might reflect a more sophisticated processing stage that encompasses higher order areas of the brain. Among these differences, timing might be the most crucial. Single-neuron onset firing to deviant sounds occurs about ~20 ms (Pérez-González et al., 2005), whereas the peak latency of the MMN occurs between 100 and 250 ms after deviant onset. Besides, neurons displaying SSA have been localized in subcortical nuclei such as the inferior colliculi (IC) (Pérez-González et al., 2005; Malmierca et al., 2009; Ayala and Malmierca, 2013), and the thalamic medial geniculate body (MGB) (Antunes et al., 2010; Antunes and Malmierca, 2011; Duque et al., 2014). Animal correlates of the MMN, however, show that activity is larger in secondary areas as compared to primary auditory and subcortical regions (Pincze et al., 2001). Besides, human generators of MMN have not been described below the level of the PAC to the best of our knowledge. Last but not least, Farley and colleagues (2010) showed that NMDA antagonists, known to disrupt the MMN, did not affect SSA sensitivity in the auditory cortex, thus suggesting that memory-related NMDA receptors do not contribute to the different degrees of SSA to standard and deviant sounds. All together, these studies suggest that MMN represents a change-detection and regularity-encoding signal generated in hierarchically superior areas than the SSA. As noted previously, no human correlates of MMN have been described below the cortical level. However, change detection and MMN-like responses in animals can be found subcortically (Kraus et al., 1994; Csépe, 1995), and recent human studies suggest that long lasting plastic changes can occur in subcortical auditory stations like the brainstem

(Chandrasekaran et al., 2009, 2014; Chandrasekaran and Kraus, 2010), thus indicating that adaptation can occur below the cortical level (Malmierca et al., 2014; Pérez-González and Malmierca, 2014). Such disparity of results motivated the investigation of human mechanisms of deviance detection in earlier time intervals than the MMN, under the assumption that regularity encoding is a pervasive phenomena observed throughout the auditory pathway.

MIDDLE LATENCY RESPONSES AND ULTRAFAST DEVIANCE DETECTION

Ascending neural activity throughout the auditory pathway can be registered by means of EEG. ERPs recorded in EEG (or event-related fields [ERF] if recorded using MEG) result from the summation of postsynaptic potentials (PSPs) that occur simultaneously in large number of cortical pyramidal cells, oriented in a similar manner with respect to the scalp (Kappenman and Luck, 2012). ERPs reflecting afferent activation in the auditory brainstem include transient auditory brainstem responses (ABR) and the steady-state frequency following response (FFR) (Pratt, 2012). ABRs can be recorded in the initial 10 ms following sound onset and are defined by 5 to 7 voltage oscillations, with peak V identified as the most prominent component in the ABR complex. Even though the exact location of neuronal generators is still a subject of debate, there is general agreement that peak I is generated in the cochlea (Pratt, 2012) and later peaks (IV-V) might be generated by terminations of the contralateral lemniscus in the inferior colliculus (Møller, 2006), close to the midbrain junction. Afferent evoked activity between 10 and 50 ms after sound onset is termed middle-latency responses (MLR). Transient evoked potentials at this range are generated by thalamo-cortical and cortical activity and include a series of oscillations termed V, N0, P0, Na, Pa, Nb, and Pb (also termed P50), where components V and N0 are actually the brainstem component V (Pratt, 2012). The Na component, between 16 and 20 ms, is originated subcortically in the midbrain or thalamo-cortical radiations as suggested by scalp topography analyses (Deiber et al., 1988; Kraus and McGee, 1988). However, Nam sources in MEG cannot be identified systematically (Mäkelä et al., 1994; Yoshiura et al., 1995; Godey et al., 2001; Yvert et al., 2001). The Pa component, around 30 ms, is the first MLR component showing a cortical origin (Celesia, 1976; Pelizzone et al., 1987), even though subcortical contributions have been described too (McGee et al.,

1992). MEG studies on the Pam component have localized its sources in more anterior and medial sites than equivalent sources of N1m (Pelizzone et al., 1987; Pantev et al., 1993) arguing for a cortical origin. In addition, Pantev and colleagues (1995) described a tonotopic organization of the Pam response that mirrored the N1m tonotopic map. In sum, it is commonly accepted that the Na-Pa complex reflects the earliest PAC activity (Yvert et al., 2001; Lütkenhöner et al., 2003). Later components of the MLR, Nb (~40 ms) and Pb/P50 (~50 ms), have been localized in lateral portions of the STG or the upper bank of the superior temporal sulcus, and little or no source separation has been found between them (Yvert et al., 2001). Yoshiura et al. (1995) also observed that the Nbm component overlapped with Pam, suggesting that a clear delineation of MLR sources can be made between early and late components (Gutschalk et al., 1999). In addition, Inui and colleagues (2006) suggested the existence of a serial model of auditory processing along the medio-lateral axis of the supratemporal plane consistent with the hierarchical organization observed in the monkey anatomy (see: Kaas et al., 1999).

At this point we might wonder whether MLR are involved in any sort of cognitive processing, or whether they just reflect afferent (bottom-up) sensory processing. With respect to the foregoing introduction, Näätänen and Winkler (1999) pointed out that formation of stimulus representations by means of regularity encoding requires of memory storages (or memory traces) available to top-down operations, that is, a separate process from afferent (bottom-up) activation in the auditory pathway. Regarding ABR and MLR, the authors stated that afferent or ascending neuronal circuits in early stages of the auditory pathway have very short recovery periods, since they must contain all the information of the incoming stimuli, but "this [afferent activation] pattern cannot be regarded as a feature trace because it lacks any form of stable existence … Hence, in this stage of auditory stimulus processing, information storage does not appear as a separate function. Rather, this stage can be characterized in terms of processes continuously transforming the stimulus information." (Näätänen and Winkler, 1999). This prevailing belief, that postulates that neuronal circuits involved in MLR generation do not maintain auditory feature traces, has changed under the light of recent findings. Some of these have already been introduced in previous sections, and some of which will be introduced below. MLR modulation has been observed

during sensory gating (Müller et al., 2001), self-initiation of sounds (Baess et al., 2009), task-related demands (Woldorff and Hillyard, 1991), and even during sound segregation (Dyson and Alain, 2004), thus pointing to a complex and cognitive nature of early auditory processing. Sonnadara and colleagues (2006) first described the modulation of the Na component of the MLR for location deviants, as compared to standard click sounds, indicating and early effect of stimulus rareness. This effect however, could be explained by the mere adaptation of sensory-specific neurons, rather than by a memory-based comparison process. In a series of experiments conducted in our laboratory, deviance detection was also assessed at early time intervals using control conditions such as those described above. In addition to the traditionally employed oddball block, Grimm et al. (2011) and Slabu et al. (2010) presented a reversed block where deviant and standard frequencies were swapped, thus allowing for a deviant minus standard comparison where both stimuli were physically identical. That prevented MLR differences to be accounted for by changes in the physical properties of the stimulus. Stimulus probability was controlled for by comparing deviant sounds to equal-probability sounds presented in a random sequence, therefore ensuring that deviance-related effect could not be accounted by the differential state of refractoriness to deviant and control sounds (Schröger and Wolff, 1996; Jacobsen and Schröger, 2001). In their respective studies, Grimm and colleagues (2011) and Slabu et al. (2010) showed "genuine" deviance-related modulations of Nb and Pa components of the MLR, respectively. Such early memory-based effects found for pure tones and band-pass filtered noises were later replicated using location deviants (Grimm et al., 2012), thus upgrading Sonnadara's et al. (2006) findings. Even more, Slabu et al. (2012) showed that the human auditory brainstem is able to encode regularities and detect novel events. The authors observed that the steady-state FFR, with putative origins in the IC, was reduced to the infrequent presentation of /ba/ syllables as compared to physically identical stimuli presented in a random control condition. This and previous results indicate that deviance-related effects at the level of MLR and brainstem might reflect a better correlate of SSA than the MMN. Together, all these data provide support for a multi-stage deviance detection system and suggest that regularity encoding is a

pervasive feature present all along the auditory pathway (Grimm and Escera, 2012; Escera and Malmierca, 2014; Escera et al., 2014).

REGULARITY ENCODING: A DIRECT APPROACH

Up to now, human studies introduced here investigated regularity encoding in an indirect manner, that is, by assessing deviance detection (MMN or deviance-related MLR effects). And under the empirically grounded assumption that deviance detection reflects a mismatch between a sound input and previously encoded regularities stored in sensory memory. While direct indices of acoustic regularity encoding have been found at the single-neuron level, human correlates of regularity encoding (or memory-trace formation) are far scarcer. Oddball paradigms might not be specially well-suited to study the encoding of online regularities, since memory traces created after standard repetitions might reflect carry-over activity developed during the stimulation session. Instead, in a "roving-standard paradigm" (Cowan et al., 1993) memory traces are continuously reestablished after each train, when a new feature starts to repeat. In roving standard paradigms trains of repeated sounds, with variable number of repetitions, are presented. Trains differ in their acoustic features, so that all stimuli in the first position of a train constitute a deviant stimulus, and subsequent presentations constitute standards that strengthen the memory trace. In other words, deviant sounds become standards after many repetitions, thus allowing to study repetition-related changes in the neuronal response to acoustic stimuli. Different versions of the roving standard paradigm have been employed to study memory processing in normal population and in psychiatric disorders like schizophrenia (Cowan et al., 1993; Baldeweg et al., 2002, 2004, 2006; Haenschel et al., 2005; Bendixen et al., 2007; Ylinen and Huotilainen, 2007; Costa-Faidella et al., 2011a; Cooper et al., 2013). Baldeweg and colleagues (1999) first observed that ERPs to standard stimuli increased its positivity between 50 and 150 ms in mastoid electrodes after the first recording block. Subsequent studies, employing a roving standard design, confirmed such findings and termed the enhancement of that slow positive drift "repetition positivity" (RP). In EEG, RP is reflected as an increase of the P50 activity, a decrease of the N1, and an enhancement of the P2 component (~250 ms post stimulus), recorded in frontocentral electrodes under

both passive and active listening conditions (Haenschel et al., 2005; Baldeweg, 2007). The RP increases with stimulus repetition and empirical evidence suggests that the enhancement to standard tones accounts for most of the MMN memory trace observed effects (Haenschel et al., 2005). Such behavior has led to the notion that RP might reflect a human scalp-recorded correlate of the animal SSA observed at the single-neuron level (Baldeweg, 2007), a candidate mechanism underlying sensory memory formation in the auditory cortex (Haenschel et al., 2005) that is sensitive to sensory encoding deficits (Baldeweg et al., 2004). In addition, the early modulation at ~50 ms suggests that primary auditory areas might be involved in its generation (Liégeois-Chauvel et al., 1991), and its extended latency over 200 ms indicates that multiple generators beyond PAC, in parietal and frontal cortices, might exist as well (Baldeweg, 2006, 2007). However, no direct examination of RP source generators by means of neuroimaging methods has been conducted to date. In this regard, the third study of the present PhD thesis aims to clarify the neuronal sources of regularity encoding.

In conclusion, the aim of the present PhD thesis is to show that auditory regularity encoding and subsequent deviance detection is structured in a hierarchical fashion in the human brain. In order to accomplish such a goal, both electrophysiological and anatomical evidence will be presented arguing for the involvement of different areas and processing stages devoted to the encoding and detection of acoustic features.

Aim of the studies

AIM OF THE STUDIES

The specific goals of each of the studies included in the present PhD thesis are:

STUDY I

To examine the neuronal generators of frequency deviance detection in the time range of the MLR and the MMN. First we aimed at corroborating recent evidence showing that genuine change detection occurs within a very short time after deviance onset, between 10 and 50 ms. Second, we aimed to show that underlying neuronal populations giving rise to early and late change detection mechanisms are located in hierarchically separated brain regions. Specifically, we hypothesized that deviance-related MLR would be generated in cortical regions near primary auditory areas, whereas subsequent activation origins of MMNm would be localized in secondary auditory regions.

STUDY II

We aimed to highlight the different role of early (MLR) and late (MMN) deviance detection mechanisms in the organization of the auditory scene, that is, whether these two mechanisms convey different information of a single auditory stimulus. We examined whether local regularity-violations of simple complexity like frequency, and global violations of regularities based on the relation between temporary non-adjacent sounds were processed in distinct temporal and spatial scales, thus providing support for the notion that the human auditory system is organized in a hierarchical fashion. Specifically we expected to obtain an MMNm response to global regularity-violations, and early areas underlying MLR to respond to violations of local rules only. Anatomically, we expected neuronal generators underlying global deviations to be located in hierarchically superior areas than those underlying local regularity violations.

STUDY III

In study III we aimed at unraveling the spatio-temporal dynamics of memory-trace formation. Our goal was to obtain a neuromagnetic correlate of the “repetition positivity” index of memory-trace formation and, secondly, reveal the neuronal

generators of repetition suppression (RS) and repetition enhancement (RE) that index the encoding of acoustic features at different time intervals. Specifically we hypothesize that distinct neuronal sources would account for RS and RE effects and that frontal and parietal regions would be involved in the formation of acoustic memory-traces.

General Methods

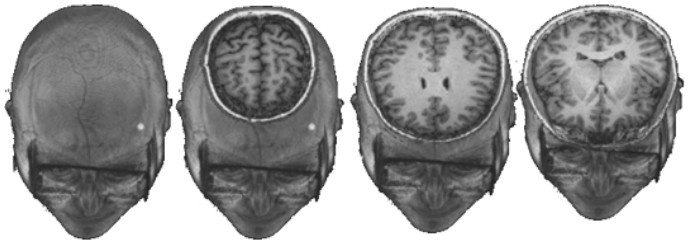

GENERAL METHODS

Specific details on the methods employed in the current PhD thesis can be found in the "methods" section included in each of the studies presented in the following section. An overview of the general methods will however be described here.

In all studies, recordings were carried out in young healthy adults (mean age across studies = 28.5 years) with ages ranging from 23 to 35 years. Normal hearing levels were assessed by means of a pure tone audiometry. Overall, audiometries were conducted at the beginning of each MEG session and subjects showing hearing levels below 20 dB were discarded. All subjects provided written consent prior to their participation in the studies and most of them received a monetary compensation (excluding laboratory members and friends who volunteered). Experimental protocols were approved by the ethical committees of the universities where experiments were conducted (University of Barcelona and University of Münster), and were in accordance with the code of ethics stated by the Declaration of Helsinki.

In all three studies frequency was used as the acoustic feature of interest. That is, both acoustic regularities and sound deviations were elicited by repetitions or changes in frequency. The frequency range employed in each study varied, but frequencies never exceeded 2500 Hz in order to avoid sound distortion. Specifically, pure sine wave sounds were employed in the three studies. The duration of pure tones was kept constant at 50 ms, including at least 10 ms rise and decay slopes in order to avoid abrupt onsets and offsets. Individual sounds were generated using Matlab or free audio editors like Audacity®. Sounds were delivered binaurally at comfortable sensation levels. Since no ferromagnetic components can be introduced into the magnetically shielded room where the MEG machine is located, sounds were delivered via MEG-compatible plastic tubes. Delay in sound transmission through the plastic tubes was compensated for by appropriate shifts in the trigger signal. Presentation rates were kept between 150 and 500 ms SOA in order to find a tradeoff between the amount of stimuli sent and the signal strength, known to diminish with extremely fast presentation rates. During experimental tasks subjects were required to stay still and relaxed in order

to avoid muscle artifacts. In study II, subjects remained in a seated position, while studies I and III were conducted with subjects lying on a comfortable stretcher. Participants were instructed to ignore the auditory stimulation in all cases and were requested to attend to muted movies with subtitles, therefore ruling out a strong attentional modulation of the auditory responses elicited by experimental stimuli. Subjects were not allowed to sleep during the MEG recordings and active video monitoring was carried out during the whole experimental session. All experimental tasks lasted for one hour approximately. The experimental stimulation was controlled using specific software applications like Presentation® or the Psychophysics toolbox for Matlab.

The MEG machine used for experiments I and III was a 4D Neuroimaging Magnes 2500WH equipped with 148 biomagnetometers. For experiment II, a CTF OMEGA system equipped with 275 axial gradiometers was used. The main difference between these two MEG-systems lie in the distinct flux transformers employed to detect the weak magnetic field generated in the brain. Flux transformers connected to superconductor sensors or SQUIDS (Superconducting Quantum Interference Device) enhance the coupling of magnetic fields. Briefly, biomagnetometers have a single pick-up coil configuration and are characterized by a higher sensitivity to distal sources. Axial gradiometers include an extra compensation coil arranged vertically that decreases sensitivity to distal sources but enhances signal-to-noise ratio. In order to determine the position of the head inside the MEG, sensor position coils were attached to the subjects' head. These coils track head movements during the recording session and were used to define an individual coordinate system. Since head movements could hamper an accurate reconstruction of brain sources, recordings showing head movements bigger than 0.7 cm in any direction were discarded from further analyses. Additionally, the head-shape of all participants was digitized using a Polhemus® wand, and magnetic resonance images (MRI) of each participant were acquired to allow an accurate co-registration of MEG and the individual MRI data. Eye movements and cardiac activity were registered using a bipolar electrooculogram and an electrocardiogram, respectively.

In all three experiments, basic data preprocessing was carried out using Matlab (the MathWorks) and the FieldTrip toolbox (Oostenveld et a., 2011). Overall,

preprocessing involved data filtering, cardiac and ocular artifact identification and rejection, epoching, and averaging. Artifact identification and rejection was carried out using independent component analysis (ICA) and an additional rejection of epochs exceeding 2.5-3 pT. Prior to the source estimation using inverse solution techniques, individual MRI were segmented and re-aligned to the MEG individual coordinate system. Individualized structural data was used to complete the *forward modeling*, where brain volumes, or cortical mantles, are used to define a source space; that is, a parcelation of the anatomical space where activity will be modeled. During the forward modeling a leadfield matrix is computed for each small parcel (or dipole) that expresses the sensitivity of the sensor array in the three-dimensional space. In studies I and II source reconstruction was conducted in Fieldtrip using a time-domain inverse solution known as *linearly constrained minimum variance* (LCMV) *beamforming*. Beamformers estimate the contribution of sources in each parcel to the overall signal at the sensors, and yield a distributed representation of activity in the brain. In study III source reconstruction was carried out using a cortically constrained *minimum-norm* approach known as *dynamic statistic parametric mapping* (dSPM) implemented in Brainstorm (Tadel et al., 2011). This approach is based on a distributed source model and tries to estimate the current at all grid (parcels) locations by fitting the model to de data. In all studies individual source spaces were transformed into a standardized template brain, thus allowing for group averaging and statistical comparison. Statistical comparisons between conditions (e.g., deviant, standard, control) were carried out using both parametric and non-parametric statistics.

STUDY I

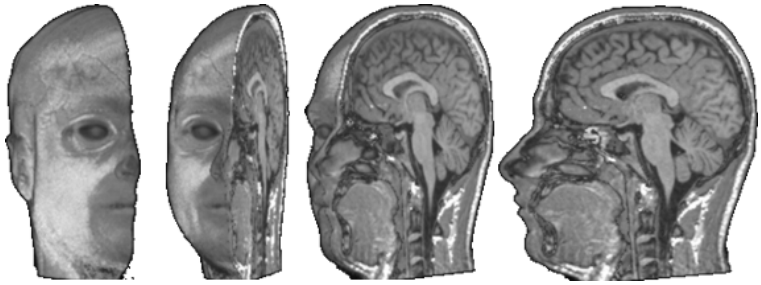

Two sequential processes of change detection in hierarchically ordered areas of the human auditory cortex

Cerebral Cortex January 2014;24:143–153
doi:10.1093/cercor/bhs295
Advance Access publication October 4, 2012

Two Sequential Processes of Change Detection in Hierarchically Ordered Areas of the Human Auditory Cortex

Marc Recasens[1,2], Sabine Grimm[1,2], Almudena Capilla[3], Rafal Nowak[4] and Carles Escera[1,2]

[1]Institute for Brain, Cognition and Behavior (IR3C), [2]Cognitive Neuroscience Research Group, Department of Psychiatry and Clinical Psychobiology, University of Barcelona, Barcelona, Spain, [3]Department of Biological and Health Psychology, Autonomous University of Madrid, Madrid, Spain and [4]Unidad de Magnetoencefalografía, Centro Médico Teknon, Barcelona, Spain

Address correspondence to Carles Escera, Department of Psychiatry and Clinical Psychobiology, University of Barcelona, P. Vall d'Hebron 171, Catalonia, 08035 Barcelona, Spain. Email: cescera@ub.edu, cescera@gmail.com

Auditory deviance detection occurs around 150 ms after the onset of a deviant sound. Recent studies in animals and humans have described change-related processes occurring during the first 50 ms after sound onset. However, it still remains an open question whether these early and late processes of deviance detection are organized hierarchically in the human auditory cortex. We applied a beamforming source reconstruction approach in order to estimate brain sources associated with 2 temporally distinct markers of deviance detection. Results showed that rare frequency changes elicit an enhancement of the Nbm component of the middle latency response (MLR) peaking at 43 ms, in addition to the magnetic mismatch negativity (MMNm) peaking at 115 ms. Sources of MMNm, located in the right superior temporal gyrus, were lateral and posterior to the deviance-related MLR activity being generated in the right primary auditory cortex. Source reconstruction analyses revealed that detection of changes in the acoustic environment is a process accomplished in 2 different time ranges, by spatially separated auditory regions. Paralleling animal studies, our findings suggest that primary and secondary areas are involved in successive stages of deviance detection and support the existence of a hierarchical network devoted to auditory change detection.

Keywords: auditory change detection, magnetoencephalography, middle latency responses, mismatch negativity, source localization

Introduction

The rapid discrimination of novel sounds in complex acoustic environments enables us to reallocate our attentional resources to rare and potentially relevant events (Escera et al. 1998; Escera and Corral 2007). In humans, the processing of such rarely occurring sounds is indexed by an automatic event-related brain potential/event-related field (ERF) peaking at 150–250 ms: The mismatch negativity (MMN; Näätänen et al. 2007) or its magnetic counterpart (MMNm). However, recent findings by our group have shown that violations of an auditory stimulus feature trace are also reflected at much earlier latencies in the auditory brain as indexed by amplitude modulations of the auditory middle latency responses (MLRs: Na, Pa, Nb, and Pb), in the initial 50 ms after change onset (Slabu et al. 2010; Althen et al. 2011; Grimm et al. 2011, 2012; Leung et al. 2012). Specifically, enhancements of Pa (Slabu et al. 2010), Nb (Grimm et al. 2011), and Na components of the MLR (Grimm et al. 2012), in addition to the MMN in long-latency responses (LLRs), were elicited as "genuine" deviance-related responses, that is, controlling for confounding frequency-specific adaptation effects. Such results suggest that change detection is hierarchically structured in different processing stages along the auditory pathway (Grimm and Escera 2011; Slabu et al. 2012), thus paralleling other properties of the auditory system such as spectral (Wessinger et al. 2001; Kumar et al. 2007), temporal-scale (Kiebel et al. 2008; Lerner et al. 2011), or speech processing (Scott and Johnsrude 2003). A hierarchically organized deviance detection network would be in line with the "predictive coding" hypothesis (Friston 2005), stating that the brain predicts the nature of forthcoming events based on hierarchical message passing among cortical areas (Garrido et al. 2009). Indeed, such hypothesis has been recently implemented in a neuronal model accounting for several MMN findings (Wacongne et al. 2012).

Additional evidence in favor of a hierarchical auditory deviance detection system comes from animal studies showing that stimulus-specific adaptation (SSA), that is, the reduction of the spiking rate to standard stimuli while keeping robust responses to deviant stimuli (Ulanovsky et al. 2003) is a widespread property of the auditory system, including cortical (Ulanovsky et al. 2003, 2004; von der Behrens et al. 2009) and subcortical structures (Pérez-González et al. 2005; Malmierca et al. 2009; Antunes et al. 2010).

In humans, source localization studies have yielded generators of MMN and MMNm confined to bilateral secondary auditory areas like the anterior Heschl's gyrus (HG) and superior temporal gyrus (STG; Opitz et al. 2005; Schönwiesner et al. 2007). On the other hand, MLRs are known to follow a medio-lateral and postero-anterior propagation starting in medial portions of the HG (Liegeois-Chauvel et al. 1994; Pantev et al. 1995; Yvert et al. 2005) with Pa/Pb complex thought to reflect a processing stream from primary auditory cortex (PAC) to STG (Howard et al. 2000). To our knowledge, no studies assessing the anatomical generators of change detection in the time range of MLR have been conducted yet.

We aim to show that hierarchically distinct areas of the auditory cortex are involved in early and late auditory change detection, thus supporting that detection of deviant sounds is functionally organized in a hierarchical fashion. We hypothesize that generators of deviance processing in the time range of MLR will be located in or close to PAC, whereas those accounting for MMNm will be located in secondary areas such as STG.

Materials and Methods

Subjects

Thirteen healthy, normal-hearing subjects (7 females) aged 22–34 years (27 years, mean age, standard deviation [SD] = 3.7) took part in

the experiment. Hearing level was assessed binaurally with a pure tone audiometry for 5 frequencies (250, 500, 1000, 3000, and 8000 Hz) before or just after the task. The experimental protocol was approved by the Ethical Committee of the University of Barcelona and was in accordance with the Code of Ethics of the World Medical Association (Declaration of Helsinki). Participants gave written informed consent before the experiment.

Stimuli and Procedure

Auditory stimuli consisted of 50-ms pure sine wave sounds (5 ms rise, 20 ms fall) delivered at 60-dB sound pressure level. Sounds were binaurally delivered by an Etymotic ER-30 system (Etymotic Research, Inc. United States of America) via plastic earpieces. The 18-ms delay in the transmission of sound was compensated for by an appropriate shift of the trigger signal.

The stimulus-onset asynchrony was randomly jittered between 150 and 350 ms. The experimental design consisted of an oddball block including 800-Hz frequency deviant tones occurring at a probability of 0.20- and 1040-Hz repetitive standard tones occurring at a probability of 0.80. In a reversed oddball block, the roles of deviant and standard stimuli were switched in order to allow the comparison between physically identical stimuli. Only standard stimuli from the reversed block and deviants from the oddball block were used in further analyses. For the sake of clarity, we will refer to "reversed standard" as "standard" condition from now on. A control block, comparable with the one first introduced by Schröger and Wolff (1996) was used, in which stimuli of 5 different frequencies (800, 1040, 1280, 1664, and 2040 Hz) were randomly presented, each at a probability of 0.20. This was done to preclude refractoriness confounds. The 3 blocks were split into 6 blocks, which were presented randomly. In sum, a total amount of 1200 stimuli of each condition (deviants from the oddball block, standards from the reversed block, and controls) were used in the subsequent analyses.

Data Acquisition

During the recording session, subjects were required to lie as still as possible on a bed with their head inside the helmet-like device for approximately 1 h. Participants were instructed to relax, to ignore the auditory stimulation, and to attend to a silent movie with subtitles. A whole-head magnetoencephalography (MEG) system (148 biomagnetometers, 4D Neuroimaging Magnes 2500WH, San Diego, CA, United States of America) recorded the magnetic currents at 1017 Hz sampling rate. Data were on-line high-pass filtered at 1 Hz and stored for off-line analysis. A bipolar electrooculogram was recorded to identify eye movements. Five small sensor position coils were attached to the forehead and to the periauricular points in order to determine the position of the head and to track any head movement occurring during the recording. Data sets in which the relative position of the head changed by >0.7 cm throughout the recording session were discarded from further analyses. For each subject, the headshape including the forehead, the nose, and the location of the sensor position coils were digitized using a digitizer wand (Polhemus Fastrak, Polhemus Inc., Colchester, VT, United States of America). Additionally, T_1-weighted, 3-dimensional (3D) spoiled gradient-echo, magnetic resonance images (MRIs) of each individual brain were acquired using a 1.5-T Signa CV (General Electric, Milwaukee, WI, United States of America) to allow superimposition of MEG and MRI data.

Data Analysis

Data analysis was performed using Matlab 7.10 (The MathWorks) and FieldTrip (Oostenveld et al. 2011; www.ru.nl/neuroimaging/fieldtrip, 20101006 release). The signal was digitally low-pass filtered at 150 Hz. The strongest components corresponding to cardiac and ocular artifacts were projected out of the MEG signal using independent component analysis (ICA; "runica" algorithm implemented in FieldTrip/EEGLAB, http://sccn.ucsd.edu/eeglab/). Eight hundred samples (1 s length) including data from each condition were used for ICA. On average, 3.4 components per subject were identified as blinks, saccades, or cardiac artifacts (maximum of 5 components in subject 7) on the basis of their scalp topography and continuous activity (Jung et al. 2000). Additionally, a rejection threshold of 4 pT was applied to remove high amplitude artifacts. Finally, LLR data were epoched in 400-ms time windows (including 100-ms pre-stimulus baseline) and low-pass filtered at 30 Hz (2-pass Butterworth filter; filter order of 4). For MLR analysis, epoch length was 200 ms (including 50-ms pre-stimulus baseline) and a high-pass filter of 15 Hz was applied (2-pass Butterworth filter; filter order of 4). Artifact-free trials were averaged separately for each condition (deviant, standard, and control).

For the source localization analysis, we first coregistered the MEG and the anatomical MRI coordinate systems by using a semiautomatic procedure. Three landmarks (nasion, and the 2 periauricular points) were localized in each individual MRI and used for a first alignment with the MEG coordinate system. We then performed an automatic fit between the digitized headshape and the scalp surface extracted from the MRIs based on an iterative procedure. In each iteration, we applied a modified version of the iterative closest point algorithm (Besl and Mckay 1992; icp2©: http://www.csse.uwa.edu.au/~ajmal/code/icp2.m) to a different initial position of the digitized headshape. The location of the headshape relative to the scalp surface was updated, in each iteration, to the one providing the minimum distance error between them. Based on the segmentation of the brain surface of each individual's MRI, we obtained a semirealistic single-shell head model for each participant. Subsequently, a standard 3D grid (6 mm spacing, 12773 voxels inside the head) derived from the Montreal Neurological Institute (MNI) T1 template brain was adapted to each individual's brain volume by means of an inverse-normalization procedure based on a linear affine transformation (SPM2, Wellcome Trust Center for Neuroimaging, London, United Kingdom; http://www.fil.ion.ucl.ac.uk/). The use of the standard MNI grid would thus allow for group averaging and statistical comparison of results. Leadfields were computed for each grid voxel on the basis of a quasistatic approximation of the brain surface as a single shell (Nolte 2003). The weakest orthogonal component at each voxel of the leadfield matrix was excluded. Neuronal sources of interest were identified using a time-domain minimum-variance spatial filter: The linearly constrained minimum variance beamformer, designed to detect a signal corresponding to a specific location and attenuate signals from all other locations (Van Veen et al. 1997). A single covariance matrix was computed for each subject from the combined datasets from all 3 conditions (deviant, standard, and control), both for MLR (from −50 to 100 ms) and for LLR (from −100 to 200 ms). The covariance matrix and the leadfield matrix were used to compute common spatial filter weights with regularization set to 10% of the mean power. By using common filter weights, we ensured that differences in source activity across conditions were not due to differences between filters. Subsequently, we projected the sensor-level signal of each condition and trial into each voxel of source space through the common spatial filter corresponding to a dipole at this location with fixed optimal orientation. Finally, single-trial data were subsequently averaged separately for each condition. This procedure thus provided an averaged time course of activity in source space for every subject and condition. To reduce spatial filter biases toward the center of the head, voxel activity was normalized using the neural activity index where the estimated power at each grid point is divided by an estimate of the noise (Van Veen et al. 1997).

Individual mean amplitude pseudo-Z maps of the ERF components in each condition were computed by averaging pseudo-Z values within a time window of 6 and 20 ms around the peak latencies of the MLR (Nam, Pam, Nbm, and Pbm) and LLR (N1m/MMNm) components, respectively. Peak latencies for the mentioned components were derived from the root-mean-squared grand-average computation for deviant, standard, and control stimuli. Evoked auditory activity of different conditions was statistically compared using nonparametric cluster-based permutation t-tests (Singh et al. 2003; Maris and Oostenveld 2007). This allowed us to determine which voxels showed statistically significant activity by comparing the grand-mean pseudo-Z value of a given voxel to a distribution of permuted pseudo-Z values. Permutation methods have been widely used in studies applying

beamforming techniques on event-related data since no explicit parametric distribution of the population is required (Herdman et al. 2003, 2007; Chau et al. 2004; Cheyne et al. 2006).

Significant sources of MMNm and deviance-related effects for MLR were computed by pairwise comparisons of ERF pseudo-Z maps against conditions (deviant vs. standard; deviant vs. control) for all components of interest in the above-mentioned time intervals (Nam, Pam, Nbm, and Pbm for MLR; MMNm for LLR) using a nonparametric cluster-based procedure that effectively corrects for multiple comparisons (see Maris and Oostenveld 2007, for details on the method). This type of test defines the clusters of interest based on the actual distribution of the data and tests the statistical differences between condition waveforms in each particular voxel using a Monte-Carlo randomization method. Clusters were defined as spatially adjacent voxels where a dependent samples t-test with respect to the pseudo-Z values in 2 conditions exceeded an a priori threshold ($P < 0.001$ for LLR and $P < 0.01$ for MLR). A lower significance level for MLR was chosen in order to obtain cluster volumes (for MLR and LLR) of comparable size. For each cluster, a statistical analysis was calculated by taking the sum of all individual voxel t-statistics within a cluster. The Type I error rate for the complete set of 12773 voxels was controlled by evaluating the cluster-level test statistic under the randomization null distribution of the maximum cluster-level test statistic. Specifically, the null distribution was obtained by randomly permuting the data between the 2 experimental conditions within each participant 5000 times.

Similarly, we estimated the sources of the transient N1m fields in the temporal lobe in order to identify those cortical regions showing distinctive activity to identical stimuli embedded in the different conditions (deviant, standard, and control). Pairwise comparisons of the baseline maps against the N1m maps were carried out. Baseline maps were obtained by averaging pseudo-Z values in each condition between −100 and 0 ms. N1m pseudo-Z maps were obtained by averaging each condition between 105 and 140 ms. By defining a broad interval, we included the N1m component in each condition. Clusters were defined as spatially adjacent voxels where dependent samples t-test with respect to the pseudo-Z values in the 2 time intervals exceeded an a priori threshold ($P < 0.0002$ for deviant, $P < 0.0002$ for control, and $P < 0.005$ for standard). The null distribution was obtained by randomly permuting the data between the baseline and the N1m response within each participant 5000 times.

Determination of across-subject differences in the localization of deviance-related auditory areas between MLR and LLR was performed by pairwise comparisons of the location of those individual voxels showing the largest pseudo-Z values, "peak-voxels," in the subtracted activation maps. Individual pseudo-Z maps for MMNm and MLR components were computed by averaging the pseudo-Z values within a time window of 6 and 20 ms around the individual peak latencies of the MLR (Nam, Pam, Nbm, and Pbm) and LLR (N1m/MMNm) components, respectively. Peak-voxel coordinates in the 3 axes (x, y, and z) were exclusively extracted from previously computed clusters in order to ensure that all locations were inside an area showing statistically significant deviance-related effects. Results were considered significant when Student's t-tests yielded P-values (2-tailed) <0.05. Likewise, localization differences of N1m peak-voxels for the 3 experimental conditions were estimated across subjects. Peak-voxel coordinates in the 3 axes (x, y, and z) were extracted solely from previously computed clusters showing a significant effect for N1m. For each axis, a repeated-measures analysis of variance (ANOVA) including the factor condition (deviant, standard, and control) was calculated. Results were considered significant when $P < 0.05$ using a 2-tailed analysis. Bonferroni correction was used for multiple pairwise contrasts.

Results

We delivered low-probability sounds interspersed in a context of frequently repeated tones to show that auditory change detection can be traced by both LLR and MLR. The event-related beamforming approach allowed us to estimate the contribution of different neural generators involved in deviance detection. Figure 1 shows the ERF and topographies of the grand-averaged magnetic fields corresponding to LLR and MLR for the 3 different conditions. N1m component peaked at 115 and 118 ms after sound onset in the deviant and control condition, respectively. The N1m field in the standard condition showed a clear adaptation as a result of repetitive stimulation. Unexpectedly, N1m in response to control tones elicited a higher magnetic response than deviant tones. Middle latency evoked fields were approximately 3 times smaller in amplitude when compared with LLR fields. On average, Nam component peaked at 23 ms; Pam peaked at 32 ms; Nbm peaked at 43 ms; and Pbm peaked at 55 ms. As shown in Figure 1, the field distribution of both MLR (Nbm) and LLR (N1m) responses showed a clear dipolar distribution over sensors located in the Sylvian fissure.

For LLR, deviant versus standard comparison resulted in one cluster where pseudo-Z values were significantly higher for deviant when compared with standard tones ($P < 0.001$, corrected for multiple comparisons) in the latency range of N1m/MMNm. Figure 2 shows the grand-mean source estimate of deviant versus standard (MMNm) activity exceeding the statistical threshold in the long-latency range. This cluster was clearly located in the right temporal lobe, specifically, in both medial and lateral portions of STG, HG, and middle temporal gyrus. The peak-voxel in the thresholded grand-mean source estimate of MMNm was located between the right middle temporal gyrus (MTG) and the right STG. This area, posterior to Heschl's sulcus, is usually defined as planum temporale (PT; MNI coordinates: 54, −18, −2). No clusters over left auditory cortex areas exceeded the imposed statistical threshold for MMNm. As can be inferred from the virtual channel waveform obtained from the peak-voxel in Figure 3, MMNm peaked in the grand-average waveform at 115 ms. Deviant versus control comparisons, intended to provide a clearer picture of net memory-based comparison processes than the "classic MMN", resulted in no statistically significant voxels. Tones in the control condition elicited stronger activity than deviant tones; however, this difference in activity did not reach statistical significance.

In the middle latency time range, the same procedure was repeated for the main MLR components. Deviant versus standard comparisons for the Nam, Pam, and Pbm components showed no active voxels exceeding the mentioned a priori threshold. Only deviant versus standard pairwise comparison for the Nbm component resulted in a significant cluster of activity ($P < 0.01$). As shown in Figure 4, this cluster was localized over the right temporal lobe, specifically, in areas including HG, a small aspect of the medial STG, and extending anteriorly to the insula. The peak-voxel in the thresholded grand-mean source estimate of Nbm (deviant vs. standard) was located in the anterior part of the medial HG, next to the long insular gyri (MNI coordinates: 42, −18, 4). Figure 5 shows the virtual channel obtained from the peak-voxel in Nbm (deviant vs. standard) peaking at 43 ms. Cluster-based t-test for paired differences between deviant and control tones yielded no statistically significant clusters for any of the components. Unlike LLR, Nbm deviant condition elicited numerically larger activity than control tones; however, the difference did not reach statistical significance.

To further investigate location differences in the generators of MMNm and Nbm differential activities across subjects,

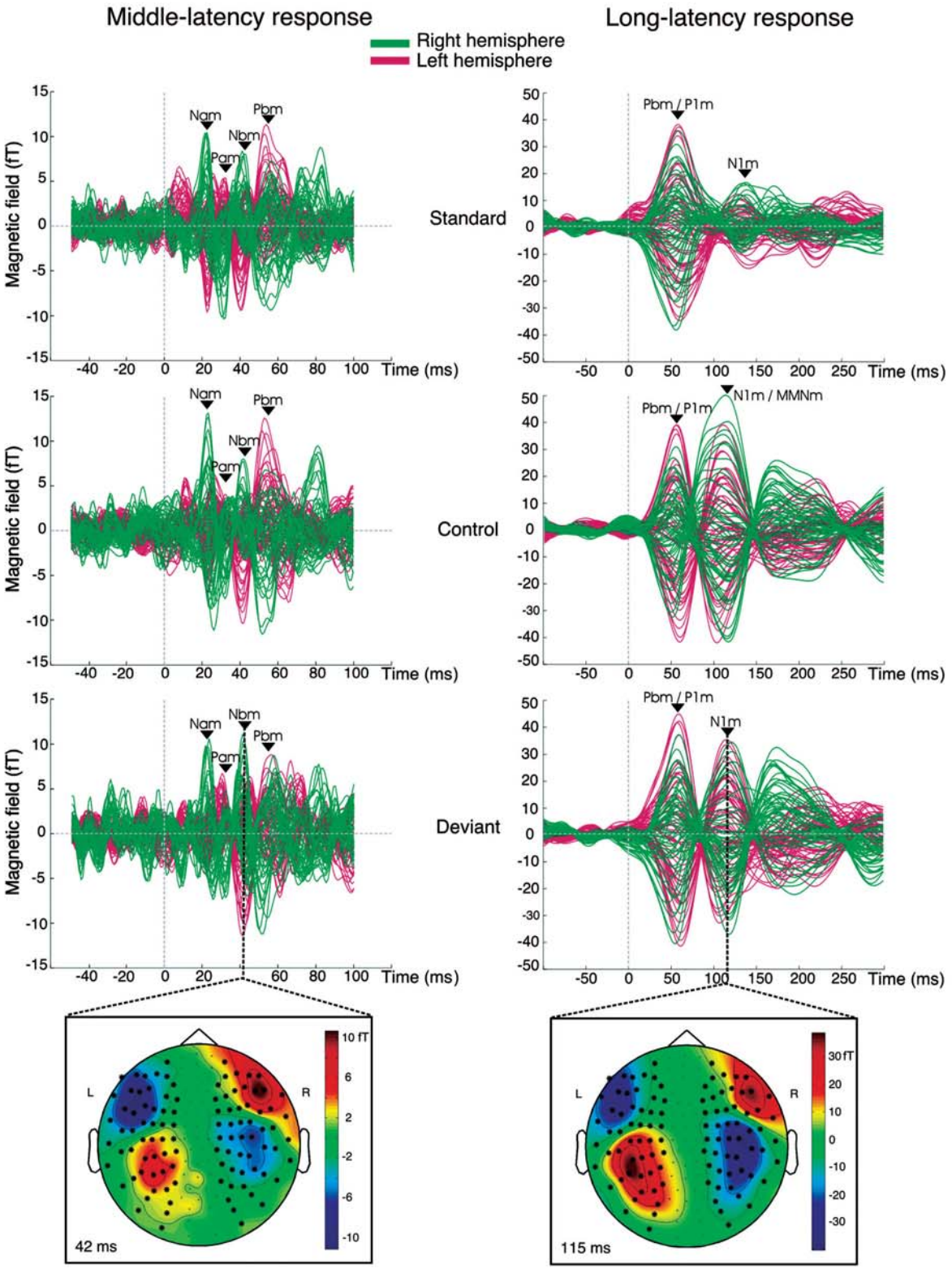

Figure 1. (Top) Grand-averaged ERFs from MLR (left) and LLR (right). Fifty-three sensors from each hemisphere are displayed. Midline sensors have been excluded. (Bottom) Magnetic field distribution for MLR (Nbm component) and LLR (N1m component) in the deviant condition. The 53 sensors used for the waveform computation are depicted.

individual peak-voxels from the deviant minus standard subtraction waveforms were extracted. To ensure that chosen peak-voxels' activity represented a significant deviance enhancement, individual peaks of maximal activity were only extracted from those areas showing statistically significant effects in the grand-averaged activity maps. Accordingly,

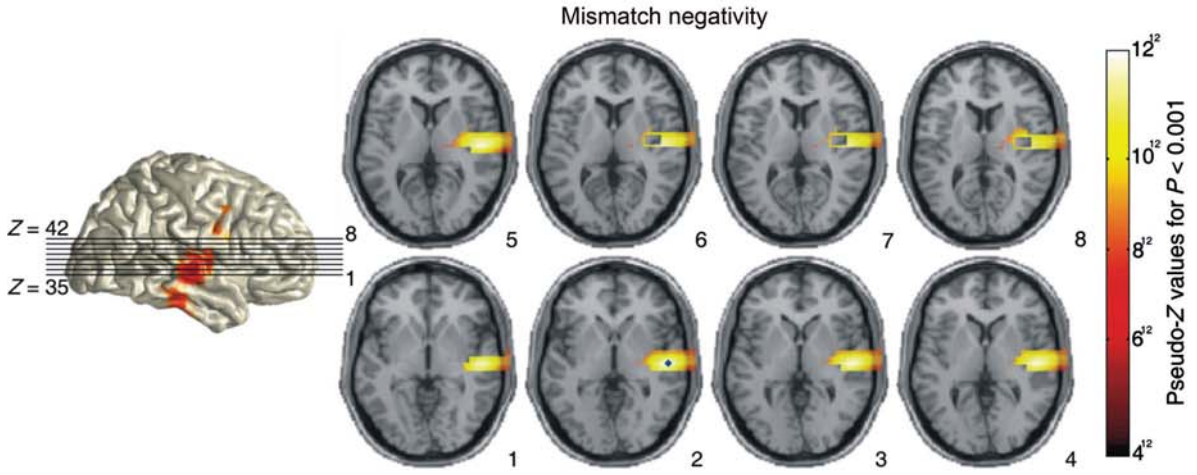

Figure 2. Thresholded grand-mean pseudo-*Z* activity for MMNm (Deviant minus reverse standard) after nonparametric cluster-based analysis. Significant voxels ($P < 0.001$, corrected) are projected to the surface of a normalized MRI. The blue diamond (shown on slice 2) indicates grand-mean peak-voxel for MMNm (Deviant minus reverse standard). Pseudo-*Z* values represent the ratio of signal-to-noise power of the evoked response.

MMNm and Nbm (deviant–standard) individual peak-voxel coordinates (*x*, *y*, and *z*) were pairwise compared among our sample of participants. Figure 6 shows the location of the individual peak-voxels for LLR (MMNm) and MLR (Nbm) located inside a cluster reflecting significant deviance detection activity. Results derived from repeated measures *t*-test showed that there was a significant difference in the *y*-axis (antero-posterior; $t = 3.288$, $P = 0.006$) between the peak-voxels for MMNm (mean = −16.77, SD = 7.17) and Nbm differential activity (mean = −5.54, SD = 11.26). In the *x*-axis (medio-lateral; $t = -2.334$, $P = 0.038$), Nbm difference peak-voxel positions (mean = 46.92, SD = 11.3) were located more medial than MMNm peak-voxels (mean = 56.3, SD = 11.84). No statistically significant differences were found in the *z*-axis (inferio-superior).

As a priori-defined region of interest (ROI) for each latency range could bias localization results, we decided to repeat the procedure but using only one cluster or ROI for both MLR and LLR subtracted responses. This cluster contained all possible voxels that appeared as statistically significant in both LLR and MLR cluster-based analyses. We found that a difference between MMNm (mean = 53.31, SD = 11.84) and Nbm (mean = 46.62, SD = 11.72) peak-voxels existed in the *x*-axis ($t = -2.51$, $P = 0.027$). Also, for the *y*-axis, MMNm peak-voxels (mean = −16.77, SD = 7.17) were posterior to deviance-related Nbm peak-voxels (mean = −7.54, SD = 12.65; $t = 2.43$, $P = 0.032$).

Additional analyses on the localization of the N1m response to the different conditions provided means to argue in favor for a genuine involvement of change detection. N1m in response to deviant and control tones resulted in one cluster on the right hemisphere where pseudo-*Z* values were significantly higher for N1m when compared with baseline levels ($P < 0.002$, corrected for multiple comparisons). For N1m to standard tones, the same procedure yielded 2 clusters located bilaterally on the supratemporal planes ($P < 0.005$, corrected for multiple comparisons). Results are displayed in Figure 7. These statistically significant clusters were subsequently used as spatial constrains to compute statistics across individual peak-voxels. One-way ANOVAs for each of the 3 axes (*x*, *y*, and *z*) revealed statistically significant differences between conditions. In the *x*-axis ($F_{1,12} = 8.03$, $P < 0.003$), pair-wise comparisons showed that deviant-related N1m sources were located lateral to standard-related N1m sources ($t = 3.597$; $P < 0.012$). Deviant–control contrast did not yield a statistically significant difference when Bonferroni correction was applied ($t = 2.61$; $P < 0.07$). In the *y*-axis (*y*-axis: $F_{1,12} = 18.670$, $P < 0.001$), both deviant and control conditions showed more anterior N1m source locations than the standard condition ($t = 4.98$, $P < 0.002$; $t = 4.726$, $P < 0.002$). Finally, in the *z*-axis ($F_{1,12} = 21.956$, $P < 0.001$), deviant and control conditions yielded N1m source locations being more superior than the standard condition ($t = 6.236$, $P < 0.001$; $t = 5.162$, $P < 0.002$).

In sum, both grand-average mean locations and intersubject peak-voxel results showed that the deviance-related enhancement of activity reflected in the Nbm component was

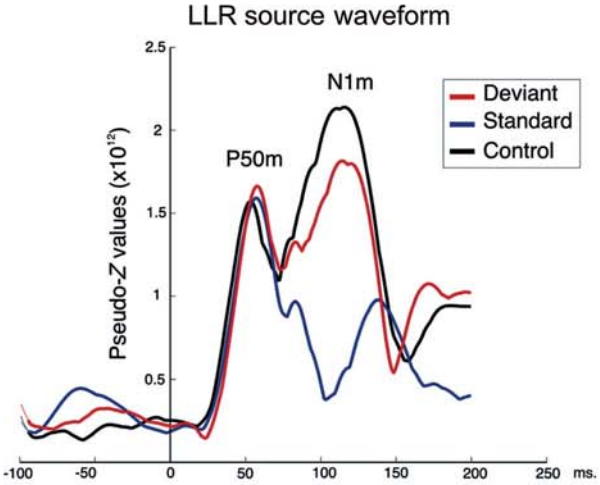

Figure 3. Grand-mean virtual channel waveform for the 3 conditions in the long-latency range: Deviant (red), reversed standard (blue), control (black). The virtual channel corresponds to peak-voxel (voxel with maximal activity) for MMNm (Deviant minus reverse standard) in the pseudo-*Z* activity map, shown in Figure 2. Time zero indicates tone onset. Absolute values are given.

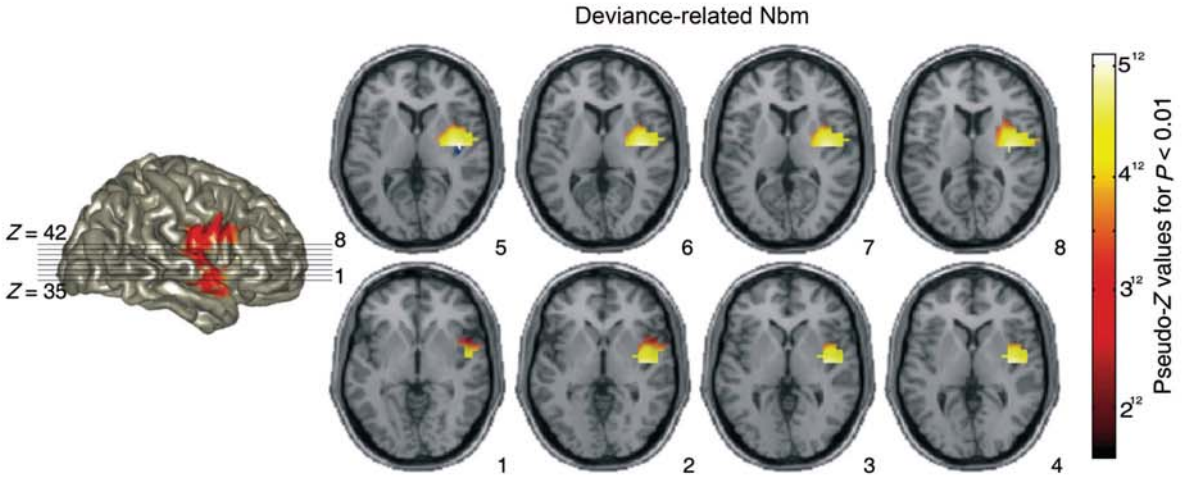

Figure 4. Thresholded grand-mean pseudo-*Z* activity for Nbm (Deviant minus reverse standard) after nonparametric cluster-based analysis. Significant voxels ($P < 0.01$, corrected) are projected to the surface of a normalized MRI. The blue diamond (shown on slice 5) indicates grand-mean peak-voxel for Nbm (Deviant minus reverse standard). Pseudo-*Z* values represent the ratio of signal-to-noise power of the evoked response.

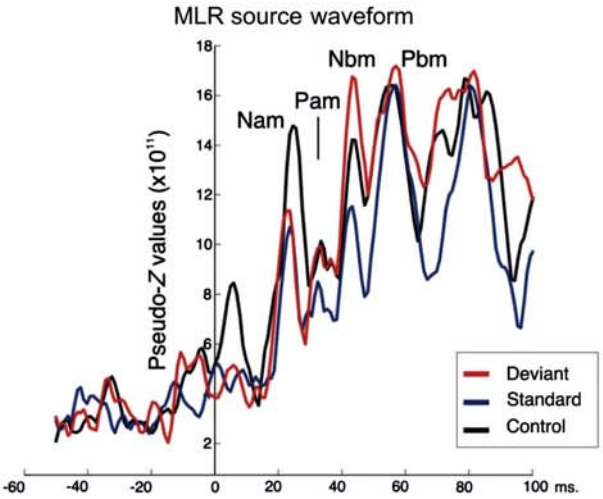

Figure 5. Grand-mean virtual channel waveform for the 3 conditions in the middle latency range: Deviant (red), reversed standard (blue), control (black). The virtual channel corresponds to the peak-voxel (voxel with maximal activity) for the Nbm (Deviant minus reverse standard) in the pseudo-*Z* activity map, shown in Figure 4. Time zero indicates tone onset. Absolute values are given.

generated by sources located medially and anteriorly to the ones of the deviance-related activity in the MMNm time range. In addition, analyses of transient responses in the long-latency range revealed spatially distinct source generators involved in the N1m response to the 3 different stimulus conditions.

Discussion

Results from this study have shown that areas involved in auditory deviance detection in the human brain exist in 2 separated spatial and temporal domains. Regions showing larger activity for deviant events in the time range of MLR were located in the right hemisphere, anterior and medial to those of the MMNm, and overlapping anterior aspects of HG, temporoinsular areas, and antero-medial portions of the right STG. Consistent with recent electroencephalography (EEG) findings (Grimm et al. 2011, Leung et al. 2012), unexpected pure tones elicited larger Nbm responses than physically identical tones occurring in a repetitive fashion. Source estimates for deviance-related Nbm overlapped the anterior rim of HG, including its medial and central aspects, a region equivalent to the cytoarchitechtonically koniocortical Te1 area (Brodmann area 41). Te1.0 subdivisions have been described in cytoarchitechtonic and probabilistic maps of the human auditory cortex as the PAC (Morosan et al. 2001; Rademacher et al. 2001). The grand-averaged peak-voxel was located medially in a site overlapping the medial aspect of HG. These results are in line with previous electrophysiological studies pointing at different regions along the medio-lateral and posterior–anterior axes of HG as the neuronal generators of the Pa/Pb components of the MLR. Intracranial recording studies (Liegeois-Chauvel et al. 1991, 1994) localized generators of auditory MLR between 30 and 50 ms in medial and central parts of HG, respectively. These findings were further confirmed by means of MEG recordings, showing an origin of MLR at 20 ms in medial HG (Scherg et al. 1989; Scherg and von Cramon 1990; Lütkenhöner et al. 2003). Similarly, MEG studies (Yoshiura et al. 1995; Gutschalk et al. 1999; Inui et al. 2006) showed 2 different sources accounting for the early and late part of the MLR, located in the medial and lateral parts of HG, respectively. Their findings, suggestive of a serial activation, are consistent with anatomical findings in monkeys showing strong connections between core and adjacent belt regions (Merzenich and Brugge 1973; Galaburda and Pandya 1983). Source generators of transient Nbm component (peaking around 40 ms after sound onset) have been located over lateral areas of the STG (Yvert et al. 2001; Inui et al. 2006). Source localization discrepancies might stem from differences in the time intervals chosen to delineate event-related activity in this latency, different reconstruction techniques, and experimental design. Still, the localization of the deviance-related activity found here is highly consistent with localization of MLR components shown by the above-mentioned MEG studies and intracranial recordings (Liegeois-Chauvel et al. 2001). To our knowledge, this is the

first time that the sources of deviance-related MLR have been localized in a region overlapping medial and lateral HG.

Source estimates of MMNm (deviant minus standard) spanned right hemisphere regions of STG, MTG, superior temporal sulcus (STS), and posterior portions of HG. Our results are in agreement with the bulk of MMN localization studies, where, independently of the technique or stimulation employed, STG is the most consistent finding (Opitz et al. 1999, 2002; Tervaniemi et al. 2000, 2006; Doeller et al. 2003; Schall et al. 2003; Rinne et al. 2005; Schönwiesner et al. 2007; but see Maess et al. 2007). Specifically, the grand-average peak-voxel for MMNm was localized in STG, bordering posteriorly with HG. Source estimates as a whole overlapped cyto- and receptoarchitectonic Te2.2 and Te3 subdivisions of the auditory cortex (corresponding to BA 42 and BA 22; Morosan et al. 2005), thought to correspond to secondary auditory areas. Also, activity overlapping HG was found, consistent with previous findings (Opitz et al. 2005; Maess et al. 2007; Schönwiesner et al. 2007). Schönwiesner et al. (2007) reported activation in STG and in both medial and lateral HG, suggesting contributions of PAC areas to deviance detection. Similarly, Opitz et al. (2005) disentangled the existence of a cognitive mechanism (deviant vs. control) in secondary areas, and a sensory mechanism (standard vs. control) generated in a primary auditory area of HG. The right lateralization of the MMNm observed in our study is consistent with previous non-linguistic studies showing larger MMN amplitude in the right hemisphere, irrespective of the stimulated ear (Scherg et al. 1989; Giard et al. 1990; Paavilainen et al. 1991; Grimm et al. 2006). Similarly, sources of Nbm were lateralized to the right hemisphere. This might point to the fact that the MLR change-related enhancement is an upstream index of contextual deviance processing preceding MMNm. Nevertheless, a complementary explanation based either on the greater spectral variation sensitivity of the right hemisphere for pure-tone processing (Liegeois-Chauvel et al. 2001; Zatorre and Belin 2001; Jamison et al. 2006) or methodological differences cannot be ruled out.

The arrangement of the distinct auditory regions found here is comparable with the structures described in previous studies using intracranial recording in humans (Howard et al. 2000; Brugge et al. 2003), showing a functional differentiation between the mesial-HG and the postero-lateral STG. In functional magnetic resonance imaging, a source location of the MMN posterior to the source of the P50 component has been shown (Mathiak et al. 2002). In accordance, our results suggest that generators of MMNm are partially located in secondary areas, whereas deviance-related Nbm arises from primary auditory areas (Borgmann et al. 2001).

Our source localization results extend the notion of a multistage organization of deviance detection (Boutros et al. 1995;

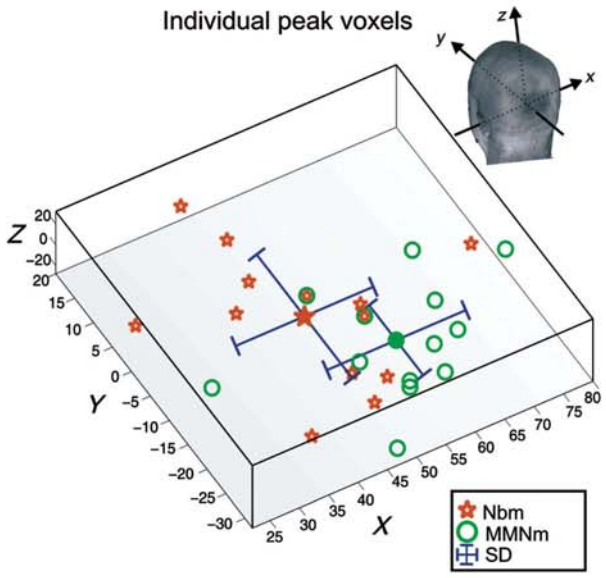

Figure 6. Locations of MMNm and Nbm (Deviant minus reverse standard) peak-voxels for the one-cluster analysis. Empty circles and stars indicate individual subjects ($n = 13$), filled circles and stars represent mean locations across all subjects. The blue cross represents standard deviation. Axis values indicate millimeters (MNI coordinates). The cube covers a reduced area of the right temporal lobe.

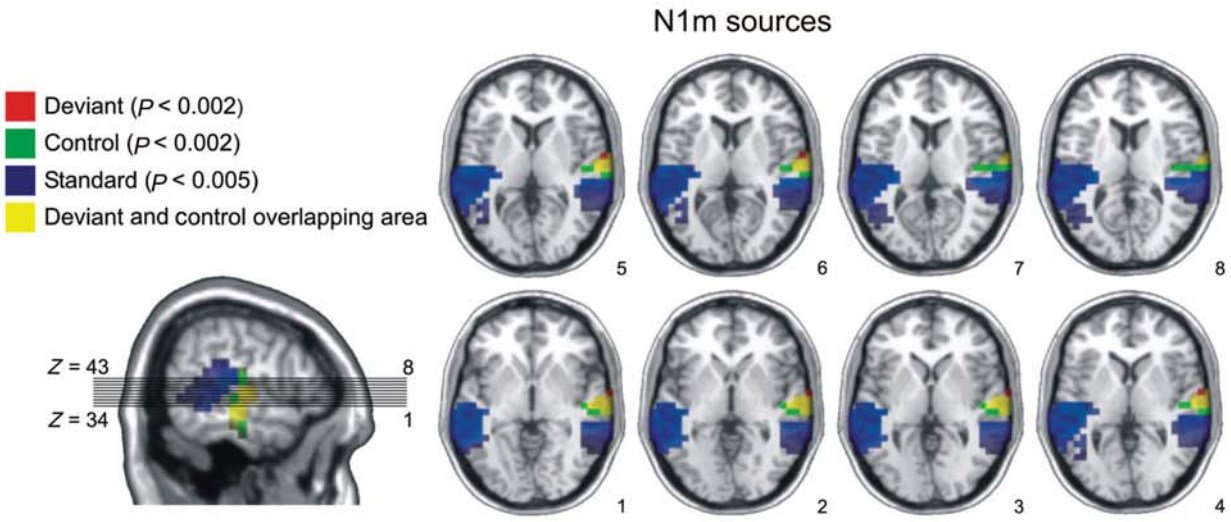

Figure 7. Thresholded grand-mean pseudo-Z activity maps (105–140 ms) for deviant ($P < 0.002$; in red), control ($P < 0.002$; in green), and standard ($P < 0.005$; in blue) N1m (N1m minus baseline) after nonparametric cluster-based analysis. Overlapping voxels between deviant and control N1m source estimates are also displayed (in yellow).

Sonnadara et al. 2006; Slabu et al. 2010, 2012; Althen et al. 2011; Grimm and Escera 2011; Grimm et al. 2011, 2012; Leung et al. 2012) by showing differences in the anatomical domain. Our results suggest that the existence of a sequential and redundant transition of change-related activity occurs between ~40 and ~100 ms, spreading from anterior areas of HG to lateral and posterior areas of the auditory cortex. It is a widely held view that redundant information in the brain is efficiently reduced as stimuli are successively processed in different stations (Barlow 1961; Friston 2005). Deviance detection, as shown in the present study, fits well with the idea of hierarchically organized areas devoted to increasing levels of auditory regularity and acoustic violation processing (Grimm and Escera 2011). Only further studies using more complex levels of acoustic regularities will allow for disentangling a differentiation between the functional role of early and late change detection. Modulations of early auditory activity during oddball situations have been broadly interpreted as early indexes of deviance detection (Boutros et al. 1995; Sonnadara et al. 2006; Slabu et al. 2010, 2012). However, according to the lack of results delineating pure memory-based deviance detection processes, alternative interpretations might be taken into account. MLR amplitude enhancements could be indexing stimulus change per se, irrespective of the previously encoded regularity. Under this view, the early mechanism indexed by modulations of Nbm in primary areas would act as a stimulus detector signaling to higher order mechanisms devoted to memory-based change detection, the MMNm. This interpretation is in line with a study by Schönwiesner et al. (2007) which observed the sources of the MMN to duration changes located in lateral and medial portions of HG, PT, and along the STG and STS, whereas only STG and PT showed a deviance magnitude modulation. Based on that finding, the authors suggest that changes are initially detected in primary auditory areas, whereas STG and PT might be enrolled in a detailed analysis of acoustic changes. Similarly, Leung et al. (2012) suggested that, with the exception of frequency, deviance detection at early latencies is feature unspecific, whereas MMN indexed feature specific changes. Altogether, interpretations based on the different functional role of MMN and deviance-related MLR support the notion of deviance detection as a hierarchically organized network in the human brain Although the idea of an early noncomparator mechanism processing stimulus change per se is feasible, previous results showing enhanced responses to frequency deviants when compared with control sounds would not support this view (Slabu et al. 2010; Grimm et al. 2011; 2012). Similarly, the numerically largest deviant response found in the MLR time range of the present study argues in favor of a sequential activation of a change detection network.

Even though a direct functional relationship between change detection in the MLR and MMN time range cannot be drawn from the present study, the existence of 2 brain mechanisms of change detection operating at different spatial and temporal scales leads to the hypothesis that deviance processing might be framed under the same hierarchic model described for the auditory cortex of the macaque monkey (Kaas and Hackett 1998; Rauschecker 1998; Kaas et al. 1999). Single-cell and multiunit recordings in animals studying SSA have described an ubiquitous presence of neurons responding to deviant events along the auditory pathway, from anatomically low levels such as the inferior colliculi (Malmierca et al. 2009), the auditory thalamus (Antunes et al. 2010), and extending up to the PAC (Ulanovsky et al. 2003, 2004; von der Behrens et al. 2009). Although SSA has been regarded as the single-neuron correlate of the MMNm (Nelken and Ulanovsky 2007), remarkable differences contradict the assumption that the former directly accounts for the latter (von der Behrens et al. 2009). Instead, the most parsimonious explanation is that SSA in the PAC is reflecting a process "upstream" of MMN generation, that is to say, PAC first detects changes that subsequently would elicit MMN in higher areas. Since the sources of the deviance-elicited Nbm component described here (peaking at about 40 ms from stimulus onset) were estimated in, or near, the vicinity of PAC, our findings are not only suggestive of an upstream deviance detection mechanism, but provide anatomical evidence to support the hypothesis that deviance-related MLR may be the human analog of single-cell firing and local-field potential patterns found in PAC of animals (Ulanovsky et al. 2003, 2004; von der Behrens et al. 2009). This notion is further supported by the fact that both scalp-recorded MLR and single-neuron spikes share a common firing time interval, responding to deviant stimuli at about 20 ms from stimulus onset (Pérez-González et al. 2005; von der Behrens et al. 2009).

Differences between deviant minus control conditions yielded no significant effects, neither for MLR, nor for LLR. In this regard, it should be argued that we were not able to delineate pure memory-based deviance detection processes from contributions of a differential state of refractoriness (Jacobsen et al. 2003). Despite the differential brain response to deviant tones and their homologous control tones is a well established finding in the EEG literature pointing to the memory comparison nature of the MMN (Schröger and Wolff 1996; Jacobsen et al. 2003; Slabu et al. 2010; Grimm et al. 2011, 2012), it is also acknowledged that the genuine comparison underestimates the MMN due to a higher refractory state of neurons responding to deviants compared with controls (Schröger 2007). The unobserved genuine MMNm effect could be related to the tendency of the control condition to "overcontrol", yielding less adaptation to control tones when compared with deviants (Kujala et al. 2007; Schröger 2007; Taaseh et al. 2011). It could also be related to the extremely fast presentation rate yielding amplitude-diminished transient responses (May and Tiitinen 2010). In agreement with the notion that the traditional MMN comparison yields a combination of memory comparison-based and memory comparison-unrelated deviance-related effects (Jacobsen and Schröger 2001; Taaseh et al. 2011), our analyses on the sources of N1m showed a clear distinction between the localization of pseudo-Z maps for the different conditions. Our results suggest that neural generators for infrequent tones deviating in frequency were located in different positions of each axis when compared with repeating tones. The difference between neural generators for N1m to deviant and standards in the anterior–posterior axis is consistent with previous MEG studies arguing for the involvement of separate change-specific neural populations underlying MMNm (Hari et al. 1992; Tiitinen et al. 1993; Korzyukov et al. 1999). The different location of N1m in response to deviant tones when compared with standard tones supports the existence of separate change-specific neural populations giving rise to the MMN/MMNm (Korzyukov et al. 1999; Näätänen et al. 2005).

The lack of controlled results poses interpretative limitations regarding the genuine nature of memory-based deviance detection reported here, since hypothesis based on combined contributions of adaptation and memory comparison cannot be ruled out. In the time range of the MLR, lack of deviant versus control effects might point to the existence of a stimulus detection mechanism that is not related to memory comparison, as suggested previously. In any case, evidence points to the areas underlying the aforementioned components being acting in a sequential fashion during auditory deviance detection.

To our knowledge, this is the first study that applied spatial filter source reconstruction to both early and late deviance-related responses. Results in the present study nicely delineated the sources of auditory deviance detection on right hemispheric auditory areas. The use of spatial filters to estimate auditory activity has been, from a theoretical and computational point of view, limited by the fact that high correlations between sources deteriorate the performance of beamformers by introducing distortion in time courses, spatial blurring of sources, and reduction in reconstructed source intensities (Van Veen et al. 1997; Sekihara et al. 2002). Yet, it has been shown that standard beamformers are able to adequately reconstruct the magnitude of simulated correlations up to a relatively high level of source correlation ($\mu = 0.7–0.8$) and low signal-to-noise ratios (Sekihara et al. 2002). Belardinelli et al. (2012) drew the same conclusion by assessing the impact of correlation on real data. Authors showed that phantom generated parallel dipoles in the 2 hemispheres (as might be the case in our data) separated by 3 cm were just slightly distorted in location and still recognizable when correlation levels reached 0.55, but clearly more blurred, with a high correlation of 0.95. The use of common filters and non-averaged data for the covariance matrix computation makes high correlation between hemispheres less likely to occur in our data (Brookes et al. 2010).

In summary, we provide evidence for 2 temporally and spatially separated neuronal sources indexing auditory deviance detection in the human auditory cortex. Our findings strongly support the presence of a neuronal assembly in the PAC located medially and anteriorly to the source generators of MMN. The existence of hierarchically different areas responding to auditory deviances is highly suggestive of a large distributed cortical network devoted to the processing of rare and unexpected auditory events.

Funding

This work was supported by the program Consolider-Ingenio 2010 (grant number CDS2007-00012), the National Program for Fundamental Research (reference number PSI2009-08063) of the Spanish Ministry of Science and Innovation, the 2009SGR11 grant of the Generalitat de Catalunya, the ICREA Academia Distinguished Professorship awarded to Carles Escera, and the FPI grant (BES-2010-030160) of the Spanish Ministry of Science and Innovation.

Notes

The authors thank Joachim Gross, Gavin Paterson, and Jan-Mathijs Schoffelen for their contribution in the development of the coregistration algorithm. *Conflict of Interest*: None declared.

References

Althen H, Grimm S, Escera E. 2011. Fast detection of unexpected sound intensity decrements as revealed by human evoked potentials. PLoS One. 6:e28522.

Antunes F, Nelken I, Covey E, Malmierca M. 2010. Stimulus-specific adaptation in the auditory thalamus of the anesthetized rat. PLoS One. 5:e14071.

Barlow HB. 1961. Possible principles underlying the transformation of sensory messages. In: Rosenblith WA, editor. Sensory communication. Cambridge (MA): MIT Press.

Belardinelli P, Ortiz E, Braun C. 2012. Source activity correlation effects on LCMV beamformers in a realistic measurement environment. Comput Math Methods Med. doi:10.1155/2012/190513.

Besl P, Mckay N. 1992. A method for registration of 3-d shapes. IEEE Trans Pattern Anal Machine Intell Mater. 14:239–256.

Borgmann C, Ross B, Draganova R, Pantev C. 2001. Human auditory middle latency responses: influence of stimulus type and intensity. Hear Res. 158:57–64.

Boutros NN, Torello MW, Barker BA, Tueting PA, Wu SC, Nasrallah HA. 1995. The P50 evoked potential component and mismatch detection in normal volunteers: implications for the study of sensory gating. Psychiatry Res. 57:83–88.

Brookes M, Zumer JM, Stevenson CM, Joanne RH, Barnes GB, Vrba J, Morris PG. 2010. Investigating spatial specificity and data averaging in MEG. Neuroimage. 49:525–538.

Brugge JF, Volkov IO, Garell PC, Reale RA, Howard MA. 2003. Functional connections between auditory cortex on Heschl's gyrus and on the lateral superior temporal gyrus in humans. J Neurophysiol. 90:3750–3763.

Chau W, McIntosh AR, Robinson SE, Schulz M, Pantev C. 2004. Improving permutation test power for group analysis of spatially filtered MEG data. Neuroimage. 23:983–996.

Cheyne D, Bakhtazad L, Gaetz W. 2006. Spatiotemporal mapping of cortical activity accompanying voluntary movements using an event-related beamforming approach. Hum Brain Mapp. 27:213–229.

Doeller C, Opitz B, Mecklinger A, Krick C, Reith W, Schröger E. 2003. Prefrontal cortex involvement in preattentive auditory deviance detection: neuroimaging and electrophysiological evidence. Neuroimage. 20:1270–1282.

Escera C, Alho K, Winkler I, Näätänen R. 1998. Neural mechanisms of involuntary attention to acoustic novelty and change. J Cogn Neurosci. 10:590–604.

Escera C, Corral MJ. 2007. Role of mismatch negativity and novelty-P3 in involuntary auditory attention. Int J Psychophysiol. 21:251.

Friston K. 2005. A theory of cortical responses. Philos Trans R Soc Lond B Biol Sci. 360:815–836.

Galaburda A, Pandya D. 1983. The intrinsic architectonic and connectional organization of the superior temporal region of the rhesus-monkey. J Comp Neurol. 221:169–184.

Garrido M, Kilner J, Kiebel S, Friston K. 2009. Dynamic causal modeling of the response to frequency deviants. J Neurophysiol. 101:2620–2631.

Giard MH, Perrin F, Pernier J, Bouchet P. 1990. Brain generators implicated in the processing of auditory stimulus deviance: a topographic event-related potential study. Psychophysiology. 27:627–640.

Grimm S, Escera C. 2011. Auditory deviance detection revisited: evidence for a hierarchical novelty system. Int J Psychophysiol. doi:10.1016/j.ijpsycho.2011.05.012.

Grimm S, Escera C, Slabu L, Costa-Faidella J. 2011. Electrophysiological evidence for the hierarchical organization of auditory change detection in the human brain. Psychophysiology. 48:377–384.

Grimm S, Recasens M, Althen H, Escera C. 2012. Ultrafast tracking of sound location changes as revealed by human auditory evoked potentials. Biol Psychol. 89:232–239.

Grimm S, Roeber U, Trujillo-Barreto N, Schröger E. 2006. Mechanisms for detecting auditory temporal and spectral deviations operate over similar time windows but are divided differently between the two hemispheres. Neuroimage. 32:275–282.

Gutschalk A, Mase R, Roth R, Ille N, Rupp A, Hahnel S, Picton TW, Scherg M. 1999. Deconvolution of 40 Hz steady-state fields reveals two overlapping source activities of the human auditory cortex. Clin Neurophysiol. 110:856–868.
Hari R, Rif J, Tiihonen J, Sams M. 1992. Neuromagnetic mismatch fields to single and paired tones. Electroencephalogr Clin Neurophysiol. 82:152–154.
Herdman AT, Pang EW, Ressel V, Gaetz W, Cheyne D. 2007. Task-related modulation of early cortical responses during language production: an event-related synthetic aperture magnetometry study. Cereb Cortex. 17:2536–2543.
Herdman AT, Wollbrink A, Chau W, Ishii R, Ross B, Pantev C. 2003. Determination of activation areas in the human auditory cortex by means of synthetic aperture magnetometry. Neuroimage. 20:995–1005.
Howard MA, Volkov IO, Mirsky R, Garell PC, Noh MD, Granner M, Damasio H, Steinschneider M, Reale RA, Hind JE et al. 2000. Auditory cortex on the human posterior superior temporal gyrus. J Comp Neurol. 416:79–92.
Inui K, Okamoto H, Miki K, Gunji A, Kakigi R. 2006. Serial and parallel processing in the human auditory cortex: a magnetoencephalographic study. Cereb Cortex. 16:18–30.
Jacobsen T, Schröger E. 2001. Is there pre-attentive memory-based comparison of pitch? Psychophysiology. 38:723–727.
Jacobsen T, Schröger E, Horenkamp T, Winkler I. 2003. Mismatch negativity to pitch change: varied stimulus proportions in controlling effects of neural refractoriness on human auditory event-related brain potentials. Neurosci Lett. 344:79–82.
Jamison HL, Watkins KE, Bishop DVM, Matthews PM. 2006. Hemispheric specialization for processing auditory nonspeech stimuli. Cereb Cortex. 16:1266–1275.
Jung TP, Makeig S, Westerfield M, Townsend J, Courchesne E, Sejnowski TJ. 2000. Removal of eye activity artifacts from visual event-related potentials in normal and clinical subjects. Clin Neurophysiol. 111:1745–1758.
Kaas J, Hackett T. 1998. Subdivisions of auditory cortex and levels of processing in primates. Audiol Neurootol. 3:73–85.
Kaas J, Hackett T, Tramo M. 1999. Auditory processing in primate cerebral cortex. Curr Opin Neurobiol. 9:164–170.
Kiebel S, Daunizeau J, Friston K. 2008. A hierarchy of time-scales and the brain. PLoS Comput Biol. 4:e1000209.
Korzyukov O, Alho K, Kujala A, Valentina G, Ilmoniemi R, Virtanen J, Kropotov J, Näätänen R. 1999. Electromagnetic responses of the human auditory cortex generated by sensory-memory based processing of tone-frequency changes. Neurosci Lett. 276:169–172.
Kujala T, Tervaniemi M, Schröger E. 2007. The mismatch negativity in cognitive and clinical neuroscience: theoretical and methodological considerations. Biol Psychol. 74:1–19.
Kumar S, Stephan KE, Warren JD, Friston KJ, Griffiths TD. 2007. Hierarchical processing of auditory objects in humans. PLoS Comput Biol. 3:e100.
Lerner Y, Honey C, Silbert L, Hasson U. 2011. Topographic mapping of a hierarchy of temporal receptive windows using a narrated story. J Neurosci. 31:2906–2915.
Leung S, Cornella M, Grimm S, Escera C. 2012. Is fast auditory change detection feature-specific? An electrophysiological study in humans. Psychophysiology. 49:933–942.
Liegeois-Chauvel C, Giraud K, Badier J, Marquis P, Chauvel P. 2001. Intracerebral evoked potentials in pitch perception reveal a functional asymmetry of the human auditory cortex. Ann N Y Acad Sci. 930:117–132.
Liegeois-Chauvel C, Musolino A, Badier JM, Marquis P, Chauvel P. 1994. Evoked potentials recorded from the auditory cortex in man: evaluation and topography of the middle latency components. Electroencephalogr Clin Neurophysiol. 92:204–214.
Liegeois-Chauvel C, Musolino A, Chauvel P. 1991. Localization of the primary auditory area in man. Brain. 114:139–151.
Lütkenhöner B, Krumbholz K, Lammertmann C, Seither-Preisler A, Steinstrater O, Patterson RD. 2003. Localization of primary auditory cortex in humans by magnetoencephalography. Neuroimage. 18:58–66.
Maess B, Jacobsen T, Schröger E, Friederici AD. 2007. Localizing pre-attentive auditory memory-based comparison: magnetic mismatch negativity to pitch change. Neuroimage. 37:561–571.
Malmierca MS, Cristaudo S, Pérez-González D, Covey E. 2009. Stimulus-specific adaptation in the inferior colliculus of the anesthetized rat. J Neurosci. 29:5483–5493.
Maris E, Oostenveld R. 2007. Nonparametric statistical testing of EEG- and MEG-data. J Neurosci Methods. 164:177–190.
Mathiak K, Rapp A, Kircher TT, Grodd W, Hertrich I, Weiskopf N, Lutzenberger W, Ackermann H. 2002. Mismatch responses to randomized gradient switching noise as reflected by fMRI and whole-head magnetoencephalography. Hum Brain Mapp. 16:190–195.
May PH, Tiitinen H. 2010. Mismatch negativity (MMN), the deviance-elicited auditory deflection, explained. Psychophysiology. 47:66–122.
Merzenich M, Brugge J. 1973. Representation of cochlear partition on superior temporal plane of macaque monkey. Brain Res. 50:275–296.
Morosan P, Rademacher J, Schleicher A, Amunts K, Schormann T, Zilles K. 2001. Human primary auditory cortex: cytoarchitectonic subdivisions and mapping into a spatial reference system. Neuroimage. 13:684–701.
Morosan P, Schleicher A, Amunts K, Zilles K. 2005. Multimodal architectonic mapping of human superior temporal gyrus. Anat Embryol. 210:401–406.
Näätänen R, Jacobsen T, Winkler I. 2005. Memory-based or afferent processes in mismatch negativity (MMN): a review of the evidence. Psychophysiology. 42:25–32.
Näätänen R, Paavilainen P, Rinne T, Alho K. 2007. The mismatch negativity (MMN) in basic research of central auditory processing: a review. Clin Neurophysiol. 118:2544–2590.
Nelken I, Ulanovsky N. 2007. Mismatch negativity and stimulus-specific adaptation in animal models. Int J Psychophysiol. 21:214.
Nolte G. 2003. The magnetic lead field theorem in the quasi-static approximation and its use for magnetoencephalography forward calculation in realistic volume conductors. Phys Med Biol. 48:3637–3652.
Oostenveld R, Fries P, Maris E, Schoffelen JM. 2011. FieldTrip: open source software for advanced analysis of MEG, EEG, and invasive electrophysiological data. Comput Intell Neurosci. 2011:156869.
Opitz B, Mecklinger A, von Cramon D, Kruggel F. 1999. Combining electrophysiological and hemodynamic measures of the auditory oddball. Psychophysiology. 36:142–147.
Opitz B, Rinne T, Mecklinger A, von Cramon D, Schröger E. 2002. Differential contribution of frontal and temporal cortices to auditory change detection: fMRI and ERP results. Neuroimage. 15:167–174.
Opitz B, Schröger E, von Cramon D. 2005. Sensory and cognitive mechanisms for preattentive change detection in auditory cortex. Eur J Neurosci. 21:531–535.
Paavilainen P, Alho K, Reinikainen K, Sams M, Näätänen R. 1991. Right-hemisphere dominance of different mismatch negativities. Electroencephalogr Clin Neurophysiol. 78:466–479.
Pantev C, Bertrand O, Eulitz C, Verkindt C, Hampson S, Schuierer G, Elbert T. 1995. Specific tonotopic organizations of different areas of the human auditory cortex revealed by simultaneous magnetic and electric recordings. Electroencephalogr Clin Neurophysiol. 94:26–40.
Pérez-González D, Malmierca MS, Covey E. 2005. Novelty detector neurons in the mammalian auditory midbrain. Eur J Neurosci. 22:2879–2885.
Rademacher J, Morosan P, Schormann T, Schleicher A, Werner C, Freund H. 2001. Probabilistic mapping and volume measurement of human primary auditory cortex. Neuroimage. 13:669–683.
Rauschecker J. 1998. Cortical processing of complex sounds. Curr Opin Neurobiol. 8:516–521.
Rinne T, Degerman A, Alho K. 2005. Superior temporal and inferior frontal cortices are activated by infrequent sound duration decrements: an fMRI study. Neuroimage. 26:66–72.

Schall U, Johnston P, Todd J, Ward P, Michie P. 2003. Functional neuroanatomy of auditory mismatch processing: an event-related fMRI study of duration-deviant oddballs. Neuroimage. 20:729–736.
Scherg M, Vajsar J, Picton TW. 1989. A source analysis of the late human auditory evoked potentials. J Cogn Neurosci. 1:336–355.
Scherg M, von Cramon D. 1990. Dipole source potentials of the auditory cortex in normal subjects and in patients with temporal lobe lesions. Adv Audiol. 6:165–193.
Schönwiesner M, Novitski N, Pakarinen S, Carlson S, Tervaniemi M, Näätänen R. 2007. Heschl's gyrus, posterior superior temporal gyrus, and mid-ventrolateral prefrontal cortex have different roles in the detection of acoustic changes. J Neurophysiol. 97:2075–2082.
Schröger E. 2007. Mismatch negativity: a microphone into the auditory memory. Int J Psychophysiol. 21:138–146.
Schröger E, Wolff C. 1996. Mismatch response of the human brain to changes in sound location. Neuroreport. 7:3005–3008.
Scott S, Johnsrude I. 2003. The neuroanatomical and functional organization of speech perception. Trends Neurosci. 26:100–107.
Sekihara K, Nagarajan SS, Poeppel D, Marantz A. 2002. Performance of an MEG adaptive-beamformer technique in the presence of correlated neural activities: effects on signal intensity and time-course estimates. IEEE Trans Biomed Eng. 49:1534–1546.
Singh KD, Barnes GR, Hillebrand A. 2003. Group imaging of task-related changes in cortical synchronisation using nonparametric permutation testing. Neuroimage. 19:1589–1601.
Slabu L, Escera C, Grimm S, Costa-Faidella J. 2010. Early change detection in humans as revealed by auditory brainstem and middle-latency evoked potentials. Eur J Neurosci. 32:859–865.
Slabu L, Grimm S, Escera C. 2012. Novelty detection in the human auditory brainstem. J Neurosci. 32:1447–1452.
Sonnadara RR, Alain C, Trainor LJ. 2006. Occasional changes in sound location enhance middle latency evoked responses. Brain Res. 1076:187–192.
Taaseh N, Yaron A, Nelken I. 2011. Stimulus-specific adaptation and deviance detection in the rat auditory cortex. PLoS One. 6:e23369.
Tervaniemi M, Medvedev S, Alho K, Pakhomov S, Roudas M, van Zuijen T. 2000. Lateralized automatic auditory processing of phonetic versus musical information: a PET study. Hum Brain Mapp. 10:74–79.
Tervaniemi M, Szameitat A, Kruck S, Schroger E, Alter K, De Baene W. 2006. From air oscillations to music and speech: functional magnetic resonance imaging evidence for fine-tuned neural networks in audition. J Neurosci. 26:8647–8652.
Tiitinen H, Alho K, Huotilainen M, Ilmoniemi RJ, Simola J, Näätänen R. 1993. Tonotopic auditory cortex and the magnetoencephalographic (MEG) equivalent of the mismatch negativity. Psychophysiology. 30:537–540.
Ulanovsky N, Las L, Farkas D, Nelken I. 2004. Multiple time scales of adaptation in auditory cortex neurons. J Neurosci. 24:10440–10453.
Ulanovsky N, Las L, Nelken I. 2003. Processing of low-probability sounds by cortical neurons. Nat Neurosci. 6:391–398.
Van Veen B, van Drongelen W, Yuchtman M, Suzuki A. 1997. Localization of brain electrical activity via linearly constrained minimum variance spatial filtering. IEEE Trans Biomed Eng. 44:867–880.
von der Behrens W, Bauerle P, Kossl M, Gaese B. 2009. Correlating stimulus-specific adaptation of cortical neurons and local field potentials in the awake rat. J Neurosci. 29:13837–13849.
Wacongne C, Changeux JP, Dehaene S. 2012. A neuronal model of predictive coding accounting for the mismatch negativity. J Neurosci. 32:3665–3678.
Wessinger C, VanMeter J, Tian B, Van Lare J, Pekar J, Rauschecker J. 2001. Hierarchical organization of the human auditory cortex revealed by functional magnetic resonance imaging. J Cogn Neurosci. 13:1–7.
Yoshiura T, Ueno S, Iramina K, Masuda K. 1995. Source localization of middle latency auditory evoked magnetic fields. Brain Res. 703:139–144.
Yvert B, Crouzeix A, Bertrand O, Seither-Preisler A, Pantev C. 2001. Multiple supratemporal sources of magnetic and electric auditory evoked middle latency components in humans. Cereb Cortex. 11:411–423.
Yvert B, Fischer C, Bertrand O, Pernier J. 2005. Localization of human supratemporal auditory areas from intracerebral auditory evoked potentials using distributed source models. Neuroimage. 28:140–153.
Zatorre R, Belin P. 2001. Spectral and temporal processing in human auditory cortex. Cereb Cortex. 11:946–953.

STUDY II

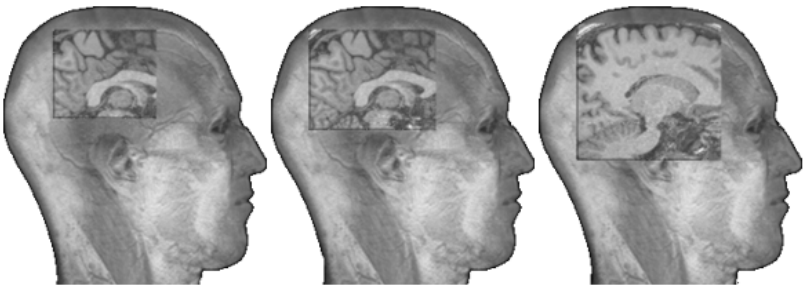

Encoding of nested levels of acoustic regularity in hierarchically organized areas of the human auditory cortex

Encoding of Nested Levels of Acoustic Regularity in Hierarchically Organized Areas of the Human Auditory Cortex

Marc Recasens,[1,2] Sabine Grimm,[1,2] Andreas Wollbrink,[3] Christo Pantev,[3] and Carles Escera[1,2]*

[1]*Institute for Brain, Cognition and Behavior (IR3C), University of Barcelona, 08035 Catalonia, Spain*
[2]*Cognitive Neuroscience Research Group, Department of Psychiatry and Clinical Psychobiology, University of Barcelona, 08035 Catalonia, Spain*
[3]*Institute for Biomagnetism and Biosignalanalysis, University of Münster, 48149 Münster, Germany*

Abstract: Our auditory system is able to encode acoustic regularity of growing levels of complexity to model and predict incoming events. Recent evidence suggests that early indices of deviance detection in the time range of the middle-latency responses (MLR) precede the mismatch negativity (MMN), a well-established error response associated with deviance detection. While studies suggest that only the MMN, but not early deviance-related MLR, underlie complex regularity levels, it is not clear whether these two mechanisms interplay during scene analysis by encoding nested levels of acoustic regularity, and whether neuronal sources underlying local and global deviations are hierarchically organized. We registered magnetoencephalographic evoked fields to rapidly presented four-tone local sequences containing a frequency change. Temporally integrated local events, in turn, defined global regularities, which were infrequently violated by a tone repetition. A global magnetic mismatch negativity (MMNm) was obtained at 140–220 ms when breaking the global regularity, but no deviance-related effects were shown in early latencies. Conversely, Nbm (45–55 ms) and Pbm (60–75 ms) deflections of the MLR, and an earlier MMNm response at 120–160 ms, responded to local violations. Distinct neuronal generators in the auditory cortex underlay the processing of local and global regularity violations, suggesting that nested levels of complexity of auditory object representations are represented in separated cortical areas. Our results suggest that the different processing stages and anatomical areas involved in the encoding of auditory representations, and the subsequent detection of its violations, are hierarchically organized in the human auditory cortex. *Hum Brain Mapp 00:000–000, 2014.* © **2014 Wiley Periodicals, Inc.**

Key words: mismatch negativity; middle-latency responses; deviance detection; auditory cortex; magnetoencephalographic; beamforming

Contract grant sponsor: Spanish Ministry of Economy and Knowledge; Contract grant number: PSI2012-37174; Contract grant sponsor: Catalan Government; Contract grant number: SGR2009-11; Contract grant sponsor: ICREA Academia Distinguished Professorship (to C. E.)

*Correspondence to: Carles Escera, Cognitive Neuroscience Research Group, Department of Psychiatry and Clinical Psychobiology, University of Barcelona, P. Vall d'Hebron 171, 08035-Barcelona, Catalonia-Spain. E-mail: cescera@ub.edu

Received for publication 4 December 2013; Revised 29 April 2014; Accepted 28 June 2014.

DOI: 10.1002/hbm.22582
Published online 00 Month 2014 in Wiley Online Library (wileyonlinelibrary.com).

INTRODUCTION

Sounds do not occur in isolation but are generally integrated into more complex patterns, as occurs in speech, animal vocalizations, or even in common sounds like our alarm ringtone. In such cases, the temporal integration of the ongoing sensory input plays an important role of organizing the acoustic background and, thus, guiding our perception [Bregman, 1990; Winkler et al., 2009]. Modeling our auditory scene in search for regularities is essential not only to organize our perceptual background into meaningful percepts but also to predict future sensory events [Friston, 2005; Winkler et al., 2009]. Hence, regularity-violation signals like the mismatch negativity (MMN), an auditory evoked potential to unexpected stimuli [Näätänen et al., 1978], serve as an appropriate tool to investigate the mechanism underlying perceptual organization and predictive processing in the human brain [Bendixen et al., 2012]. The MMN, generated in supratemporal areas between 100 and 250 ms after stimulus onset [Näätänen et al., 2007], indexes sudden changes in previously encoded regularities and is an indirect marker of the auditory memory-trace formation [Haenschel et al., 2005].

Remarkably, recent human studies have revealed the existence of earlier indices of deviance detection and regularity encoding preceding the MMN. Slabu et al. [2010] and Grimm et al. [2011] showed that different deflections of the middle-latency response (MLR), peaking between 10 and 50 ms after stimulus onset, were significantly enhanced in response to simple deviations as compared to control stimuli, suggesting that dynamic modeling of the acoustic regularity rather than adaptation underlies deviance detection well before MMN. In parallel, a large group of animal findings support the existence of very early indices of deviance detection in the mammal brain [Ayala et al., 2013; Taaseh et al., 2011]. Single-unit and multiunit recordings, as well as local field potentials, showed that particular auditory neurons display stimulus-specific adaptation (SSA), an attenuated response to repetitive stimuli, just 20 ms after sound onset [Malmierca et al., 2009; Ulanovsky et al., 2003]. Although SSA has been considered a possible single-neuron correlate of the MMN [Nelken and Ulanovsky, 2007], differences in the underlying pharmacological properties [Farley et al., 2010], the different anatomical generators involved [Malmierca et al. 2009], and their time scale, make MLR a better correlate of the animal SSA. Yaron et al. [2012] showed that neurons in the primary auditory cortex of the cat displayed a reduced firing when stimuli were presented in regular sequences, in contrast to typically random oddball sequences. Results showed that neural responses were sensitive to the structure of sound sequences; however, the decrease in neural discharge was present both in repeated and deviated stimuli, leaving open the question of whether early levels of the auditory pathway can encode complex or pattern-like regularities, and detect subsequent deviations. In humans, Cornella et al. [2012] showed that simple sound features like location are rapidly encoded at the level of MLR, and subsequently in the time range of the long-latency responses (LLR) by the MMN [Grimm et al., 2012; Sonnadara et al., 2006]. Notably, rare frequency repetitions in a sound alternation sequence were only detected at the level of MMN but not in earlier latencies. Similarly, results by Althen et al. [2013] showed that simple sound regularities (i.e., frequency) were processed earlier than complex regularities (i.e., frequency-location combinations). Together, the above mentioned findings suggest that regularity encoding is a ubiquitous property of the mammal auditory system that may be organized in ascending levels of complexity [Escera and Malmierca, 2014; Grimm and Escera, 2012]. However, two important points are still unresolved: First, previous human studies did not allow for testing whether deviance-related MLR and MMN mechanisms interplay when processing nested levels of regularity of growing complexity [Althen et al., 2013; Cornella et al., 2012], as occur in most real-life acoustic events. Second, it is not clear whether these mechanisms are supported by anatomically distinct areas and whether these sources show a hierarchical arrangement.

Previous studies have shown distinct MMN generators for simple rules as compared to more complex types of regularity. Magnetic mismatch negativity (MMNm) sources to deviations in feature conjunctions (i.e., pitch-location) have been located in more anterior portions of the auditory cortex when compared to sources derived from simple frequency changes [Takegata et al., 2000]. Similar results were obtained for abstract, but still local, changes in frequency direction [Korzyukov et al., 2003]. Alho et al. [1996] showed that equivalent current dipoles in response to changes in a serial tone pattern were located 1 cm medially as compared to sources of the MMNm elicited by simple frequency changes. Although accurate localization of the MMNm to complex changes might differ across studies depending on the stimuli used, the complexity of the regularity at play, or the source localization techniques used, overall findings suggest that the neural circuits underlying deviance detection vary as a function of the perceptual context [Alain et al. 1999a]. On this line, Sussman et al. [1998] showed that the MMN was abolished for predictable occurrences of a frequency change when tones in a sequence were presented at a fast pace. Their results suggest that sound organization changed from a local single-repeating tone rule to a global tone-repeating pattern. Despite that previous studies have elucidated the neuronal sources of both deviance-related MLR and MMNm [Recasens et al., 2014], as well as the generators underlying local and global deviations [Bekinschtein et al., 2009; Wacongne et al., 2011], this is, to our knowledge, the first attempt to localize multiple neuronal generators underlying local and global deviations in very early latencies during an unattended condition task.

In this magnetoencephalographic (MEG) study, we used similar sound structures to Yaron et al. [2012] and Sussman et al. [1998] with the difference that pattern

deviations (an unexpected tone repetition) were included in addition to local-rule deviations (a frequency change) [see also: Bekinschtein et al., 2009; Herholz et al., 2009, 2011; Wacongne et al., 2011]; therefore, putting the stress on both local (based on relations between temporary adjacent stimuli) and global (based on the relation between temporary nonadjacent sounds) types of regularity. We aimed to highlight the different roles of the early and late mechanisms in the organization of the auditory scene by showing that the neuronal generators underlying the representation of local and global invariance are mapped in distinct areas of the human brain and in distinct time scales, thus providing support for the notion that the human auditory system is organized in a hierarchical fashion. We expected to obtain an MMNm response to global regularity violations, thus indexing pattern-object representation, and early areas underlying MLR to respond to violations of local rules only; thus showing that beyond the acoustic feature at play, different auditory mechanisms assist the representation of local and global acoustic regularities. At the anatomical level, we hypothesized that multiple sources in the vicinity of the primary auditory cortex allocated the neuronal generators of local deviance detection as obtained in different time ranges [Recasens et al., 2014]. Moreover, we predicted that a clear anatomical separation would exist between sources underlying local and global acoustic regularity processing. We expected neuronal generators underlying global deviations to be located in hierarchically superior areas than those underlying local regularity violations.

MATERIALS AND METHODS

Participants

Fifteen healthy subjects (eight female, age: 27.4 ± 3, mean ± SD) participated in the experiment. All subjects had normal hearing as evaluated by clinical audiometry at the beginning of each MEG session for each ear. All subjects provided written consent prior to their participation in the study and received monetary compensation for it. The experimental protocol was approved by the ethics committee of the Medical Faculty of the University of Münster and the study was conducted according to the Declaration of Helsinki.

Stimuli and Procedure

Stimuli consisted of 50-ms pure tones (10 ms rise and decay time) delivered binaurally at 60 dB SL (Sensation level) via 90 cm long MEG-compatible plastic tubes (Etymotic Research). Two close sinusoidal tones, 988 Hz ("A" tone) or 880 Hz ("B" tone), were presented isochronously at 200 ms SOA (stimulus-onset-asynchrony) within repeating patterns of either four tones randomly occurring at a probability of 0.8 (AAA**B**: Standard patterns) or five tones

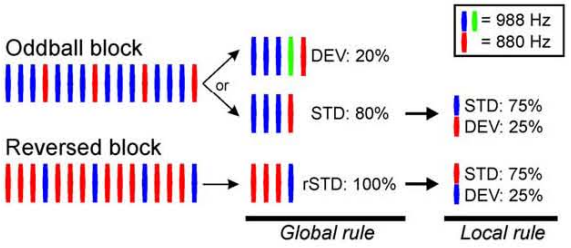

Figure 1.

Experimental design. Oddball and reversed blocks were composed of four-tone repeating sequences (200 ms SOA). Frequencies, and the role of deviant and standard, were interchanged in reversed blocks (left). Global rules (middle) were composed by sequences containing three repetitions and one pure tone deviation when standard (STD), and four repetitions and one pure tone deviation when deviants (DEV). The global deviation was defined by the fourth 988 Hz pure tone. Sequences in the reversed block contained standard global rules only (rSTD). Local rules (right) were defined by the pure tones within global sequences (standards only). Three standard repetitions (STD) defined the local rule, violated by a frequency change (DEV).

occurring at a probability of 0.2 (AAA**a**B: Deviant patterns). The interval between global sequences was also kept at 200 ms, thus, leading to a continuously ongoing tone presentation. A fast presentation rate was used to facilitate automatic grouping of nested local objects under global patterns [Sussman et al., 1998; Sussman and Gumenyuk, 2005]. Additionally, a reversed block consisting of frequency-reversed standard patterns (BBB**A**) was presented to contrast against physically identical tones (Fig. 1). This prevented frequency-specific effects to mask real change-dependent effects, particularly for MLR. The global condition was assessed by comparing the activity from the rare fourth **a**-tone against the previous A-tone. We assessed the local condition by comparing the activity from local deviants, within standard patterns only, against physically identical standard tones preceding the frequency change. Thus, two local conditions, one per each frequency, were obtained (A vs. reversed-A; and B vs. reversed-B). In total, 660 rare repetitions of the **a**-tone (global deviants), 1992 B-tones (local deviants) in the oddball block, and 1105 A-tones in the reversed block (reversed local deviants) were delivered. Local deviants appearing after a global deviant were excluded from the analysis. The presentation of the experimental sequence was split in four pseudorandomized runs (consisting of three oddball blocks and one reversed block). Stimuli were presented using Presentation (Neurobehavioral Systems).

Data Acquisition and Analysis

Evoked magnetic fields were recorded with a 275-sensor whole-head system (OMEGA 2005, CTF Systems) in a magnetically shielded room. Data were acquired continuously

during each run with a sampling rate of 1200 Hz. Subjects were seated upright and were asked to relax, ignore acoustic stimulation and focus on a muted self-selected movie with no subtitles. The subject's alertness and compliance were verified by video monitoring. Recording lasted for 1 h approximately and subjects were not allowed to move their head between runs. No subjects were discarded due to head movement across runs (maximum head displacement throughout the session did not exceed 0.7 cm along the inferior–superior axis).

Analyses were carried out using the FieldTrip toolbox [Oostenveld et al., 2011] under Matlab 2012 (The MathWorks Inc.). For LLR analysis, datasets were epoched in intervals of 400 ms (100 ms baseline). Epoch intervals of 150 ms (50 ms baseline) were cut for MLR analysis. An offline band-pass filter (2-pass Butterworth, filter order of 4) was applied from 1 to 30 Hz for LLR, and from 15 to 150 Hz for MLR. Additionally, a DFT filter with 600 ms of sample padding was used to clean the data from the 50 Hz component and its harmonics. Epochs were baseline corrected using the whole baseline interval. On a separate analysis, the strongest components corresponding to cardiac and ocular artifacts were identified and rejected from the above mentioned dataset by means of independent component analysis, using the runica algorithm [Makeig et al., 1997]. To carry out independent component analysis, 100 samples (1 s length) from each run were downsampled and filtered between 1 and 150 Hz. A mean of 3.3 independent components per subject were rejected manually by visual inspection on the basis of their scalp topography and continuous activity [Jung et al., 2000]. Subsequent epochs containing channels having a signal amplitude range larger than 2.5 pT were considered artifact-contaminated and excluded from the averaging. To correct for intraindividual head position in the MEG sensor array across runs, artifact-free data were interpolated to a common sensor array template using a minimum-norm projection method [Knösche, 2002], and subsequently concatenated across runs. Remaining artifact-free epochs were averaged separately for each condition (global, local, and local-reversed). All subsequent analyses were performed separately for LLR and MLR.

Differences between deviant and standard events in each condition and latency were assessed nonparametrically using cluster-based permutation *t*-tests [for more details on the method see: Maris and Oostenveld, 2007]. This test controls for type I error rate in situations involving multiple comparisons (in our case, due to many comparisons of time-point by sensor). Moreover, this method requires no a priori hypotheses about the time intervals and distribution of the expected differences. Thus, we used this test in the sensor-space to determine, in an unbiased way, the presence of effects and the time windows where brain responses statistically differed between stimuli in each condition. Time windows showing significant effects were, then, used to reconstruct the activity in the source-space.

A planar gradient transformation of the axial gradiometer-recorded data were calculated by taking, for each sensor, the average of the absolute values of the first spatial derivatives in two orthogonal directions [Bastiaansen and Knösche, 2000]. Planar transformation simplified the interpretation of sensor-level results as it places a single field extrema right above the source [Hämäläinen et al., 1993]. Nonparametric statistical testing was applied on the transformed data to statistically compare deviant and standard stimuli in all possible conditions and latencies. Cluster-based permutation *t*-tests considered two dimensions, thus we assessed the existence of significant clusters of differential activity along the temporal (time-bin clusters) and spatial dimension (sensor clusters). For LLR, deviant and standard amplitude differences were assessed between 40 and 300 ms in steps of 20 ms. For MLR, a time window between 20 and 100 ms with steps of 5 ms was evaluated. A minimum of three neighboring significant sensors was required to form a significant cluster. Distance at which channels were considered neighbors was set in such a way that each channel had an average of 7.4 neighbors. Deviant and standard stimuli from the local and the local-reversed conditions were collapsed together prior to statistical analysis. A total amount of 1000 random permutations of the observed data were drawn and the critical alpha level for dependent-samples *t*-test (two-tailed, corrected) comparisons was set to 0.05. Only those conditions showing statistically significant differences in the sensor-space between deviant and standard stimuli in each time range were subsequently analyzed in source-space.

To obtain a more detailed localization, sources of evoked brain activity for standards and deviants were modeled using a time-domain spatial filter, the linearly constrained minimum variance (LCMV) beamformer [Van Veen et al., 1997]. Based on the segmentation of the brain surface of each individual's MRI, we obtained a semirealistic single-shell head model for each participant. Each brain volume had 5 mm resolution (23869 voxels inside the head). The leadfield matrix was computed for each grid voxel on the basis of a quasistatic approximation of the brain surface as a single shell [Nolte, 2003]. The weakest orthogonal component at each voxel of the leadfield matrix was excluded. To model the sources underlying each condition, we first computed common filter weights for LLR and MLR based on a balanced combination of deviant and standard responses in each condition (non-transformed data), thus ensuring that differences in source activity were not related to spatial filter differences. Therefore, the covariance matrix was computed on the average of 3000 trials derived from that combination. Power regularization was set to 1% of the mean power to maximize the sensitivity of the beamformer to focal sources. Subsequently, we projected nontransformed sensor-level data in each condition through the common spatial weights. The LCMV beamformer was independently

applied only on those statistically significant time intervals derived from the sensor-space analysis: the local MMNm (120–160 ms), global MMNm (160–200 ms), local Nbm (45–55), and local Pbm (60–75). Resulting source-space deviant and standard trials were averaged separately. Finally, source strengths were normalized using the neural activity index (NAI), where the estimated power at each grid point is divided by an estimate of the noise. Individual Pseudo-Z or NAI values were overlaid on the corresponding anatomical MRI. Anatomical and functional data were spatially normalized using SPM8 (Statistical Parametric Mapping; http://www.fil.ion.ucl.ac.uk/spm) to the MNI (Montreal Neurological Institute) template. Detailed determination of localization differences between the four deviance-related responses of interest (global MMNm, local MMNm, local Nbm, and local Pbm) was performed by means of analysis of variance (ANOVA) including the factor condition and hemisphere, independently for each of the three axes (*X*, *Y*, and *Z*). Individual single voxels showing the largest pseudo-Z values were retrieved from the beamformer source reconstructions thresholded at half-maximum. Additionally and as a measure of reliability, we repeated the same analysis using the 50 highest individual peak voxels (Top50) instead of the individual best voxel. Medial-lateral values were transformed into absolute values to assess hemispheric differences. For all statistical analyses, results were considered significant when $P < 0.05$. All post hoc comparisons were carried out using the Bonferroni correction for multiple comparisons. The Greenhouse–Geisser (G–G) correction was applied if the assumption of sphericity was violated. Effect sizes were reported for analyses of variance (partial eta squared, η_p^2) and post hoc comparisons (Cohen's *d*).

RESULTS

No statistical differences at any sensor were found between the local and the local-reversed difference waveforms (deviant minus standard: **A** vs. A = **B** vs. B), neither for LLR nor for MLR. Therefore, both conditions were merged and analyzed as a unique condition. In the LLR time range, local deviant and standard sounds at 120–140 ms elicited maximum activity on lateral and central scalp sensors (Fig. 2A, left and middle). Figure 2B, showing the time course of the root mean square (RMS) for deviant, standard, and their difference waveform, illustrates that local deviations elicited a statistically significant response between 120 and 160 ms after change onset ($P < 0.05$) when compared to local standards. Even though activity was higher on right hemisphere sensors, significant clusters of sensors emerged on both hemispheres (Fig. 2A, right). A smaller cluster of channels showing greater activity for deviant sounds as compared to standards emerged on right frontal areas between 240 and 260 ms. No clusters were found where standard stimuli elicited higher activity than deviant stimuli. In the LLR time range, infrequent repetitions of the standard tone, representing a global violation, elicited strong bilateral responses on lateral and central sensors between 160 and 180 ms (Fig. 3A, left and middle). Despite that maximum response activity for deviant and standard stimuli occurred between 160 and 180 ms, clusters of sensors showing significant ($P < 0.05$) global MMNm effects spanned from 140 to 220 ms after sound onset (Fig. 3B). Significant clusters were located bilaterally (Fig. 3A, right). No clusters were found where standard stimuli elicited higher activity than deviant stimuli. Additional clusters showing an enhanced activity ($P < 0.05$) for deviant stimuli were found between 240 and 280 ms, probably representing an enhanced response to local changes occurring after the rare global deviant within a deviant pattern. The same conditions were assessed throughout the MLR time range to identify whether early mechanisms of regularity encoding and change detection were functionally comparable to later mechanisms. Auditory tones elicited strong neuromagnetic activity over the scalp during the time intervals corresponding to the peaks of the typical MRL deflections: Nam (24.3 ms), Pam (32.6 ms), Nbm (46.4), and Pbm (62.5). For the local condition, statistically significant differences between deviant and standard tones emerged during the time course of the Nbm and Pbm waveforms, between 45 and 55 ms, and 60 and 75 ms after change onset, respectively (Fig. 4B). Both deviant and standard stimuli in the Nbm and Pbm time intervals showed maximum activity distributed bilaterally over lateral and central sensors (Fig. 4A, left and middle columns). For the Nbm component, clusters showing a significant differential activity ($P < 0.05$) appeared over left hemisphere sensors only (Fig. 4A, upper right). During the time interval of the Pbm component, significant clusters ($P < 0.05$) emerged on both hemispheres, (Fig. 4A, lower right). No clusters were found where standard stimuli elicited higher activity than deviant stimuli. Additional significant clusters ($P < 0.05$) emerged between 85 ms after change onset till the end of the epoch, probably reflecting an enhanced response to local deviants, as found in the LLR time range. For the global condition, auditory stimuli elicited strong evoked activity over the same time intervals as for local condition (Fig. 5A, left and middle columns); however, no significant differences were found between deviant and standard tones during the time course of MLR (Fig. 5A right column, and 5B).

Beamformer differential activity between local deviant and standard tones in the LLR time range (between 120 and 160 ms) yielded main sources of the local MMNm over anterior supratemporal cortices bilaterally (Fig. 6, first row). The peak voxel, showing the highest pseudo-Z value, on the right hemisphere was located on the anterior part of the superior temporal gyrus (STG, 64 −16 6), whereas a weaker peak activity on the left hemisphere overlapped areas of the middle temporal gyrus (MTG,

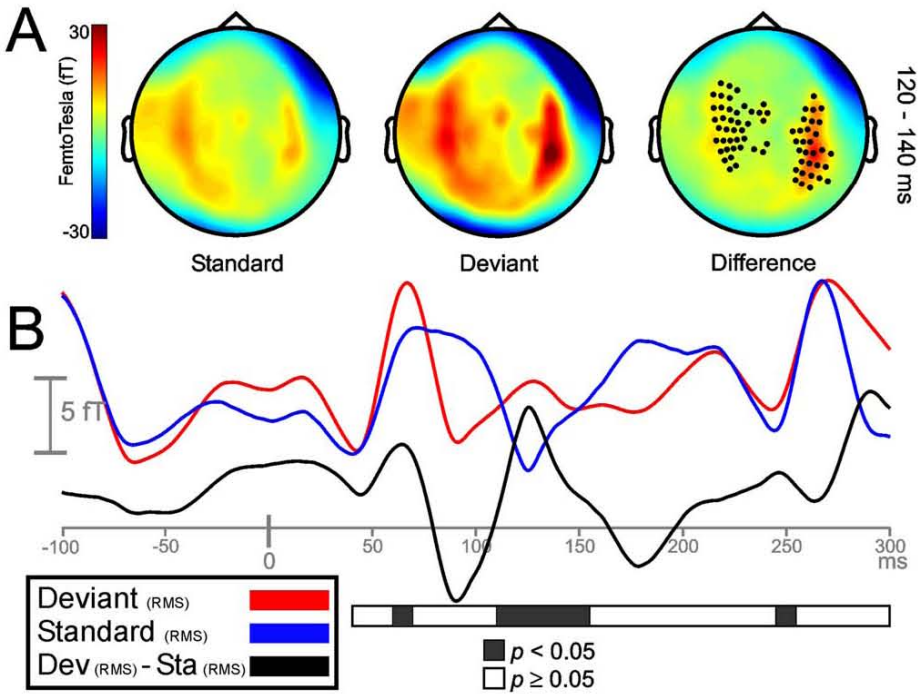

Figure 2.

Sensor-space activity for the local condition during LLR time range. **A**: The grand average of the topography of magnetic fields (planar transformed) between 120 and 140 ms after sound onset for standard (Sta), deviant (Dev), and their difference (Dev − Sta). Two bilateral clusters of sensors showed a significant increase in response to local frequency deviations ($P < 0.05$). **B**: Grand-averaged RMS waveforms (all sensors, not planar transformed) for deviant (red line), standard (blue line), and its difference RMS time course (black line). Black portions within the horizontal bar representing statistically significant time intervals ($P < 0.05$; in steps of 20 ms) show enhanced responses to deviant tones between 120 and 160 ms after the onset of the local deviation.

−60 −10 −6). Beamformer results for global deviants minus standard tones (between 160 and 200 ms) localized the generators of the global MMNm on posterior portions of the supratemporal cortex bilaterally (Fig. 6, second row). The peak voxel was located on posterior regions of the right STG (70 −34 16), and a weaker peak voxel on the left hemisphere fell on the posterior tip of STG (−64 −34 20). Using the same approach, we also investigated the location of neuronal sources underlying local regularity violations in the MLR time range. Sources of local deviants minus standard tones during the time interval of the Nbm MLR component (between 45 and 55 ms) were located bilaterally on supratemporal cortices. Consistent with sensor-level results (Fig. 4A), the left hemisphere showed stronger Pseudo-Z values than the right hemisphere (Fig. 6, third row). Peak voxels were located on the right anterior STG (66 −20 10) and the left post-central gyrus, just above the anterior tip of the left STG (−64 −20 14). During the time interval of the Pbm component (between 60 and 75 ms), beamformer results for the difference wave yielded bilateral activation on supratemporal regions, with the right hemisphere showing stronger pseudo-Z values (Fig. 6, fourth row). Peak voxels were located on the right (64 −10 4) and left (−66 −24 10) STG.

A more detailed analysis of the spatial differences between neuronal sources was carried out by examining the distribution, in each coordinate axis, of the individual peak voxels in each condition (Fig. 7). In these analyses, right hemisphere peak voxels from Subject 2 were excluded from all conditions on the basis that peak voxels in the *Y*-axis, for LLR conditions, were 1.5 standard deviations above the mean. The same type of analysis was repeated using the top 50 highest individual peak voxels in each condition to assess spatial differences in more detail. ANOVA of individual's highest peak voxels revealed a main effect of the condition in the *Y*-axis, indicating that individual peak voxels in the anterior–posterior axis differed between conditions ($F(3,39) = 16.29$, $P < 0.0001$, $\eta_p^2 = 0.56$). As no differences were found between hemispheres, data from the two hemispheres

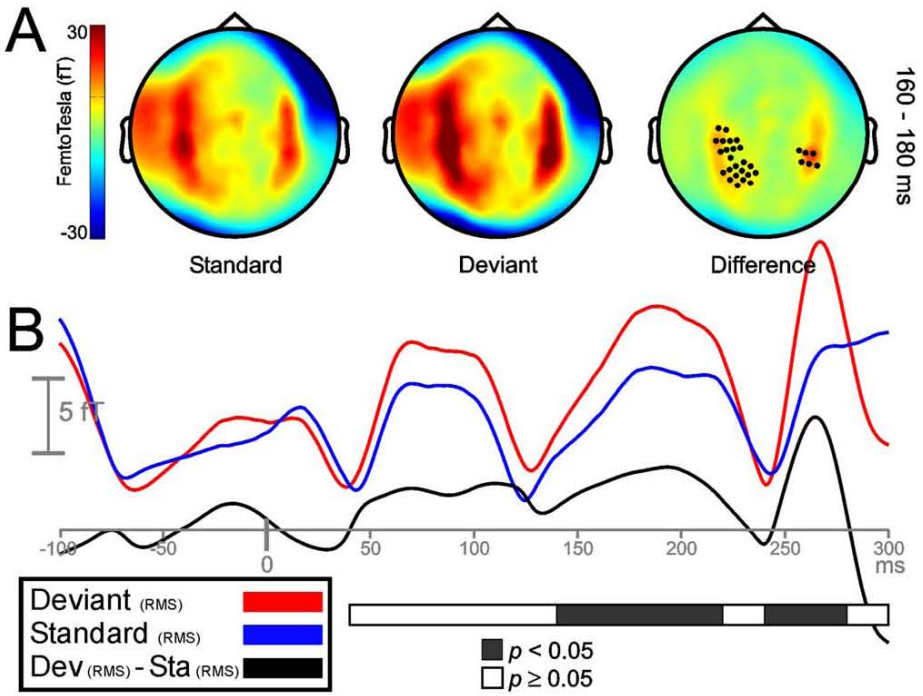

Figure 3.

Sensor-space activity for the global condition during LLR time range. **A**: The grand average of the topography of magnetic fields (planar transformed) between 160 and 180 ms after sound onset for standard (Sta), deviant (Dev), and their difference (Dev − Sta). Two bilateral clusters of sensors showed a significant increase in response to global frequency repetitions ($P < 0.05$). **B**: Grand-averaged RMS waveforms (all sensors, not planar transformed) for deviant (red line), standard (blue line), and its difference RMS time course (black line). Black portions within the horizontal bar representing statistically significant time intervals ($P < 0.05$; in steps of 20 ms) show enhanced responses to deviant tones between 140 and 220 ms after the onset of the global violation.

were collapsed for post hoc comparisons. Pairwise analyses showed that global MMNm peak voxels were located more posterior than the local MMNm ($t(28) = -6.01$, $P < 0.0001$, $d = 1.69$), Nbm ($t(28) = -3.37$, $P < 0.05$, $d = 0.77$), and Pbm ($t(28) = -4.75$, $P < 0.001$, $d = 1.28$). Local MMNm peak voxels were located significantly more anterior than those for the Nbm ($t(28) = 4.13$, $P < 0.005$, $d = 1.08$). The same procedure was repeated using the average coordinates from the best 50 individual peak voxels in each condition. This analysis showed an interaction between the factors condition and hemisphere ($F(3, 39) = 5.56$, $P < 0.01$, $\eta_p^2 = 0.3$). Separate analyses in each hemisphere showed that conditions differed significantly in the left hemisphere only ($F(3,42) = 28.12$, $P < 0.0001$ (G–G), $\eta_p^2 = 0.67$). Post hoc contrasts showed, for the left hemisphere, the same results reported using one single peak voxel, with the addition that local MMNm showed a more anterior location than Pbm ($t(14) = 5.35$, $P < 0.001$, $d = 1.98$). In the *Z*-axis, an interaction between the factors condition and hemisphere was found ($F(3,39) = 3.36$, $P < 0.05$, $\eta_p^2 = 0.21$). Separate analyses in each hemisphere showed that conditions differed significantly in the left ($F(3,42) = 11.96$, $P < 0.0001$, $\eta_p^2 = 0.46$) and right hemispheres ($F(3,39) = 5.15$, $P < 0.005$, $\eta_p^2 = 0.28$). Pairwise post hoc comparisons showed that the local MMNm was located significantly more inferior than global MMNm ($t(14) = 5.49$, $P < 0.0001$, $d = 1.37$), Nbm ($t(14) = 4.3$, $P < 0.005$, $d = 0.93$), and Pbm peak voxels in the left hemisphere ($t(14) = 3.99$, $P < 0.01$, $d = 0.89$). In the right hemisphere, only peak voxels in the global MMNm condition differed significantly from those in the Pbm condition ($t(13) = 3.48$, $P < 0.05$, $d = 0.89$). Identical results were found in the *Z*-axis when using the average of the Top50 individual peak voxels in each condition. Finally, no statistically significant differences were found in the *X*-axis when taking the best single peak voxel. However, Top50 analysis revealed a condition effect ($F(3, 39) = 4.73$, $P < 0.01$, $\eta_p^2 = 0.27$), and post hoc analysis, using collapsed

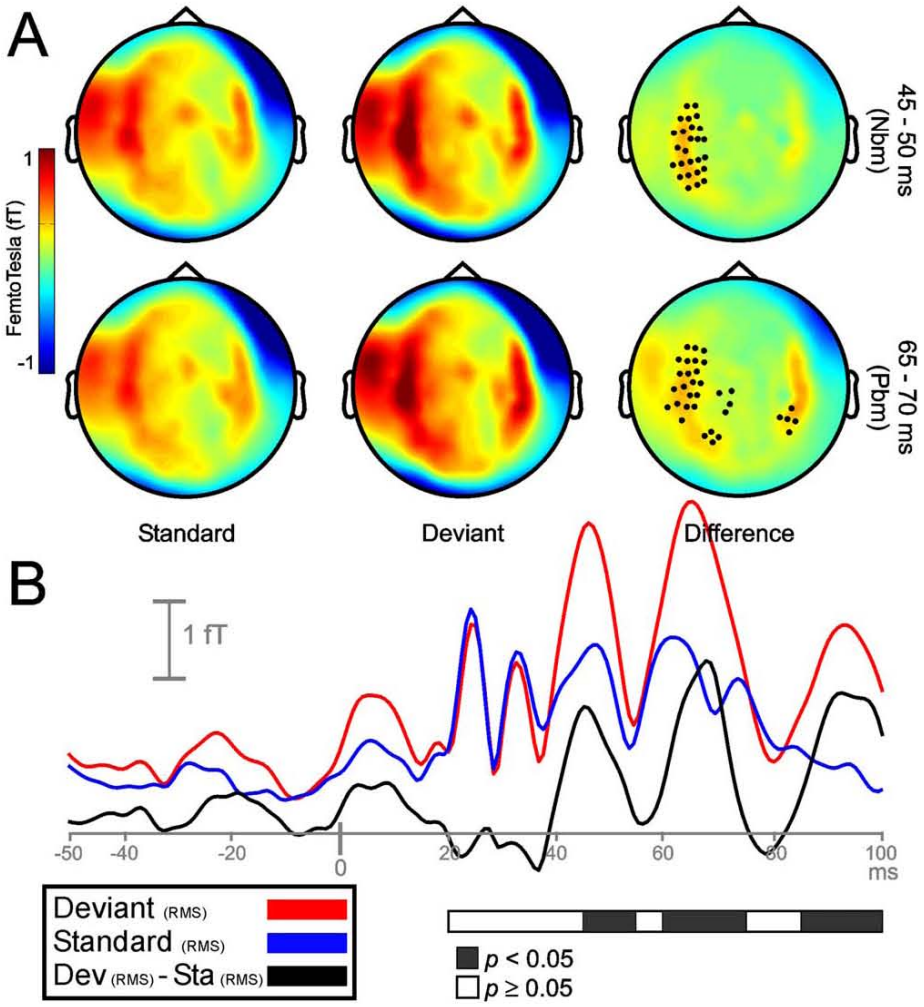

Figure 4.

Sensor-space activity for the local condition during MLR time range. **A**: The grand average of the topography of magnetic fields (planar transformed) between 45 and 50 ms (upper row), and between 65 and 70 ms (lower row) after sound onset for standard (Sta), deviant (Dev), and their difference (Dev − Sta). One cluster of sensors on left hemisphere for the Nbm component (upper row) and two bilateral clusters of sensors for the Pbm component (lower row) showed a significant increase in response to local frequency deviations ($P < 0.05$). **B**: Grand-averaged RMS waveforms (all sensors, not planar transformed) for deviant (red line), standard (blue line), and its difference RMS time course (black line). Black portions within the horizontal bar representing statistically significant time intervals ($P < 0.05$; in steps of 5 ms) show enhanced responses to deviant tones between 45 and 55 ms, and between 60 and 75 ms after the onset of the local violation.

data from the two hemispheres, showed statistically significant differences between Nbm and local MMNm peak voxels, the latter being more medial ($t(28) = 3.09$, $P < 0.05$, $d = 0.72$). In short, statistically significant local effects were found in the time intervals of the Nbm, Pbm, and MMNm, when comparing deviant and standard stimuli. No global effects were found in the time range of the MLR, and only a late MMNm response indexed global regularity violations. Source analysis of deviant minus standard tones for the aforementioned conditions revealed a significant spatial separation between neuronal sources underlying local and global regularity encoding mechanisms. Analyses revealed consistent differences in peak voxels' distribution along the inferior–superior and anterior–posterior axes. In addition, Top50 voxel analyses revealed that differences across conditions in the anterior–

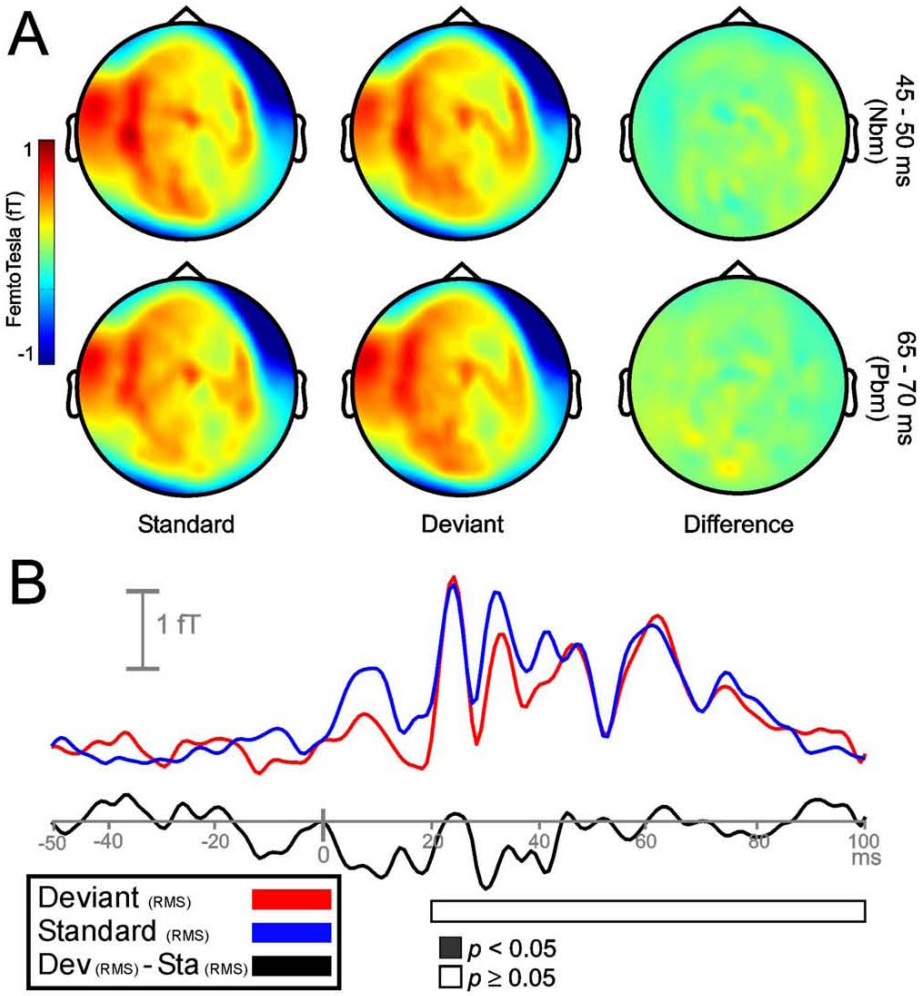

Figure 5.

Sensor-space activity for the global condition during MLR time range. **A**: The grand average of the topography of magnetic fields (planar transformed) between 45 and 50 ms (upper row), and between 65 and 70 ms (lower row) after sound onset for standard (Sta), deviant (Dev), and their difference (Dev − Sta). No cluster of sensors for any MLR deflections showed a significant increase in response to global frequency repetitions (n.s.). **B**: Grand-averaged RMS waveforms (all sensors, not planar transformed) for deviant (red line), standard (blue line), and its difference RMS time course (black line). Horizontal bar representing statistically significant time intervals (in steps of 5 ms) show the lack of significant differences between global deviant and standard tones.

posterior axis were carried by the left hemisphere mainly, and showed additional differences in the medial-lateral axis between MLR and LLR conditions.

DISCUSSION

Our results show that global regularity violations are indexed by a late MMNm (~160 ms) in the LLR time range, but not at earlier latencies during the time course of the MLRs. Likewise, we show that the processing of local rule violations is carried out in several time scales, in the LLR (~120 ms) and MLR (Nbm: ~45 ms, and Pbm: ~65 ms) time ranges. Source localization results describe a clear anatomical separation between neuronal sources allocating local and global types of regularity. Posterior areas in perisylvian region showed enhanced responses to global violations only, while anterior areas located near primary auditory cortices were only activated by local changes. Our results show that multiple anatomical regions in the

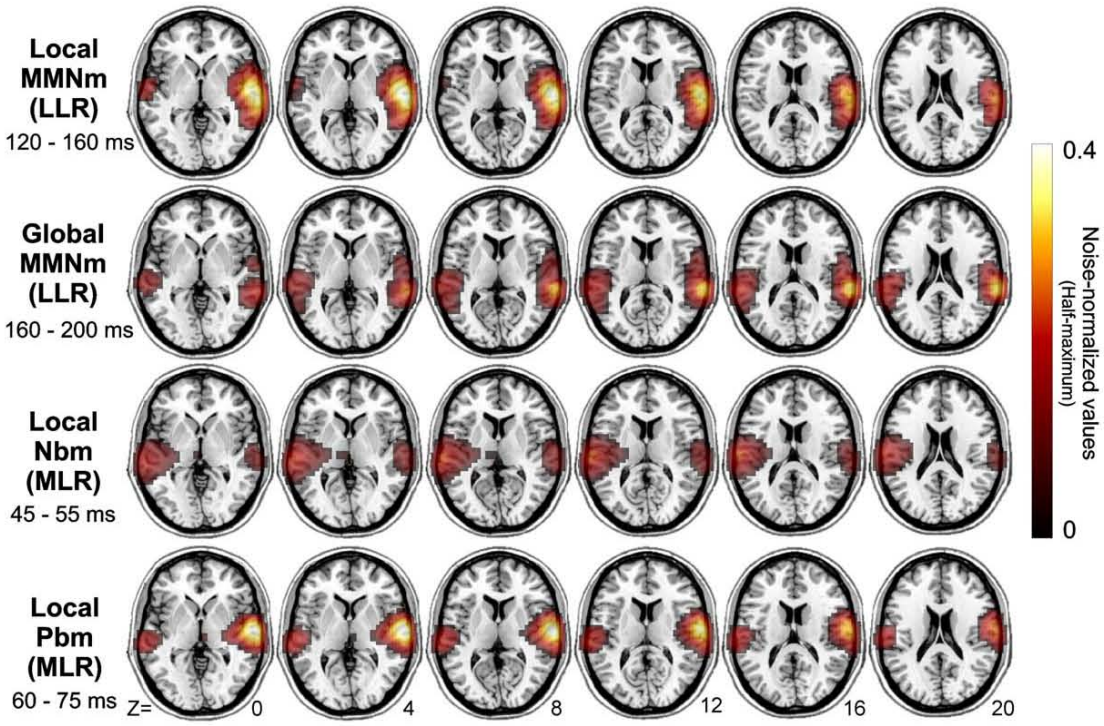

Figure 6.

Group-averaged source localization of the contrasts (deviant minus standard) for the four different conditions. The power (noise normalized pseudo-*Z* values) of the source representations is thresholded at half-maximum and overlaid onto the MNI standard brain. All conditions showed bilateral activation with main activity overlapping auditory regions. Only the global condition (second row), in the LLR time range, showed peak voxels localized in posterior regions of the supratemporal cortex. *Z* MNI coordinates (inferior–superior) are given at the lowest row on the corresponding slice.

auditory cortex sustain parallel sensitivities to different levels of acoustic regularity. We suggest that both early and late mechanisms of change detection are concurrently engaged during the processing of nested levels of sound organization, and their neural generators are located in separate auditory areas.

Enhanced responses to frequency changes occurred for MLR and LLR, indicating that the local regularity defined by the three repeated tones of each microsequence was extracted recursively in two consecutive and clearly separated time intervals. In accordance with these results, previous studies found MMNm responses to local violations in the LLR time range using a similar "global–local" experimental design [Bekinschtein et al., 2009; Herholz et al., 2009; Wacongne et al., 2011]. Sussman et al. [Sussman et al., 1998; Sussman and Gumenyuk, 2005] showed that a short SOA, as the one used here, abolished the MMN to local deviations when stimuli were presented in regular microsequences, suggesting that patterns were processed as a global entity. Disparate results between those studies and ours could be accounted for by the presence of interspersed global deviants acting as a contextual modification, and reactivating the dormant local regularity [Ritter et al., 1998; Sussman and Winkler, 2001]. The 200 ms SOA used in this study, lying right at the temporal edge for automatic grouping to occur [Sussman and Gumenyuk, 2005], might explain why a local MMNm still emerged in the reversed block where no global deviations were presented. In earlier time intervals, Nbm and Pbm waveforms of the MLR reflected deviance-related enhancements preceding MMNm. In consonance with our data, previous studies showed that spectral deviations elicit amplitude modulations in the Nbm component of the MLR [Alho et al., 2012; Althen et al., 2013; Grimm et al., 2011; Puschmann et al., 2013; Recasens et al., 2014]. Similarly, effects on the Pbm/P50m component have been previously interpreted as an indicator of gating-in, that is, a dishabituation to significant stimuli occurring after redundant stimulation [Boutros and Belger, 1999; Paraskevopoulos et al., 2012]. The early modulation of MLR in the local condition can be paralleled to animal findings showing very fast SSA to the repeated presentation of a particular frequency, and the subsequent increment in the response to deviant stimuli [Malmierca et al., 2009; Ulanovsky et al., 2003].

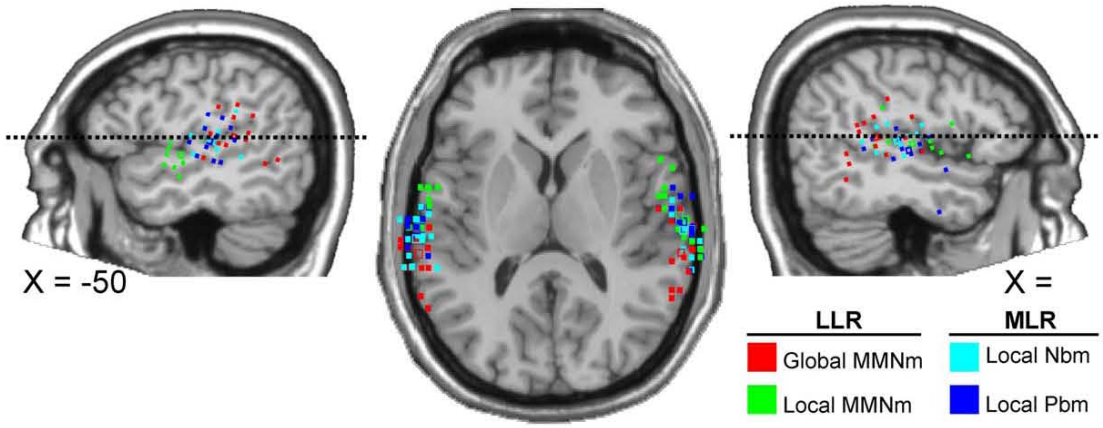

Figure 7.

Individual peak voxel locations for the four different conditions (deviant minus standard) superimposed on a template brain (Montreal Neurological Institute, MNI) tilted 16° down to assist the visualization of peak voxels on the supratemporal planes. Peak voxels are projected on one sagittal slice (lateral panels), thus omitting the *X*-axis; and on a tilted axial slice (central panel), thus omitting the *Z*-axis coordinate. Dotted lines on sagittal views indicate the height of the axial slice.

With regard to the global condition, our results are in line with previous research showing mismatch-like responses to infrequent sound repetitions [Alain et al., 1994, 1999b; Boh et al., 2011; Chait et al., 2008; Herholz et al., 2009, 2011; Horvath et al., 2001; Tervaniemi et al., 2001]. Previous attempts to probe complex regularity processing in the MLR and LLR range designed complex regularities based on feature combinations [Althen et al., 2013] or simple patterns, whose regularity was defined by the interrelationship of adjacent tones [Cornella et al., 2012]. Here, we tested complex regularity processing and early deviance detection using nested and more realistic acoustic events. The global MMNm indicates the presence of temporally integrated stimulus representations, which could correspond to the subjective pattern percept [Näätänen and Winkler, 1999]. Recent studies using similar global–local paradigms and active listening tasks have investigated the conscious processing of global regularities [Bekinschtein et al., 2009; Wacongne et al., 2011] discovering that a P3b, but not MMN, was elicited during global violations. Dissimilarities in the responses indexing global changes (global MMN or P3b) between Bekinschtein et al. [2009] and other studies including ours [see also: Herholz et al., 2009, 2011; Horvath et al., 2001] might be accounted for by the different task demands. In this line, our results support that active or conscious listening is not a prerequisite for the automatic encoding of global regularities and that different brain mechanisms might be involved in the automatic processing of global regularity violations. It is worth noting that a sustained field between about 50 and 130 ms, with a dipolar field equivalent to the P50/P1 EEG response, characterized the time course of the standards and repetition violations, but not that of the frequency deviants. Such differences in spatial distribution, which are probably explained by the fast and regular presentation rate, could reflect the distinct neuronal generators involved in the processing of local and global deviations [Lütkenhöner, 2003]. The absence of earlier activity preceding the global MMNm is in line with previous findings showing that sound transitions from a regular sequence to a constant pure-tone elicited a peak at 160 ms after transition but no earlier activity in the P50 time range, suggesting that early mechanisms of deviance detection may be limited by the kinds of regularity they can compute [Chait et al., 2008]. Based on the lack of global deviance-related effects in the time range of the MLR, we suggest that very early deviance detection mechanisms work, at least for frequency [Leung et al., 2012], at the feature level [Alho et al., 2012; Althen et al., 2011; Grimm et al., 2012; Leung et al., 2013], and reflect an early stage prior to feature combination, sequential grouping, or the extraction of regularities based on the interrelationship between sounds. In sum, our study refine previous findings by Cornella et al. [2012] and Althen et al. [2013] and provide additional evidence showing that deviance detection is hierarchically organized consistently with the level of complexity in which the auditory input can be organized. In other words, the detection of simple regularities is already accomplished at early stages of the auditory hierarchy, in the time range of the MLR, whereas complex levels of regularity are encoded in higher levels along the novelty system's hierarchy [Escera and Malmierca, 2014].

Source reconstruction revealed neuronal generators that were consistent with sensor-level data, pointing to the overall robustness of beamforming results. As expected, sources of MMNm and deviance-related MLR deflections to local deviations were located on anterior areas of STG and lateral aspects of HG (Heschl's gyrus) bilaterally

[Doeller et al., 2003; Inui et al., 2006; Opitz et al., 1999; Schönwiesner et al., 2007; Yvert et al., 2001]. Consistent with sensor-level data and previous findings, MMNm was larger on the right hemisphere [Paavilainen et al., 1991; Recasens et al., 2014]. Similarly, left- and right-ward lateralization of deviance-related effects in the Nbm and Pbm components, respectively, was in agreement with sensor-level data. The individual peak-voxel distribution for the different local conditions (deviance-related MLR and MMN) revealed a spatial separation along the sylvian fissures between very early deviance-related Nbm sources and MMNm sources to local changes. That difference was even clearer on the left hemisphere, where MMNm neuronal sources were located more inferior than deviance-related MLR sources. Our results replicate previous localization results obtained by Recasens et al. [2014] showing a mediolateral and anterior–posterior separation between MLR and MMNm sources. The lack of differences in the mediolateral axis might be accounted for by the different sensitivity of axial gradiometers to deep sources as compared to magnetometers [Hämäläinen et al., 1993]. Anterior MMNm sources, as compared to N1m generators, have been reported by classic MMN studies using small frequency separations. Jääskeläinen et al. [2004] showed that such source configuration could be explained by the relatively different adaptation sensitivity of anterior and posterior N1m sources. Using similar paradigms, focal activation in or near primary auditory cortex has been previously reported for local MMN [Bekinschtein et al., 2009; Wacongne et al., 2011]. Uhrig et al. [2014] registered fMRI in the monkey brain also revealing a much more distributed cortical network for local novelties that included subcortical nuclei and primary auditory cortices. In agreement, our findings suggest that multiple loci near HG support the processing of local events in successive time intervals. Sources underlying violations of the global regularity were located in posterior STG, or planum temporale (PT), more posterior than neuronal activity underlying all remaining local conditions. Our data agree with previous findings suggesting that physical dimensions-like frequency and more complex regularities are encoded in distinct auditory areas [Alain et al., 1999a; Alho et al., 1996; Levänen et al., 1996]. Previous studies revealed the involvement of a global workspace network during the processing of global rule violations that included auditory, prefrontal, parietal, and cingulate regions [Bekinschtein et al., 2009; Wacongne et al., 2011]. Even though strong parallelisms with our source reconstruction results should be avoided since P3b was elicited in these studies, Uhrig et al. [2014] showed the involvement of posterior auditory regions, the temporo-parietal area, in the preprocessing of global violations. This posterior localization for pattern processing, understood as sequences of sounds unfolding on a multidimensional space [Bregman, 1990], can be related to neuroimaging findings showing auditory and motor interactions during rhythm processing [Chen et al., 2009]. PT is frequently reported during auditory spatial tasks as part of the dual-stream model [Alain et al., 2001; Rauschecker and Tian, 2000], which has been criticized as over-simplistic [Belin and Zatorre, 2000; Hall, 2003], and recently re-examined as an auditory-action related area [for a review see: Arnott and Alain, 2011]. Thus, posterior STG activation might reflect the spectrotemporal analysis of complex sounds sequences [Zatorre et al., 2002] or the breaking of previously encoded auditory-motor representation of the global sequence [Chen et al., 2009; Karabanov et al., 2009]. Under the dual-stream framework, findings showing sources underlying intelligible speech processing located in anterior portions of the superior temporal sulcus [Evans et al., in press; Scott et al., 2000] could be explained in terms of a ventral pathway involved in mapping sound into meaning, and a dorsal pathway involved in mapping sound into an articulatory-based representation [Arnott and Alain, 2011; Hickok and Poeppel, 2007]. In line, Griffiths and Warren [2002] suggested that PT contains mechanisms for parsing the different types of auditory information included in complex sounds, which work in a template-matching fashion [Näätänen et al., 2005; Winkler et al., 2009]. In sum, source localization results are in agreement with a putative role of posterior STG in the encoding of discrete local units into an ordered and extended global auditory signal [Warren et al., 2005]. Our results suggest that while different anterior regions participate in the encoding of features at the local level, posterior and hierarchically superior regions may be engaged in the encoding of more complex or global patterns. Despite converging evidence shows the existence of MMN generators in the frontal lobe [Doeller et al., 2003; Schönwiesner et al., 2007], no frontal areas were observed in this study. Previous studies described the involvement of frontal regions when using listening tasks and by recording EEG or intracranial activity during global–local paradigms [Bekinschtein et al., 2009; Chennu et al., 2013]. However, MEG findings, or the lack of them, suggest that the frontal MMNm component is either located deeper in the brain or is radially oriented and, hence, almost silent to MEG sensors [Hämäläinen et al., 1993; Rinne et al., 2000]. More sophisticated source analyses (e.g., using regions of interest) or design parameters might allow future studies to reveal frontal generators using MEG.

A long debate exists about whether MMN can be explained solely on the differential states of refractoriness of neurons specifically responding to given stimulus attributes that characterize the standard sound [May and Tiitinen, 2010], or denotes a predictive coding mechanism supported by genuine memory-based comparisons between a deviant input and the previously encoded regularity [Jacobsen and Schröger, 2001; Näätänen et al., 2005; Winkler et al., 2009]. Although both alternatives are not mutually exclusive, several conditions controlling for stimulus probability have been designed to differentiate

adaptation from genuine memory-based effects in the MMN response [Jacobsen and Schröger, 2001; Jacobsen et al., 2003; Ruhnau et al., 2012; Schröger and Wolff, 1996]. Given that this study did not implement such a condition, it may be argued that one cannot be sure whether "sensory" or "cognitive" deviance detection mechanisms [Opitz et al., 2005] are participating in the local effects of both MLR and LLR. However, our previous research using controlled designs showed that genuine deviance detection is preserved in both LLR and MLR time ranges for rare changes in frequency or location [Grimm et al., 2011, 2012; Slabu et al., 2010, 2012]. Also Wacongne et al. [2011] showed that novelty responses to local violations remain present when the final sound is omitted, an effect that cannot be explained under the adaptation hypothesis. Nevertheless, an alternative interpretation of our local effects is that amplitude enhancements indexed stimulus change per se, irrespective of the previously encoded regularity, and hence, acted as a simple stimulus detector signaling to higher-order mechanisms [Recasens et al., 2014]. Similar interpretations have been offered by previous studies suggesting that early deflections index a sensory change detection mechanism based on differential states of refractoriness during a "minimal integration window," and later MMN responses reflect the construction of a new memory-trace based regularity [Chait et al., 2007, 2008]. Similarly, Schönwiesner et al. [2007] found that only high-order regions in the temporal cortex were sensitive to the magnitude of deviation whereas hierarchically lower areas were not, suggesting that medial portions of the HG are devoted to a nonmemory-based mechanism of change detection. Regarding the global effects, an interpretation based on the different refractory states for deviant and standard responses could not be applied. Whereas a higher degree of adaptation was expected for the global deviant, the rare four-tone repetition, an enhanced response was obtained indicating that global regularities were extracted and its deviations detected in spite of the expected greater degree of adaptation. In sum, local violations presented here are likely reflecting a combination of genuine memory-based and refractoriness effects, whereas global rules are probably extracted by means of more complex memory-based processes. Nevertheless, beyond the underlying neurophysiological mechanism that triggers deviance detection, the hierarchical notion we support is in agreement with the ideas of Schönwiesner et al. [2007] proposing different roles for hierarchically distinct areas involved in the MMN generation process, namely the detection of changes in global as opposed to local regularities. Our suggestion that early and late regularity encoding and deviance detection mechanisms work in a parallel fashion is based on the fact that hierarchically inferior regions of the auditory cortex sustain local rules (frequency invariance), and respond to local deviations; Concurrently with the presentation of the same stimulus, higher-order regions do not show enhanced responses, as local deviations represent an integral part of the global regularity template. In line with Bregman's [1990] view of multiple preattentive processes that analyze the input in parallel, our source reconstruction results support the notion that a late MMNm to global changes, located in posterior areas of the auditory cortex, underlies an unconscious mechanism that organizes regularity inputs into meaningful objects, while representation of necessary local features is concurrently maintained in hierarchically lower levels.

CONCLUSIONS

This study proposes that temporally and spatially distinct deviance detection mechanisms underlie growing levels of regularity encoding in the human auditory system, which in turn, support parallel levels of acoustic organization. Using sequences composed of interrelated sounds, with local deviants nested into global patterns, we showed that only late mechanisms of deviance detection reflect the spectrotemporal integration of single events into a global organization. Noteworthy, anterior areas near primary auditory cortex, and posterior regions in PT, interplay to maintain local and global sensory representations, thus showing that different regularity levels are encoded in parallel within hierarchically organized regions of the human auditory cortex.

REFERENCES

Alain C, Woods D, Ogawa K (1994): Brain indices of automatic pattern processing. Neuroreport 6:140–144.

Alain C, Achim A, Woods DL (1999a): Separate memory-related processing for auditory frequency and patterns. Psychophysiology 36:737–744.

Alain C, Cortese F, Picton TW (1999b): Event-related brain activity associated with auditory pattern processing. Neuroreport 10: 2429–2434.

Alain C, Arnott SR, Hevenor S, Graham S, Grady CL (2001): "What" and "where" in the human auditory system. Proc Natl Acad Sci USA 98:12301–12306.

Alho K, Tervaniemi M, Huotilainen M, Lavikainen J, Tiitinen H, Ilmoniemi R, Knuutila J, Näätänen R (1996): Processing of complex sounds in the human auditory cortex as revealed by magnetic brain responses. Psychophysiology 33:369–375.

Alho K, Grimm S, Mateo-León S, Costa-Faidella J, Escera C (2012): Early processing of pitch in the human auditory system. Eur J Neurosci 36:2972–2978.

Althen H, Grimm S, Escera C (2011): Fast detection of unexpected sound intensity decrements as revealed by human evoked potentials. PLoS One 6:e28522.

Althen H, Grimm S, Escera C (2013): Simple and complex acoustic regularities are encoded at different levels of the auditory hierarchy. Eur J Neurosci 38:3448–3455.

Arnott SR, Alain C (2011): The auditory dorsal pathway: Orienting vision. Neurosci Biobehav Rev 35:2162–2173.

Ayala YA, Pérez-González D, Duque D, Nelken I, Malmierca MS (2013): Frequency discrimination and stimulus deviance in the inferior colliculus and cochlear nucleus. Front Neural Circuits 6:119.

Bastiaansen MC, Knösche TR (2000): Tangential derivative mapping of axial MEG applied to event-related desynchronization research. Clin Neurophysiol 111:1300–1305.

Bekinschtein T, Dehaene S, Rohaut B, Tadel F, Cohen L, Naccache L (2009): Neural signature of the conscious processing of auditory regularities. Proc Natl Acad Sci USA 106:1672–1677.

Belin P, Zatorre R (2000): "What", "where" and "how" in auditory cortex. Nat Neurosci 3:965–966.

Bendixen A, SanMiguel I, Schröger E (2012): Early electrophysiological indicators for predictive processing in audition: A review. Int J Psychophysiol 83:120–131.

Boh B, Herholz SC, Lappe C, Pantev C (2011): Processing of complex auditory patterns in musicians and nonmusicians. PLoS One 6:e21458.

Boutros NN, Belger A (1999): Midlatency evoked potentials attenuation and augmentation reflect different aspects of sensory gating. Biol Psychiatry 45:917–922.

Bregman AS (1990): Auditory Scene Analysis: The Perceptual Organization of Sound. Cambridge MA: MIT Press.

Chait M, Poeppel D, de Cheveigné A, Simon JZ (2007): Processing asymmetry of transitions between order and disorder in human auditory cortex. J Neurosci 27:5207–5214.

Chait M, Poeppel D, Simon JZ (2008): Auditory temporal edge detection in human auditory cortex. Brain Res 1213:78–90.

Chen JL, Penhune VB, Zatorre R (2009): The role of auditory and premotor cortex in sensorimotor transformations. Ann N Y Acad Sci 1169:15–34.

Chennu S, Noreika V, Gueorguiev D, Blenkmann A, Kochen S, Ibáñez A, Owen AM, Bekinschtein TA (2013): Expectation and attention in hierarchical auditory prediction. J Neurosci 33: 11194–11205.

Cornella M, Leung S, Grimm S, Escera C (2012): Detection of simple and pattern regularity violations occurs at different levels of the auditory hierarchy. PLoS One 7:e43604.

Doeller C, Opitz B, Mecklinger A, Krick C, Reith W, Schröger E (2003): Prefrontal cortex involvement in preattentive auditory deviance detection: Neuroimaging and electrophysiological evidence. Neuroimage 20:1270–1282.

Escera C, Malmierca MS (2014): The auditory novelty system: An attempt to integrate human and animal research. Psychophysiology 51:111–123.

Evans S, Kyong JS, Rosen S, Golestani N, Warren JE, McGettigan C, Mourão-Miranda J, Wise RJ, Scott SK: The pathways for intelligible speech: Multivariate and univariate perspectives (in press).

Farley BJ, Quirk MC, Doherty JJ, Christian EP (2010): Stimulus-specific adaptation in auditory cortex is an NMDA-independent process distinct from the sensory novelty encoded by the mismatch negativity. J Neurosci 30:16475–16484.

Friston K (2005): A theory of cortical responses. Philos Trans R Soc B Biol Sci 360:815–836.

Griffiths TD, Warren JD (2002): The planum temporale as a computational hub. Trends Neurosci 25:348–253.

Grimm S, Escera C (2012): Auditory deviance detection revisited: Evidence for a hierarchical novelty system. Int J Psychophysiol 85:88–92.

Grimm S, Escera C, Slabu L, Costa Faidella J (2011): Electrophysiological evidence for the hierarchical organization of auditory change detection in the human brain. Psychophysiology 48: 377–384.

Grimm S, Recasens M, Althen H, Escera C (2012): Ultrafast tracking of sound location changes as revealed by human auditory evoked potentials. Biol Psychol 89:232–239.

Haenschel C, Vernon DJ, Dwivedi P, Gruzelier JH, Baldeweg T (2005): Event-related brain potential correlates of human auditory sensory memory-trace formation. J Neurosci 25:10494–10501.

Hall D (2003): Auditory pathways: Are "What" and "Where" appropriate? Curr Biol 13:R406–R408.

Hämäläinen M, Hari R, Ilmoniemi RJ, Knuutila J, Lounasmaa O (1993): Magnetoencephalography—Theory, instrumentation, and applications to noninvasive studies of the working human brain. Rev Mod Phys 65:413–497.

Herholz SC, Lappe C, Pantev C (2009): Looking for a pattern: An MEG study on the abstract mismatch negativity in musicians and nonmusicians. BMC Neurosci 10:42.

Herholz SC, Boh B, Pantev C (2011): Musical training modulates encoding of higher-order regularities in the auditory cortex. Eur J Neurosci 34:524–529.

Hickok G, Poeppel D (2007): The cortical organization of speech processing. Nat Rev Neurosci 8:393–402.

Horvath J, Czigler I, Sussman E, Winkler I (2001): Simultaneously active pre-attentive representations of local and global rules for sound sequences in the human brain. Brain Res brain Res 12:131–144.

Inui K, Okamoto H, Miki K, Gunji A, Kakigi R (2006): Serial and parallel processing in the human auditory cortex: A magneto-encephalographic study. Cereb cortex 16:18–30.

Jääskeläinen IP, Ahveninen J, Bonmassar G, Dale AM, Ilmoniemi RJ, Levänen S, Lin FH, May P, Melcher J, Stufflebeam SM, Tiitinen H, Belliveau JW (2004): Human posterior auditory cortex gates novel sounds to consciousness. Proc Natl Acad Sci USA 101:6809–6814.

Jacobsen T, Schröger E (2001): Is there pre-attentive memory-based comparison of pitch? Psychophysiology 38:723–727.

Jacobsen T, Schröger E, Horenkamp T, Winkler I (2003): Mismatch negativity to pitch change: Varied stimulus proportions in controlling effects of neural refractoriness on human auditory event-related brain potentials. Neurosci Lett 344:79–82.

Jung TP, Makeig S, Westerfield M, Townsend J, Courchesne E, Sejnowski TJ (2000): Removal of eye activity artifacts from visual event-related potentials in normal and clinical subjects. Clin Neurophysiol 111:1745–1758.

Karabanov A, Blom O, Forsman L, Ullén F (2009): The dorsal auditory pathway is involved in performance of both visual and auditory rhythms. Neuroimage 44:480–488.

Knösche TR (2002): Transformation of whole-head MEG recordings between different sensor positions. Biomed Tech (Berl) 47: 59–62.

Korzyukov O, Winkler I, Gumenyuk V, Alho K (2003). Processing abstract auditory features in the human auditory cortex. Neuroimage 20:2245–2258.

Leung S, Cornella M, Grimm S, Escera C (2012): Is fast auditory change detection feature specific? An electrophysiological study in humans. Psychophysiology 49:933–942.

Leung S, Recasens M, Grimm S, Escera C (2013): Electrophysiological index of acoustic temporal regularity violation in the middle latency range. Clin Neurophysiol 124:2397–2405.

Levänen S, Ahonen A, Hari R, McEvoy L, Sams M (1996): Deviant auditory stimuli activate human left and right auditory cortex differently. Cereb Cortex 6:288–296.

Lütkenhöner B (2003): Magnetoencephalography and its Achilles' heel. J Physiol Paris 97:641–658.

Makeig S, Jung TP, Bell AJ, Ghahremani D, Sejnowski TJ (1997): Blind separation of auditory event-related brain responses into independent components. Proc Natl Acad Sci USA 94:10979–10984.

Malmierca MS, Cristaudo S, Pérez-González D, Covey E (2009): Stimulus-Specific adaptation in the inferior colliculus of the anesthetized rat. J Neurosci 29:5483–5493.

Maris E, Oostenveld R (2007): Nonparametric statistical testing of EEG- and MEG-data. J Neurosci Methods 164:177–190.

May PJ, Tiitinen H (2010): Mismatch negativity (MMN), the deviance-elicited auditory deflection, explained. Psychophysiology 47:66–122.

Näätänen R, Winkler I (1999): The concept of auditory stimulus representation in cognitive neuroscience. Psychol Bull 125:826–859.

Näätänen R, Gaillard AW, Mantysalo S (1978): Early selective-attention effect on evoked potential reinterpreted. Acta Psychol 42:313–329.

Näätänen R, Jacobsen T, Winkler I (2005): Memory-based or afferent processes in mismatch negativity (MMN): A review of the evidence. Psychophysiology 42:25–32.

Näätänen R, Paavilainen P, Rinne T, Alho K (2007): The mismatch negativity (MMN) in basic research of central auditory processing: A review. Clin Neurophysiol 118:2544–2590.

Nelken I, Ulanovsky N (2007): Mismatch negativity and stimulus-specific adaptation in animal models. J Psychophysiol 21:214–223.

Nolte G (2003): The magnetic lead field theorem in the quasi-static approximation and its use for magnetoencephalography forward calculation in realistic volume conductors. Phys Med Biol 48:3637–3652.

Oostenveld R, Fries P, Maris E, Schoffelen J-M (2011): FieldTrip: Open source software for advanced analysis of MEG, EEG, and invasive electrophysiological data. Comput Intell Neurosci 2011:156869.

Opitz B, Mecklinger A, von Cramon DY, Kruggel F (1999): Combining electrophysiological and hemodynamic measures of the auditory oddball. Psychophysiology 36:142–147.

Opitz B, Schröger E, von Cramon D (2005): Sensory and cognitive mechanisms for preattentive change detection in auditory cortex. Eur J Neurosci 21:531–535.

Paavilainen P, Alho K, Reinikainen K, Samsi M, Näätänen R (1991): Right-hemisphere dominance of different mismatch negativities. Electroencephalogr Clin Neurophysiol 78:466–479.

Paraskevopoulos E, Kuchenbuch A, Herholz SC, Pantev C (2012): Statistical learning effects in musicians and non-musicians: An MEG study. Neuropsychologia 50:341–349.

Puschmann S, Sandmann P, Ahrens J, Thorne J, Weerda R, Klump G, Debener S, Thiel CM (2013): Electrophysiological correlates of auditory change detection and change deafness in complex auditory scenes. Neuroimage 75:155–164.

Rauschecker JP, Tian B (2000): Mechanisms and streams for processing of "what" and "where" in auditory cortex. Proc Natl Acad Sci USA 97:11800–11806.

Recasens M, Grimm S, Capilla A, Nowak R, Escera C (2014): Two sequential processes of change detection in hierarchically ordered areas of the human auditory cortex. Cereb Cortex 24: 143–153.

Rinne T, Alho K, Ilmoniemi RJ, Virtanen J, Näätänen R (2000): Separate time behaviors of the temporal and frontal mismatch negativity sources. Neuroimage 12:14–9.

Ritter W, Gomes H, Cowan N, Sussman E, Vaughan HG (1998): Reactivation of a dormant representation of an auditory stimulus feature. J Cogn Neurosci 10:605–614.

Ruhnau P, Herrmann B, Schröger E (2012): Finding the right control: The mismatch negativity under investigation. Clin Neurophysiol 123:507–512.

Schönwiesner M, Novitski N, Pakarinen S, Carlson S, Tervaniemi M, Näätänen R (2007): Heschl's gyrus, posterior superior temporal gyrus, and mid-ventrolateral prefrontal cortex have different roles in the detection of acoustic changes. J Neurophysiol 97:2075–2082.

Schröger E, Wolff C (1996): Mismatch response of the human brain to changes in sound location. Neuroreport 7:3005–3008.

Scott SK, Blank CC, Rosen S, Wise RJ (2000): Identification of a pathway for intelligible speech in the left temporal lobe. Brain 123:2400–2406.

Slabu L, Escera C, Grimm S, Costa-Faidella J (2010): Early change detection in humans as revealed by auditory brainstem and middle-latency evoked potentials. Eur J Neurosci 32:859–865.

Slabu L, Grimm S, Escera C (2012): Novelty detection in the human auditory brainstem. J Neurosci 32:1447–1452.

Sonnadara RR, Alain C, Trainor LJ (2006): Occasional changes in sound location enhance middle latency evoked responses. Brain Res 1076:187–192.

Sussman ES, Gumenyuk V (2005): Organization of sequential sounds in auditory memory. Neuroreport 16:1519–1523.

Sussman E, Winkler I (2001): Dynamic sensory updating in the auditory system. Cogn brain Res 12:431–439.

Sussman E, Ritter W, Vaughan HG, Vaughan HG Jr (1998): Predictability of stimulus deviance and the mismatch negativity. Neuroreport 9:4167–4170.

Taaseh N, Yaron A, Nelken I (2011): Stimulus-specific adaptation and deviance detection in the rat auditory cortex. PLoS One 6: e23369.

Takegata R, Huotilainen M, Rinne T, Näätänen R, Winkler I (2000): Changes in acoustic features and their conjunctions are processed by separate neuronal populations. Neuroreport 12: 525–529.

Tervaniemi M, Rytkönen M, Schröger E, Ilmoniemi RJ, Näätänen R (2001): Superior formation of cortical memory traces for melodic patterns in musicians. Learn Mem 8:295–300.

Uhrig L, Dehaene S, Jarraya B (2014): A hierarchy of responses to auditory regularities in the macaque brain. J Neurosci 34:1127–1132.

Ulanovsky N, Las L, Nelken I (2003): Processing of low-probability sounds by cortical neurons. Nat Neurosci 6:391–398.

Van Veen B, van Drongelen W, Yuchtman M, Suzuki A (1997): Localization of brain electrical activity via linearly constrained minimum variance spatial filtering. IEEE Trans Biomed Eng 44:867–880.

Wacongne C, Labyt E, van Wassenhove V, Bekinschtein T, Naccache L, Dehaene S (2011): Evidence for a hierarchy of predictions and prediction errors in human cortex. Proc Natl Acad Sci USA 108:20754–20759.

Warren JE, Wise RJS, Warren JD (2005): Sounds do-able: Auditory-motor transformations and the posterior temporal plane. Trends Neurosci 28:636–643.

Winkler I, Denham SL, Nelken I (2009): Modeling the auditory scene: Predictive regularity representations and perceptual objects. Trends Cogn Sci 13:532–540.

Yaron A, Hershenhoren I, Nelken I (2012): Sensitivity to complex statistical regularities in rat auditory cortex. Neuron 76:603–615.

Yvert B, Crouzeix A, Bertrand O, Seither-Preisler A, Pantev C (2001): Multiple supratemporal sources of magnetic and electric auditory evoked middle latency components in humans. Cereb cortex 11:411–423.

Zatorre R, Belin P, Penhune V (2002): Structure and function of auditory cortex: Music and speech. Trends Cogn Sci 6:37–46.

STUDY III

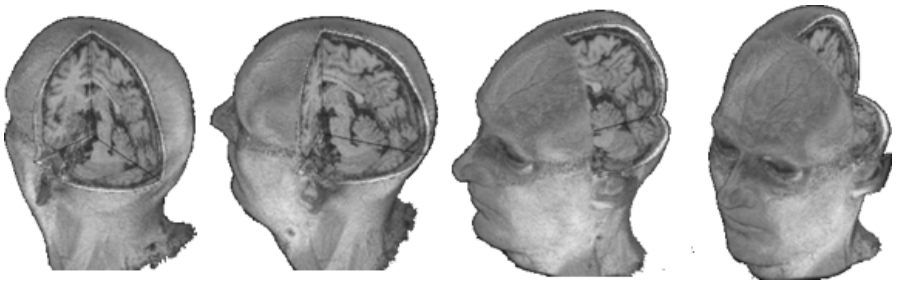

Repetition suppression and repetition enhancement underlie auditory memory-trace formation in the human brain: an MEG study

Repetition suppression and repetition enhancement underlie auditory memory-trace formation in the human brain: an MEG study

Marc Recasens[1,2], Sumie Leung[1,2], Sabine Grimm[1,2], Rafal Nowak[3], Carles Escera[1,2]

1. Institute for Brain, Cognition and Behavior (IR3C), University of Barcelona, Spain
2. Cognitive Neuroscience Research Group, Department of Psychiatry and Clinical Psychobiology, University of Barcelona, Spain
3. Unidad de Magnetoencefalografía, Hospital Quirón Teknon, Barcelona, Spain

Running title: Neuronal suppression and enhancement to auditory repetition

Type of manuscript: research article

Abstract: 247 words

Figures: 4 total

Tables: 1 total

Corresponding Author: Dr. Carles Escera

Email: cescera@ub.edu

Address: Cognitive Neuroscience Research Group,
Department of Psychiatry and Clinical Psychobiology,
University of Barcelona.
P. Vall d'Hebron 171
08035 Barcelona (Spain)

Phone: +34 933 125 048

Fax: +34 934 021 584

Abstract

The formation of echoic memory traces has traditionally been inferred from the enhanced responses to its deviations. The mismatch negativity (MMN), an auditory event-related potential (ERP) elicited between 100 and 250 ms after sound deviation is an indirect index of regularity encoding that reflects a memory-based comparison process. Recently, repetition positivity (RP) has been described as a candidate ERP correlate of direct memory trace formation. RP consists of repetition suppression and enhancement effects occurring in different auditory components between 50 and 250 ms after sound onset. However, the neuronal generators engaged in the encoding of repeated stimulus features have received little interest. This study intends to investigate the neuronal sources underlying the formation and strengthening of new memory traces by employing a roving-standard paradigm, where trains of different frequencies and different lengths are presented randomly. Source generators of repetition enhanced (RE) and suppressed (RS) activity were modeled using magnetoencephalography (MEG) in healthy subjects. Our results show that, in line with RP findings, N1m (~95–150 ms) activity is suppressed with stimulus repetition. In addition, we observed the emergence of a sustained field (~230–270 ms) that showed RE. Source analysis revealed neuronal generators of RS and RE located in both auditory and non-auditory areas, like the medial parietal cortex and frontal areas. The different timing and location of neural generators involved in RS and RE points to the existence of functionally separated mechanisms devoted to acoustic memory-trace formation in different auditory processing stages of the human brain.

Introduction

The rapid formation of echoic memory-traces is an essential property of the auditory system. It prepares us to adequately respond to potentially relevant changes in our acoustic environment and anticipate future events. One of the most widely-studied phenomena in cognitive neuroscience is repetition suppression (RS), a decrease in the neural response elicited by the repetition of a specific stimulus (Desimone, 1996). Suppression, or adaptation, has been observed in different sensory modalities, species, and in different spatial and temporal scales, using both neuroimaging and electrophysiological techniques (for a review see: Grill-Spector et al., 2006). RS is proposed to reflect the sharpening of the neural responses during stimulus encoding at different processing stages, and an increase of the precision with which future sensory events can be predicted (Friston, 2005). It is suggested as the mechanism underlying perceptual priming, implicit memory, and sensory memory-trace formation (James et al., 2000; Schacter et al., 2004; Haenschel et al., 2005). On the other hand, repetition enhancement (RE), an increase in the neural response that is also associated to stimulus recognition, learning, and prediction, has received much less attention (Segaert et al., 2013), especially in the auditory domain.

In the auditory system, individual neuron correlates of RS are provided by animal studies showing stimulus-specific adaptation (SSA), a decrease in neuronal spike firing in response to the frequent presentation of particular sound features, in cortical (Ulanovsky et al., 2003) and subcortical auditory nuclei (Perez-Gonzalez et al., 2005; Antunes et al., 2010; Antunes and Malmierca, 2011; Ayala and Malmierca, 2013; Duque and Malmierca, 2014). SSA may contribute to sensory memory formation at different processing stages, and at different time scales (Ulanovsky et al., 2004). A growing number of human studies using event-related potentials (ERP) show compatible evidence of increasing suppression of neuronal activity during memory trace formation (Baldeweg et al., 2004; Haenschel et al., 2005; Costa-Faidella et al., 2011; Cooper et al., 2013; but see: Bendixen et al., 2007; Ylinen and Huotilainen, 2007).

The bulk of human studies examined sensory encoding indirectly, by means of the mismatch negativity (MMN), a negative electroencephalographic (EEG) component elicited between 100 and 250 ms that is obtained by subtracting the ERP to a repetitive standard from the response to an infrequent deviant sound in an oddball paradigm (Näätänen et al., 1978). The MMN indexes deviance detection when an incoming stimulus is incongruent with the memory representation of the preceding stimuli (Näätänen et al., 2007). In line with animal findings, recent studies have shown that deviance detection, and hence regularity encoding, can occur very early in the time range of the middle-latency (MLR: 20 - 50 ms) and auditory brainstem (ABR: 5 - 20 ms) responses, and in hierarchically lower areas of the auditory pathway than previously expected (Slabu et al., 2010; Grimm et al., 2011, 2012; Recasens et al., 2014a), thus suggesting that regularity encoding and subsequent deviance detection might be functionally organized in a hierarchical fashion (Cornella et al., 2012; Althen et al., 2013; Escera and Malmierca, 2014; Escera et al., 2014; Recasens et al., 2014b).

A more direct investigation of stimulus encoding during stimulus repetition can be achieved by using a "roving standard paradigm", where memory-traces are forced to reset after each train of repeated features is presented (Cowan et al., 1993). Baldeweg and colleagues (1999, 2004) first identified a positive deflection at fronto-central sensors in the ERP of standard sounds that increased with increasing number of repetitions. This modulation termed repetition positivity (RP) spans between 50 and 250 ms post-stimulus and greatly contributes to the "MMN memory trace effect" (Näätänen, 1992; Javitt et al., 1998), that is, the increase of the MMN amplitude as a function of the preceding number of standards (Baldeweg et al., 2004; Haenschel et al., 2005; Costa-Faidella et al., 2011a; Cooper et al., 2013). The rapid modulation to repeated features, as well as the different adaptation sensitivity over multiple time-scales (Ulanovsky et al., 2004; Costa-Faidella et al., 2011b), suggests that RP might be a better human correlate of the animal SSA than MMN. However, it is worth noting that RP represents both an increase of P50 and P2, and a decrease of N1 components of the auditory ERP, thus it is likely to involve both RS and RE in different time-intervals. In addition, the resistance towards neural fatigue shown at P50 and P2 components, and the stable scalp distribution occurring across different experimental conditions (Costa-Faidella et al., 2011a) suggests that RP originates from a combined modulation of the ERPs involved at different time-intervals, rather than from a separate overlaying slow ERP component (Haenschel et al., 2005; Costa-Faidella et al., 2011a). Therefore, it can be assumed that different generators might exist encoding different levels of acoustic regularity in different stages of the processing hierarchy (Haenschel et al., 2005; Baldeweg, 2006, 2007; Cooper et al., 2013). However a direct assessment of the human generators of RP has not been carried out thus far.

In the auditory domain, repetition enhancement at the time range of the N1 has been established for the presentation of paired tones at very short inter-stimulus intervals (ISI), below 250-350 ms (Loveless et al., 1989; Wang et al., 2008; Heinemann et al., 2010). At longer ISI, enhancement effects are reflected at later time-intervals as a sustained negativity component, between 150 and 500 ms after stimulus onset in paired tone sequences (Heinemann et al., 2011). Näätänen and Rinne (2002), and Ylinen and Huotilainen (2007) using a roving standard paradigm, observed a later sustained negativity that was larger for repeated sounds. However, in the latter study the late enhancement only tended to increase as a function of stimulus repetitions, leaving open the question of whether late RE might reflect a mechanism of memory-trace formation analogous to RS in the auditory cortex.

In the present study we aimed at unraveling the spatio-temporal dynamics of memory-trace formation by assessing the anatomical areas underlying RS and RE during stimulus repetition using magnetoencephalography (MEG). To our knowledge, this is the first attempt to localize the neural substrates of human auditory stimulus repetition at different time intervals. This might help understanding whether RP is generated in one specific brain area or whether it is a non-unitary phenomena accounted for by the modulation of hierarchically organized processing stages devoted to the encoding of different levels of acoustic regularity. Furthermore, it has been hypothesized that frontal and parietal connections with auditory cortices might be involved during repetition suppression (Baldeweg, 2006), an idea supported by "predictive coding" accounts (Friston, 2005; Garrido et al., 2008) as part of the top-down adjustment occurring during perceptual learning. So far, the involvement of non-auditory neuronal sources in the generation of repetition effects like the RP has been scarcely studied and only indirect evidence is provided from EEG studies (Haenschel et al., 2005; Cooper et al., 2013) and anatomical findings (Romanski et al., 1999). Here, we expected to find a modulation of different anatomical generators activated at different time intervals, supportive of a non-unitary phenomenon reflecting the encoding of different aspects of the acoustic information at different stages. In addition to RS, we expected to clarify the involvement of RE as indexing memory-trace formation. Finally, we hypothesized that non-auditory areas would participate in the encoding of stimulus-specific memory traces, thus extending the notion that acoustic memory-trace formation is driven by plastic changes that extend beyond the auditory cortex.

Materials and Methods

Subjects/participants

Thirteen healthy, normal-hearing subjects (12 females, 12 right-handed) aged 23–35 years (mean age = 28 years; standard deviation = 3.3) took part in the experiment. Hearing level was assessed binaurally with a pure tone audiometry for 5 frequencies (250, 500, 1000, 3000, and 8000 Hz) before the task. All participants had hearing levels within the normal range. The experimental protocol was approved by the Ethical Committee of the University of Barcelona and was in accordance with the Code of Ethics of the World Medical Association (Declaration of Helsinki). Participants gave written informed consent before the experiment.

Stimuli and Procedure

Auditory stimuli consisted of 50-ms pure sine wave sounds (5 ms rise/fall), generated with Audacity software (version 1.3; http://audacity.sourceforge.net/). Tones were delivered binaurally at ~85 dB SPL using an Etymotic ER-30 system (Etymotic Research, Inc. United States of America) via plastic tubes and foam earpieces. The 18-ms delay in the transmission of sound was compensated for by an appropriate shift of the trigger signal. The experimental stimulation was controlled using Psychophysics Toolbox (Brainard, 1997). We used a modified version of the "roving standard" frequency paradigm (Cowan et al., 1993), also described in Baldeweg et al. (2004) and Costa-Faidella et al. (2011a). Trains of three, twelve, and 24 equal tones were randomly delivered at a constant stimulus-onset-asynchrony (SOA) of 500 ms, with no inter-train pauses (Figure 1). In total, 198 trains of three, twelve, and 24 tone repetitions were delivered, which resulted in threefold stimuli from 1st to 3rd positions, and twofold stimuli from 4th to 12th positions. Overall, the recording lasted for one hour and was split into 2 runs. Subjects were required to relax and lie as still as possible on a bed with their head inside the helmet-like device during the whole recording session. Participants were instructed to ignore the auditory stimulation, and to attend to a silent movie with subtitles. No subjects were discarded due to excessive head movement (> 0.7 cm).

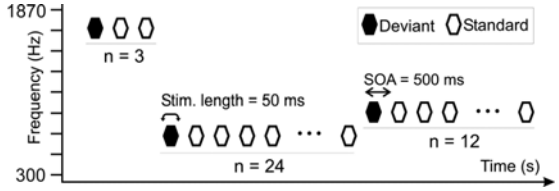

Figure 1: *Illustration of the roving standard frequency paradigm used in the present study. Trains of three, twelve, and twenty-four equal tones were randomly delivered at 500 ms SOA. Tone frequency varied randomly across trains with the only restriction that one particular frequency could not re-appear until four different frequencies had appeared before. Nine different frequencies, ranging from 300 to 1870 Hz, with a frequency ratio between adjacent frequencies of 0.23 were used (Δf = (f2 - f1) / (f2 x f1) $^{1/2}$; Ulanovsky et al. 2003). Stimuli in the first position of each train acted as low-probability events, or deviants (black hexagon). Subsequent presentations of the same tone, standards (white hexagon), were chosen in different position to assess repetition effects.*

Data acquisition

A whole-head magnetoencephalography (MEG) system (148 biomagnetometers, 4D Neuroimaging Magnes 2500WH, San Diego, CA, United States of America) recorded the magnetic currents at 678.17 Hz sampling rate. Data were on-line high-pass filtered at 1 Hz and stored for off-line analysis. A bipolar electrooculogram was recorded to identify eye movements. Five position coils were attached to the forehead and to the periauricular points in order to determine the position of the head and to track any head movement occurring during the recording. For each subject, the headshape including the forehead, the nose, and the location of the sensor position coils were digitized using a digitizer wand (Polhemus Fastrak, Polhemus Inc., Colchester, VT, United States of America). Additionally, T1-weighted, 3-dimensional (3D), magnetic resonance images (MRIs) of each individual brain were acquired to allow superimposition of MEG and MRI data.

Preprocessing

Pre-processing of sensor-level data was performed using FieldTrip (Oostenveld et al., 2011; http://fieldtrip.fcdonders.nl, 20130909 release) running under Matlab v7.14 (The MathWorks). Twenty minutes of continuous recording were used to apply independent component analysis decomposition (ICA) using the "runica" algorithm as implemented in Fieldtrip. An automatic approach based on amplitude and phase statistics of the decomposed MEG signal was used to identify the strongest components corresponding to biological artifacts (Dammers et al., 2008). On average, 6.5 components per subject were identified. Continuous MEG data was filtered from 1 to 30 Hz (two-pass Butterworth filter) and artifactual independent components were removed after manual inspection of its scalp topography and continuous activity. Epochs of 600 ms, starting 100 ms before stimulus onset and baseline corrected from -100 to 0 ms, were extracted. Epochs exceeding amplitudes of 3 pT were discarded from subsequent analyses. On average, 35.6 out of 198 trials were rejected per subject and condition.

For the analysis of repetition effects individual trials were averaged according to their position in the trains. Therefore, trials presented in the same position but belonging to trains of different length were averaged together. Only stimuli in positions 3rd to 24th were analyzed to assess repetition effects. The first tone in each train (deviant) and the second tone (first repetition) were excluded from the analyses of repetition effects, in order to avoid residual effects from the preceding deviant, or "after deviant" effects (Sams et al., 1984; Nousak et al., 1996; Roeber et al., 2003). As previously mentioned, across-position averaging yielded three times as many stimuli from 1st to 3rd positions, and twice as many stimuli from 4th to 12th positions compared to the number of stimuli from 13th to 24th positions. In order to keep signal-to-noise ratios balance, and to avoid power problems inherent with a 24-level factor design, we grouped the different positions into 6 "repetition groups": 3rd to 4th, 5th to 6th, 7th to

9th, 10th to 12th, 13th to 18th, and 19th to 24th. In a separate analysis we assessed whether responses to deviant sounds increased as a function of the preceding number of standards. Therefore, deviants after three, twelve, and twenty-four repetitions were averaged separately. In all cases, frequencies were collapses together.

We computed the global field power (GFP) of the grand averaged data and defined four intervals of interest (IOI) based on the peak latencies of the main ERP components (P50m, N1m, and the Sustained Field [SF]). Mean peak latency for P50m was at 51 ms at both hemispheres (SD = 3 ms). N1m peak latency occurred at 113 ms (SD = 13 ms) in the right hemisphere and 128 ms (SD = 14 ms) in the left hemisphere. The peak latency of the sustained field (SF), with a scalp distribution analogous to a negative EEG component, occurred at 254 ms (SD = 22 ms) and 244 ms (SD = 17 ms) in the right and left hemispheres, respectively. Given that the peak latency of the N1m grand average showed a clear difference between hemispheres, the interval of interest was split in two for the N1m time range. Intervals of interest (IOI) were finally defined as windows between 45–55 ms for P50m, 95–115 ms for the early N1m, 130–150 for the late N1m, and 230–270 for the SF. In addition, a larger IOI between 100–140 ms was defined to assess deviant effects.

Source estimation

To estimate brain sources we used an anatomically constrained MEG approach that poses an anatomical constrain to the estimated sources by assuming that each individual's recorded brain activity lies in the cortical mantle (Dale et al., 2000). First, precise co-registration of MEG and structural MRI data was accomplished using a semiautomatic procedure. Landmark (nasion, and the 2 periauricular points) information was used for a first alignment of the MEG and MRI coordinate systems. The digitized head shape and the scalp surface of each individual were then used to reduce the minimum distance error between them in an iterative process. Cortical surfaces were created for each individual subject by automatically segmenting the T1-weighted MRIs into gray and white matter and defining the border between gray and white matter as the cortical surface. Subsequent tessellation and inflation of the folded surface patterns was carried out using Freesurfer (Dale et al., 1999; Fischl et al., 1999a; http://surfer.nmr.mgh.harvard.edu/). Each individual inflated cortical surface was subsampled to ~7500 dipole locations per hemisphere, equivalent to ~5 mm spacing, as the solution space for the estimated current generators. The forward model was completed in Brainstorm (Tadel et al., 2011) using an overlapping-sphere analytical model. The activation at each latency and dipole (constrained orientation) was estimated using a noise-sensitivity normalized linear inverse solution known as dynamic statistic parametrical mapping (dSPM). Since dipole strength power is divided by the predicted noise in dSPM (Dale et al., 2000), we obtained normalized dipole strengths with a t-distribution that approaches a unit normal distribution (i.e., z-scores). Therefore, dSPM at a particular latency and location is a display of the statistical test between activity evoked by a condition and the baseline period, and can thus be interpreted as signal-to-noise ratio maps (for a similar procedure, see: Marinkovic et al., 2003, 2011; Travis et al., 2011). Results from each individual were aligned by morphing each participant's brain to an average template using a spherical morphing procedure that allowed for accurate inter-subject averaging (Fischl et al., 1999b), and a Gaussian smoothing kernel of 10 mm full-width half-maximum (FWHM) was applied. Significance levels reported on the average dSPM maps were derived by taking the square root of the F-distributed mean activity with 13 degrees of freedom in the numerator (1 constrained dipole at each location x 13 subjects), and 1632 in the denominator, derived from the number of time points used to calculate the noise covariance. Therefore, significant thresholds for all conditions were set between $p < 0.05$ corresponding to a dSPM value of 2.81, and $p < 10^{-12}$ corresponding to a dSPM value of 11.23 (Figure 2).

Whole-brain analysis

Individual dSPM maps computed for the averaged "grouped repetitions" (3rd to 4th, 5th to 6th, 7th to 9th, 10th to 12th, 13th to 18th, and 19th to 24th) were exported to SPM8 (Wellcome Trust Center for Neuroimaging, London, United Kingdom; http://www.fil.ion.ucl.ac.uk) for a whole-brain analysis. Mean activity within the 4 predefined IOIs was computed and repetition effects were assessed using a one-way repeated measures analysis of variance (ANOVA). This analysis followed a conventional General Linear Modeling (GLM) approach, and allowed us to examine which brain regions were significantly modulated by stimulus position. In order to test our initial hypothesis that both RS and RE would occur at different time intervals we carried out planned contrasts between grouped repetitions 3rd to 4th (Initial), 10th to 12th (Middle), and 19th to 24th (Late). Activation was considered significant at a conservative voxelwise threshold of $p < 0.05$ (family-wise error [FWE]-corrected). Following the same criteria, the effect of the preceding number of repetitions on the deviant was tested. Planned contrasts were carried out between deviants preceded by three, twelve, and 24 repetitions. T-tests were applied for all planned contrasts.

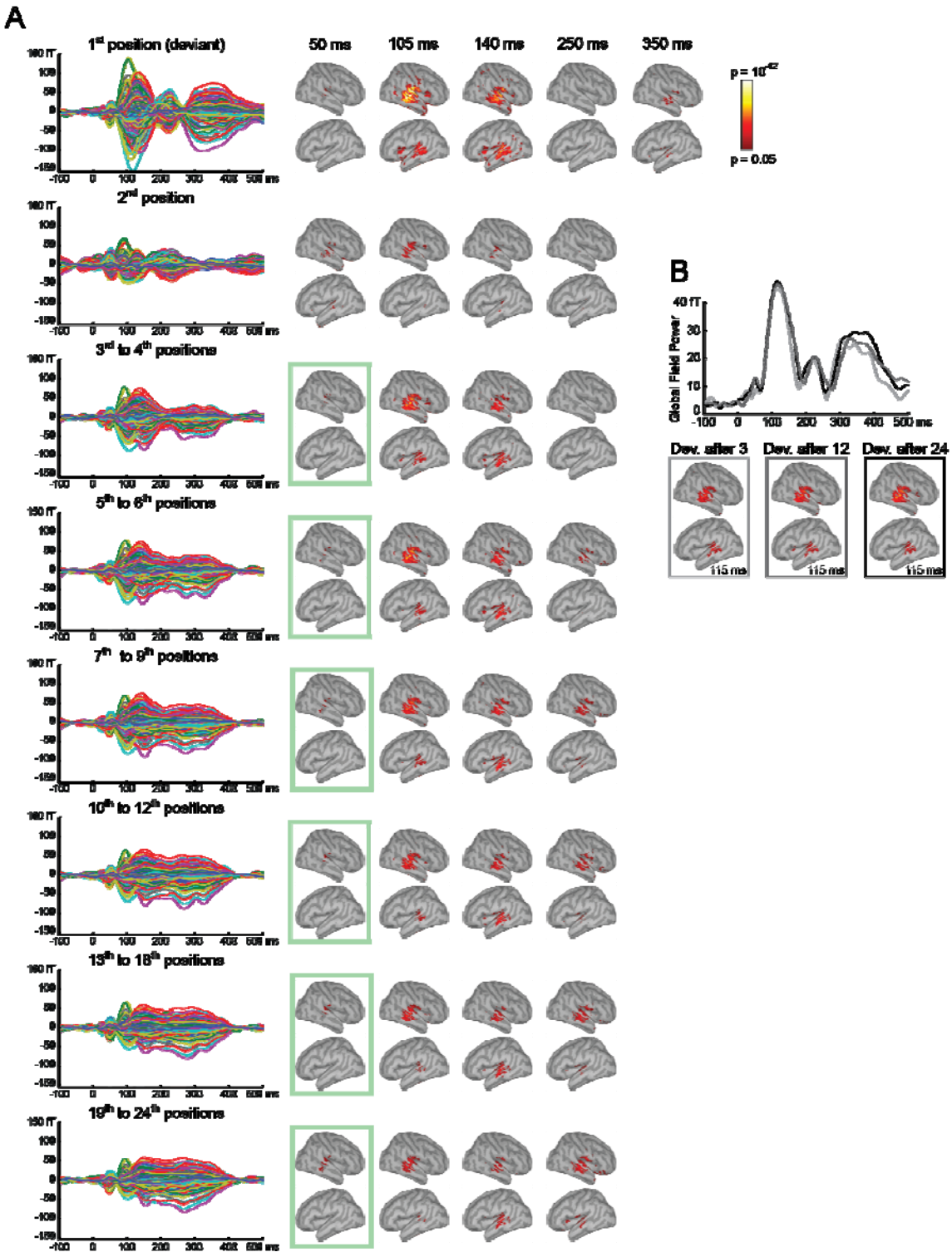

Figure 2: *Representation of group activity in the sensor and source level. (A) Grand averaged event-related fields (ERF) and dSPM activity to stimuli presented in each position group analyzed. Responses to the first and second presentation of a tone in the train are illustrated together with the grouped positions that were used for the analysis: 3rd to 4th, 5th to 6th, 7th to 9th, 10th to 12th, 13th to 18th, and 19th to 24th (rows). Colored bars and boxed in the ERF indicate the time intervals of interest (IOI) used in the analysis: 45–55 ms, 95–115 ms, 130–140 ms, and 230–270 ms. Gray bars indicate that activity from deviant and first repetition was not used in repetition effects analysis. Source-level group activity is illustrated at the center or the IOI, and also at 350 ms for the deviant stimulus. dSPM activity was thresholded from $p < 0.05$ (full red) to $p = 10^{-12}$ (full yellow). (B) Grand averaged activity of the deviant sounds (above) presented after a train of 3 (light grey), 12 (mid grey), and 24 (dark grey) stimuli. The global field power (GFP) of all channels is illustrated. (Below) dSPM activity at 115 ms after sound onset for the deviant types. Threshold are the same as in (A)*

.

ROI analysis

We additionally analyzed cortical activation in each subject using anatomically pre-defined regions of interest (ROI). This approach has the advantage of allowing the detection of weak brain activity that could be missed using whole-head approaches that require strong statistical thresholding. The same set of ROIs was used for all subjects, blind to the individual activation, by an automatic spherical morphing procedure (Fischl et al., 1999b). Due to the relatively low spatial resolution of MEG imaging, we used relatively large ROIs. The definition of the ROIs in the present study was guided both by the pre-existent literature on the anatomical sources of the MMN known to indirectly reflect sensory-memory, and the results obtained from the whole-brain analysis. We selected those anatomical regions from the Desikan-Killiany atlas (Desikan et al., 2006) that overlapped areas showing a significant modulation by stimulus position and, these areas were in accordance with previously reported sources in the literature.

In supratemporal regions, ROIs were defined according to the notion that most MMN studies localize the sources of MMN in the superior temporal gyrus (STG) and the vicinity of the Heschl's gyrus (Jääaskeläinen et al., 2004; Opitz et al., 2005; Schönwiesner et al., 2007; Recasens et al., 2014a, 2014b). Given the antero-posterior localization of effects that was observed at different intervals in the whole-head analyses, and in accordance with previous literature showing a functional separation of anterior and posterior STG regions (Jaaskelainen et al., 2004; Recasens et al., 2014b), we decided to split the STG into two equally sized portions (~28 cm^2), thus giving rise to a posterior STG ROI, and an anterior STG ROI. A separate ROI covering the HG (~5 cm^2), bilaterally, was defined according to the Desikan-Killiany atlas location. A frontal ROI (~50 cm^2) was selected on the basis that frontal generators are expected to underlie memory-trace formation (Baldeweg et al., 2004; Haenschel et al., 2005; Baldeweg, 2006, 2007; Cooper et al., 2013), and frontal MMN generators have consistently been reported in previous studies (Giard et al., 1990; Rinne et al., 2000; Yago et al., 2001). The specific location of the frontal ROI was defined by merging the pars opercularis and pars triangularis, according to the Desikan-Killiany atlas location. Finally, a large ROI (~51 cm^2) was defined on medial parietal regions, overlapping the precuneus, bilaterally. Previous studies report parietal activation as part of a broad network devoted to deviance detection (Alain et al., 2001; Molholm et al., 2005; Laufer et al., 2009; Boutros et al., 2011). Figure 4 shows an illustration of the selected ROIs.

A source-waveform for each ROI and condition was obtained by deriving the mean activity of all the vertices within each ROI. For each ROI waveform, in each hemisphere, we retrieved the individual peak amplitudes within the predefined IOIs and performed repeated-measures ANOVA with factors REPETITION (6 repetition groups) and HEMISPHERE (left and right) in each ROI and time-interval. In addition, we carried out planned contrasts on repetition groups (initial, middle, late) to assess whether RS or RE was present in the different ROIs and time-intervals. Repetition effects and planned contrasts were considered significant at $p < 0.05$ after Bonferroni correction. Greenhouse-Geisser correction (GG) was applied when the sphericity assumption was violated. Repetition effects are reported if planned contrasts show significant effects of either suppression or enhancement. The increase of the deviant as a function of the preceding number of repetitions was assessed using the same criteria in a repeated-measures ANOVA with factors PRECEDING NUMBER OF REPETITIONS (deviants after 3, 12, and 24 presentations) and HEMISPHERE (left, right). Bonferroni correction was applied to all planned contrasts.

Results

Dynamic Statistical Parametric Maps (dSPM)

Source localization using dSPM revealed the neuronal generators underlying auditory evoked activity at different time intervals (Figure 2A). At the P50m interval, around 50 ms after stimulus onset, activity was greater in the right hemisphere. Neuronal generators were located in the posterior part of the STG, bordering the posterior rim of the HG. This pattern was consistent across repetitions. Two clear subcomponents with a typically EEG-negative dipolar pattern emerged during the time interval of the N1m, between 95 and 140 ms after sound onset (see figure 2A, left column). At 105 ms activation overlapped the posterior part of the STG, MTG, and the HG, bilaterally. During the late interval of the N1m around 140 ms activation emerged more anteriorly, overlapping the HG, the MTG, and the anterior STG. This propagation towards more anterior regions in the supratemporal plane was more pronounced in the right hemisphere. Additionally, activation was found in non-auditory regions like the precuneus, the anterior insula, and prefrontal regions especially during the onset of the deviant sound. A clear P2m component around 250 ms after sound onset appeared only for the first and second sound presentation in the repetition trains. On the other hand, a late SF

appeared only after three stimulus presentations, spanning from 230 ms to 400 ms approximately. Activation during the SF interval was maximal after 24 repetitions and was located in middle and anterior portions of the supratemporal plane, overlapping the HG and the anterior part of the STG, especially in the right hemisphere. Additional activation was found in frontal areas and the medial wall of the posterior parietal cortex.

Whole-brain: Repetition effects

Using SPM8, a one-way analysis of variance was carried out to examine repetition effects in the whole-brain. Details from repetition analyses and planned contrasts analyses at the different IOIs examined are detailed in table 1. In short, no planned contrasts indicating either RS or RE were found during the P50m time interval. During the early N1m interval (Figure 3, upper row), overall suppression from initial to late repetitions occurred in the left ($P_{FWE} < 0.001$; peak MNI: -3 -47 58) and right ($P_{FWE} = 0.018$; peak MNI: 4 -49 56) precuneus. In temporal areas, a large cluster showed a significant effect of suppression in the right rolandic operculum ($P_{FWE} = 0.008$; peak MNI: 54 -10 15), and regions of the right HG, STG, and MTG ($P_{FWE} = 0.016$; peak MNI: 44 -22 9). In the left hemisphere, maximal suppression with repetitions occurred in the MTG ($P_{FWE} = 0.002$; peak MNI: -55 -37 3). A clear RS from middle to late repetitions was only observed in the right ($P_{FWE} = 0.029$; peak MNI: 4 -67 40) and left precuneus ($P_{FWE} = 0.020$; peak MNI: 0 -59 38). Similarly, during the late N1m interval only a cluster centered in the left precuneus showed significant RS from initial to middle repetitions ($P_{FWE} = 0.018$; peak MNI: -3 -51 46).

Clear RE effects were shown at the late SF interval (Figure 3, middle row). A main right-hemispheric cluster extending anteriorly towards the anterior part of the rolandic operculum overlapped the HG ($P_{FWE} < 0.001$; peak MNI: 48 -16 7), the STG ($P_{FWE} = 0.002$; peak MNI: 60 -25 11), and portions of the right insula anterior to the HG ($P_{FWE} = 0.003$; peak MNI: 46 -6 5). The same regions showed RE for the initial versus middle, and middle versus late repetitions. In the left hemisphere, a smaller clusters located in the STG ($P_{FWE} = 0.023$; k = 10; peak MNI: -61 -22 5) showed RE when comparing initial against late repetitions. Figure 3 (bottom row) shows the overlap between RS at the early N1m interval and RE at the SF interval.

In a separate analysis we assessed the localization of memory-trace effects on the deviant response. Neither overall repetition effects nor planned contrasts revealed statistically significant effects at the conservative threshold level of $P_{FWE} < 0.05$. By lowering the voxel threshold at $P < 0.001$ (uncorrected) the comparison between deviant activity after 24, and 3 repetitions revealed a large cluster located between the right HG and the rolandic operculum (*cluster*-$P_{FWE} = 0.021$; k = 539; peak MNI: 46 -18 15) where deviant activity after 24 repetitions was greater than deviant activity after 3 repetitions. Though no voxels within the cluster reached FWE-corrected values, a cluster of this size would hardly occur by chance.

ROI analysis: Repetition effects

In order to confirm the reliability of RS and RE effects in different time intervals and brain areas, statistical testing was performed on the cortically extracted source-waveforms from each of the 5 bilateral ROIS. In the same way as for the whole-brain analysis, repetition effects were analyzed and planned contrasts were performed between initial (3^{rd} to 4^{th}), middle (10^{th} to 12^{th}), and late (19^{th} to 4^{th}) repetitions in order to assess the direction of the effects (RS or RE). Results are depicted in figure 4. For bilateral ROIs delineated in the posterior STG (pSTG) at the P50m time interval (45 – 55 ms) an effect of hemisphere was found ($F(1, 12) = 13.53$; $p = 0.003$) pointing to a greater activation on the right hemisphere. At the early N1m interval (95 – 115 ms) activity was also higher in the right hemisphere ($F(1, 12) = 5.38$; $p = 0.039$). An effect of repetition was observed ($F(5, 60) = 14.99$; $p < 0.001$) and planned contrasts revealed suppression between initial and late ($p = 0.001$), and middle and late ($p = 0.009$) repetitions. At the later N1m interval (130 – 150 ms) repetition effects ($F(5, 60) = 5.99$; $p = 0.009$, GG) revealed suppression from middle to late repetitions ($p = 0.048$). In the time interval of the SF (230 – 270 ms) hemisphere effects ($F(1, 12) = 14.78$; $p = 0.002$) showed a greater activation in the right hemisphere, but planned contrasts revealed no effect of suppression or enhancement. In the ROIs located in the anterior STG (aSTG), an effect of stimulus repetition was observed for the early N1m interval ($F(5, 60) = 12.57$; $p < 0.001$), where initial repetitions showed higher activity than middle ($p = 0.009$) and late ($p = 0.003$) presentations. At the late N1m interval repetition effects ($F(5, 60) = 7.97$; $p < 0.001$) revealed suppression from initial to late repetitions ($p = 0.039$). Contrarily, at the later interval of the SF repetition effects ($F(5, 60) = 9.84$; $p < 0.001$, GG) revealed an effect of enhancement from initial to middle ($p = 0.002$), and from initial to late ($p = 0.002$) presentations. The ROI delineated in the HG revealed stronger activation in the right hemisphere during the P50m interval ($F(1, 12) = 31.61$; $p < 0.001$).

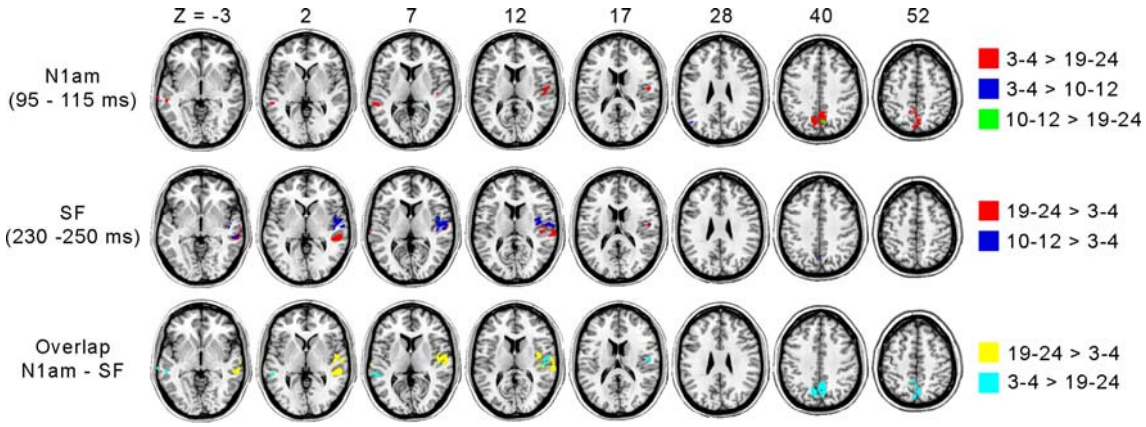

Figure 3: *Whole-brain analysis: axial sections depicting significant activity (p < 0.05, FWE corrected) for the three contrast of interest. Colored areas indicate repetition suppression (RS) at the early N1m interval (upper row), and repetition enhancement (RE) in the SF interval (middle row). Intial vs. Late (red), Initial vs. Middle (blue), Middle vs. Late (green) contrasts are illustrated when statistically significant activity occurred. The overlapping between the Initial vs. Late contrast activity, showing RS in the early N1m (cyan), and RE during the SF interval (yellow), is depicted in the bottom row.*

An interaction between hemisphere and repetition occurred at the early N1m interval ($F(5, 60) = 3.28$; $p = 0.037$, GG). Repetition effects showed up in the left hemisphere ($F(5, 60) = 6.35$; $p = 0.001$, GG), where repetition suppression occurred between initial and late ($p = 0.011$), and between middle and late ($p = 0.015$) repetitions. The same effects were reported in the right hemisphere ($F(5, 60) = 12.82$; $p < 0.001$, GG), where RS occurred between initial and late ($p = 0.006$), and between middle and late ($p = 0.004$) repetitions. At the SF interval activity was stronger in the right hemisphere ($F(1, 12) = 7.52$; $p = 0.018$). An interaction between hemisphere and repetition ($F(5, 60) = 2.77$; $p = 0.026$) revealed repetition effects in the left ($F(5, 60) = 3.78$; $p = 0.025$, GG) and right hemispheres ($F(5, 60) = 6.79$; $p = 0.002$, GG). Planned contrasts revealed repetition enhancement in the left hemisphere between initial and late ($p = 0.024$), and between middle and late ($p = 0.038$) repetitions. Similarly, RE occurred between initial and middle ($p = 0.012$), and between initial and late ($p = 0.022$) repetitions in the right hemisphere.

In the frontal ROI (Front), repetition effects occurred in the late N1m interval ($F(5, 60) = 3.69$ $p=0.006$) where suppression occurred between initial and late repetitions ($p = 0.018$), and in the later SF interval ($F(5, 60) = 6.98$; $p = 0.002$, GG), where enhancement occurred between all possible contrasts: initial and middle ($p = 0.018$), initial and late ($p = 0.002$), and middle and late ($p = 0.025$).

Finally, in the ROI delineated in the precuneus, an effect of hemisphere was found for the P50m ($F(1, 12) = 5.67$; $p = 0.035$), early N1m ($F(1, 12) = 6.58$; $p = 0.025$), late N1m ($F(1, 12) = 4.91$; $p = 0.047$), and SF ($F(1, 12) = 6.02$; $p = 0.03$). Activity was greater in the right hemisphere in all intervals. Repetition and planned contrast effects were found in the early N1m ($F(5, 60) = 9.51$; $p < 0.001$), and SF ($F(5, 60) = 6.76$; $p < 0.001$) intervals. At the N1m time range, RS occurred between initial and late ($p = 0.001$), and between middle and late ($p = 0.02$) repetitions. At the SF interval, RE occurred between initial and middle ($p = 0.026$), and between initial and late ($p = 0.021$) repetitions.

The ROI analysis carried out on the different deviant stimuli revealed hemisphere effects in the HG ($F(1, 12) = 6.13$; $p = 0.029$) and precuneus ($F(1, 12) = 5.08$; $p = 0.044$). In both regions activity was significantly higher in the right hemisphere. An effect of the preceding number of standards was found only in the HG ROI ($F(2, 24) = 3.64$; $p = 0.042$). However, planned contrasts between the three different deviant types failed to reveal a significant increase or decrease as a function of preceding repetitions.

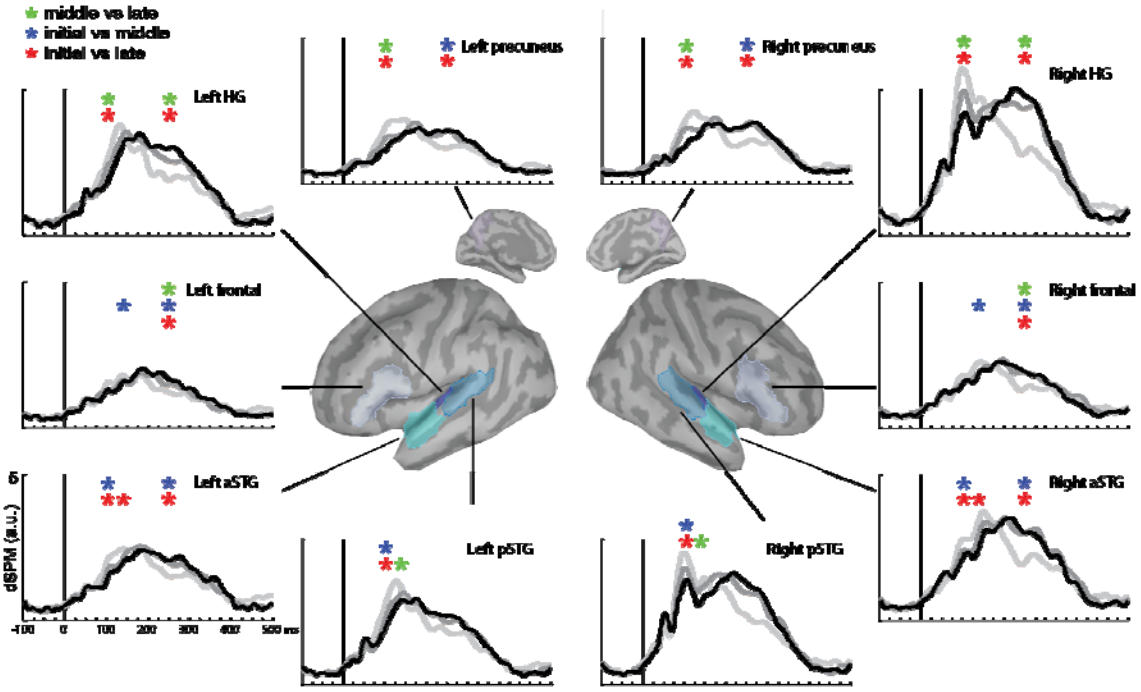

Figure 4: *ROI analysis. Center: ROIs represented in an inflated template cortical surface (medial view above, lateral view below). Surround: group averaged time courses for the estimated dSPM activity. Position-averaged activity for the Initial (light grey), Middle (mid grey), and Late (black) repetitions is represented in arbitrary noise-normalized units. Asterisks indicate statistically significant differences ($p < 0.05$, Bonferroni corrected) between the contrasts of interest: Initial vs. Late (red), Initial vs. Middle (blue), Middle vs. Late (green).*

Discussion

This study aimed to unravel the spatio-temporal dynamics underlying auditory memory-trace formation in the human brain. Results presented here describe repetition suppression (RS) and repetition enhancement (RE) as two complementary mechanisms of regularity encoding, occurring at different time scales and spatial locations. Our results indicate that N1m is suppressed during repetitive stimulation. RS at the N1m interval was found in supratemporal regions including the HG, STG, and the MTG. Notably, non-auditory regions like the precuneus, bilaterally, showed strong RS during a long time interval comprised between 95 and 150 ms after sound onset. The novel finding of the present study is, however, the source localization of repetition-based enhancement that was found at a much later time interval, between 230 and 270 ms. An increasing sustained field was evoked by stimulus repetition approximately around 200 ms after stimulus onset and lasted until 300 ms after onset. Like the suppressing N1m, the neuronal generators of this SF involved the right HG, the STG, the MTG, and extended over anterior regions of the insula and the rolandic operculum. The precuneus also showed RE at this later latency. ROI analyses confirmed that frontal regions in the pars opercularis and pars triangularis, or inferior frontal gyrus (IFG), were involved during RE between 230 and 270 ms. RS occurred in frontal areas during the later part of the N1m only, but not during the early interval around 100 ms. During the SF, no RE was found in the posterior part of the STG, suggesting that RS during the N1m interval and RE during the SF interval might have different neural generators, with early N1m sources located more posteriorly than SF generators. Overall, our findings suggest that both RS and RE, at different time- and spatial-scales, underlie the strengthening and formation of auditory memory traces. In fact, here we provide first evidence that a late sustained field is generated in both auditory and non-auditory regions, and reflects the encoding of acoustic invariances during high numbers of repetitions.

Table 1: *Whole-brain analysis: MNI coordinates, p-values, and t/F scores for brain regions exhibiting statistically significant values (peak-p < 0.05 [FWE-corrected], k > 5) in the different intervals and contrasts investigated.*

	N vox. (k)	Cluster p (FWE)	Peak p (FWE)	Peak F / t	Peak MNI coordinates X	Y	Z	Cortical region (AAL)
P50 (45 – 55 ms)								
Repetition effects	6		0.027	4.66	38	-14	11	R. Insula
N1am (95 – 115 ms)								
Repetition effects	61		0.001	12.31	42	-29	32	R. Supramarginal gyrus
	54		0.004	10.78	-11	-67	38	L. Precuneus
	11		0.009	10.04	-3	-47	48	L. Precuneus
	21		0.026	9.14	-11	-49	52	L. Precuneus
	124		0.004	10.68	0	-63	38	Precuneus bilat.
	10		0.038	4.56	-19	-69	24	L. Sup. Occipital gyrus
	131		0.005	10.53	56	-10	15	R .Rolandic Op.; HG; STG
Initial vs. Middle	32	0.009	0.004	5.56	-47	-69	26	L. Angular gyrus
Initial vs. Late	588	< 0.000	< 0.000	6.23	0	-59	38	Precuneus bilat.
	85	0.002	0.001	5.91	-11	-67	38	L. Precuneus
	32	0.009	0.004	5.58	-67	-51	-15	L. Inferior temporal gyrus
	100	0.001	0.008	5.39	54	-10	-15	R. Rolandic Op.; HG; STG
	89	0.002	0.009	5.34	-55	-37	3	L. MTG
	13	0.02	0.024	5.04	-71	-27	3	L. MTG
Middle vs. Late	33	0.009	0.02	5.11	0	-59	38	Precuneus bilat.
N1bm (130 – 150 ms)								
Repetition effects	16		0.005	10.55	58	-18	15	R. MTG
Initial vs. Middle	10	0.023	0.018	5.14	-3	-51	46	L. precuneus
SF (230 – 270 ms)								
Repetition effects	74		0.002	11.28	48	-14	7	R. HG; STG; Rolandic op.
	30		0.006	10.49	36	-6	15	R. Insula
	18		0.02	9.37	62	-29	-5	R. MTG
	6		0.034	8.91	46	-4	7	R. ant Rolandic op.
Initial vs. Middle	515	< 0.000	< 0.000	-7.06	48	-14	7	R. HG; Ins; STG
	75	0.003	0.006	-5.47	58	-29	-5	R. MTG
	6	0.029	0.017	-5.16	0	-65	40	Precuneus bilat.
Initial vs. Late	570	< 0.000	< 0.000	-7.15	48	-16	7	R. HG; STG; Ins
	233	< 0.000	0.001	-6.13	58	-31	-5	R. MTG
	10	0.023	0.023	-5.06	-61	-22	5	L. STG
Deviant (100 – 140 ms)								
After 24 vs. After 3	539	0.021	n.s.	4.56	46	-18	15	R. Rolandic op.; HG

Neuronal generators

The source estimates we obtained for the different stimulus repetitions revealed that P50m generators are located in the STG, and show a rightward lateralization. The STG origin of the early P50m response, in vicinity of the HG, is supported by previous studies using both intracranial (Liegeois-Chauvel et al., 1994; Yvert et al., 2005) and electrophysiological recordings (Huotilainen et al., 1998; Yvert et al., 2001; Huang et al., 2003). A rightward lateralization of the P50m responses is likewise supported by previous studies reporting lower signal-to-noise ratios in the left hemisphere (Korzyukov et al., 2007). Planned contrasts on the P50m interval failed to reveal significant differences between tone repetitions at different positions. However, frontal and anterior STG regions in our ROI analysis, and a small cluster located in between the right insula and the HG in our whole-brain analysis, revealed significant overall effects of repetition. In fact, previous research indicates that frontal generators contribute to the P50m response (Weisser et al., 2001), and that neuronal activity contributing to amplitude reduction or enhancement with stimulus repetition, a phenomenon known as "sensory gating", is localized in the frontal lobe (Korzyukov et al., 2007; Josef Golubic et al., 2014). While generators located in supratemporal planes are oriented tangentially, frontal sources with a radial orientation might be less suitable for source localization using MEG, which may explain why no clear effects of repetition were found in frontal areas.

The N1m peak activity at the early interval was located in posterior regions of the STG and HG bilaterally. Our results are in agreement with the intracranial localization of Yvert et al. (2005), showing that N1m sources involved almost the same areas as those active during the P50m interval. Even though the greatest N1m activity was localized in supratemporal regions in our dSPM maps, repetition effects showed the strongest suppression in the posteromedial portion of the parietal lobe, the bilateral precuneus. In the context of the MMN, parietal activation has been regarded as a sign of increased attentional switching towards salient deviations (Dittmann-Balçar et al., 2001; Molholm et al., 2005; Laufer et al., 2009). In the present study, however, we observed a suppression of parietal activation with stimulus repetition that precedes deviance detection. In consonance with results presented by Boutros et al. (2011) parietal regions might represent a mechanism involved in both information encoding and the subsequent detection of relevant changes. As reflected in the dSPM activations, SF activation involved more anterior regions of the supratemporal plane as compared to early N1m sources. This spatial pattern was mimicked in the repetition effects analysis. Whole-brain analysis revealed a temporal activation for the different repetition contrasts that spanned towards anterior regions of the right insula, below prefrontal areas, and anterior regions of the MTG. These results were confirmed by an effect of repetition enhancement in frontal and anterior STG regions, as observed in ROI analysis. Even though no previous studies have elucidated the neuronal generators underlying the sustained negativity, differences in terms of neural coding and spatial localization, as compared to N1m, might reflect the existence of separate mechanism devoted to stimulus encoding. Though speculative, differences in neuronal generators might suggest that the two processes are organized hierarchically, with different levels of information being processed serially at different time intervals. Such an organization is supported by previous studies suggesting a hierarchical organization of the deviance detection system, where more complex and integrated types of regularities are encoded in secondary auditory regions and in later time intervals (Cornella et al., 2012; Althen et al., 2013; Escera et al., 2014; Recasens et al., 2014b). Future research should specifically address whether RS and RE at different intervals reflect different information processing stages, or in other words, the encoding of different levels of acoustic information.

A neuromagnetic correlate of repetition positivity?

The ability of the brain to encode regularities has traditionally been studied using the MMN potential evoked in oddball paradigms. The MMN is suggested to reflect an automatic process of deviance detection between an incoming stimulus and the regularities previously encoded in form of sensory memory-representation (Näätänen et al., 2005). Even though MMN generation seems to be dependent on stimulus regularity encoding, oddball designs using one single standard feature do not allow explicit assessment of the mechanisms underlying regularity extraction, particularly those concerning the "standard" events. In the recent years few studies have precisely examined the role of stimulus repetition in the context of auditory memory-trace formation in the human brain. Using a roving standard presentation similar to ours, Baldeweg and colleagues (Baldeweg et al., 2004, 2006) showed that tone repetition modulates a large portion of the ERP at fronto-central scalp electrodes between 50 and 250 ms post-stimulus. This modulation, termed repetition positivity (RP), was observed as a positive polarity wave overlapping the P50-N1-P2 auditory evoked components. Further studies strengthened the idea that RP might reflect a direct index of sensory-memory formation (Baldeweg, 2006, 2007), as it is influenced both by attentional demands during active discrimination tasks (Haenschel et al., 2005), and the temporal predictability of the events during passive listening (Costa-Faidella et al., 2011a). It appears, however, that the modulation typically reflected in the RP to roving trains of standards does not hold for more complex sounds like known

vowels (Ylinen and Huotilainen, 2007), or more complex sequences where frequency repetitions are embedded in a sequence of duration-varying sounds (Bendixen et al., 2007). In the present study, a RP pattern was observed only partially. Repetition-related modulation was not found at the early time range of the P50m, between 45 and 55 ms post-stimulus onset. An enhancement at that latency would have been expected since the experimental paradigm and the long number of repetitions used was similar to previous studies (Haenschel et al., 2005; Costa-Faidella et al., 2011a). Methodological differences like the use of MEG, less sensitive to deep generators than EEG, and the subsequent decrement of statistical power, might account for the lack of early repetition-related modulations. On the other hand, a magnetic counterpart of the P2 was only observed for the first and second presentation in the trains, around 225 ms after stimulus onset. After the second sound presentation, the typical P2m scalp distribution had completely disappeared, and after three stimulus presentations scalp distribution at 225 ms resembled a typically EEG-negative component, probably reflecting the emergence of the later SF. In this regard, Shahin et al. (2007) observed that both radial and tangential sources, located in both primary and non-primary auditory regions respectively, contribute to the magnetic P2m component. The very fast adaptation, occurring after one or two presentations observed here might suggest that primary auditory areas contributing to the P2m component are highly sensitive to stimulus repetition and show a high degree of refractoriness. Contrarily, EEG might be more sensitive to generators located radially in secondary areas around the sulci, where repetition enhancement is typically observed during stimulus repetition (Baldeweg et al., 1999; Atienza et al., 2002; Costa-Faidella et al., 2011b).

In accordance with the expected RP effects, the N1m showed a clear decrement with increasing number of repetitions. A large body of literature has previously reported N1 adaptation with stimulus repetition during oddball presentations (Hari et al., 1982; Näätänen and Picton, 1987; Näätänen, 1992; Budd et al., 1998). Such strong finding has led to the alternative interpretation that non-specific N1 adaptation can in fact account for the whole of sensory memory-based effects of the MMN (Jääskeläinen et al., 2004; May and Tiitinen, 2010), or partially concur with them (Garrido et al., 2009). Suppression of the N1m component is a relatively stable effect observed in most roving standard studies and constitutes an essential part of the RP effects (Baldeweg et al., 2004, 2006; Haenschel et al., 2005; Costa-Faidella et al., 2011a; Cooper et al., 2013; but see: Bendixen et al., 2007; Ylinen and Huotilainen, 2007). Here, comparable effects were described at the anatomical level. Noteworthy, we showed RS in auditory and non-auditory regions during the N1m time range. Similarly, Boutros et al. (2011) reported a strong N1 suppression of frontal, parietal and cingulate areas that exceeded suppression found in typically auditory areas. In most cases, RS was stronger on the right hemisphere. In line with this previous research, results presented here indicate a strong suppression of the bilateral precuneus, located in the medial wall of the parietal cortex, and to a lesser degree in typical auditory regions like the HG, STG, and MTG during the early N1m interval. Both ROI and whole-brain analyses consistently showed that the precuneus was capable to track sound repetition after many presentations, as evidenced by the middle vs. late contrast. This might suggest that while rapid adaptation after few stimuli occurred in secondary auditory areas, non-auditory regions -and the HG as revealed in the ROI analysis- developed a slower long-term adaptation during the early N1m time range. Such notion would be in line with previous findings showing that auditory HG responses exhibit adaptation on multiple timescales in animals (Ulanovsky et al., 2004) and humans (Costa-Faidella et al., 2011b; Eliades et al., 2014). In addition, some empirical support for the separation we made of the N1m component in two different subcomponents was found. In the right hemisphere, dSPM estimates revealed a peak of activation in anterior areas of the STG during late N1m interval, whereas the early N1m interval had its loci located in the posterior STG. Jääskeläinen and collegues (2004) reported a similar pattern for N1m to novel sounds and suggested that anterior N1m sources might be more narrowly tuned to sound frequency, and thus, reflect a lesser degree of adaptation. Similarly, our results show few RS effects in the late N1m time range as compared to the posterior and early N1m subcomponent.

As mentioned above, repetition enhancement of the P2m component, typically found in RP studies, was not observed here. Instead, an enhancing sustained field (SF) with stimulus repetition was found. The earliest indication of a correlate of such a sustained field was reported by Näätänen and Rinne (2002). The authors found a late negative response between 150 and 280 ms after sound onset that was elicited by stimulus repetition within a sequence of otherwise randomized sounds. In addition, Bendixen et al. (2007) reported an increasing negativity with repetition in the 240 – 350 ms interval, which was interpreted as a decreasing P3a to standards. Ylinen and Houtilainen (2007) showed that a sustained potential between 250 and 400 ms increased for familiar vowels as compared to unfamiliar sounds. This sustained negativity tended to increase with larger number of repetitions. In this particular study, the reduced number of repetitions used probably hampered the elicitation of RP-like events like an N1 suppression, and statistically significant RE of the sustained component. Notably, our whole-brain and ROI analyses indicated a more anterior distribution of

neuronal generators underlying RE of the SF, suggesting a spatial dissociation between RE and RS as indexes of memory-trace formation. In auditory regions like the HG, and the anterior STG, RE showed gradual effects. Notably, no RE was found in more posterior regions of the STG, were activation was greater for N1m. The frontal ROI exhibited a fast adaptation during initial to middle repetitions in the time range of the late N1m. Contrarily, the increase of the SF occurred more progressively with stimulus repetition, thus suggesting the involvement of frontal areas in memory-formation processes. Similarly, Bendixen et al. (2007) showed that such an effect of RE was mirrored by decreases in reaction time, therefore suggesting that RE gradually strengthened memory-based rules, and that stimulus encoding conferred benefits in behavioral terms. Heinemann et al. (2010) showed an enhancement of a late sustained response with negative polarity (150 – 350 ms) to repetitions of frequency-modulated sounds in a paired-stimulus paradigm. Surprisingly, the same effect was absent for unmodulated tones. The authors argued that RE resulted from the interaction between a large frequency separation and the short interstimulus-interval (ISI: 200 ms) used, leading to facilitatory effects, as usually observed for the N1m (Wang et al., 2008). Given the longer ISI employed in the current study, and the larger number of stimulus repetitions, it is hard to accommodate such an interpretation to our findings, which support a memory representation process. Therefore, we suggested an alternative interpretation. To date, RE of a late sustained component has been found in quite predictable scenarios, where the number of repeating trains or repetitions were fixed (see: Näätänen and Rinne, 2002; Ylinen and Huotilainen, 2007), and thus, its regularities could be pre-attentively organized and anticipated even without overt attention directed to sensory inputs (Näätänen et al., 2001). In this line, a functional interpretation of RE in terms of temporal predictability could be argued. Jaramillo and Zador (2011) observed enhanced responses in primary auditory regions of the rat in response to expected temporal cues. Resembling results obtained by Bendixen et al. (2007), enhanced neuronal responses to valid expectation were correlated with decreases in reaction time. The present study, however, did not specifically test if RE was modulated by the temporal predictability of the deviant sounds or the transitional probabilities in the sound sequence. Therefore, strong conclusions regarding the functional role of the increasing SF cannot be drawn, and future studies might help to elucidate a putative dissociation between memory-based and predictive mechanisms.

Effects on deviant stimuli

As noted above a widely accepted interpretation of the MMN states that it reflects the violation of a previously encoded memory trace, as exemplified by the MMN increase with preceding number of standards (Imada et al., 1993; for a review see: Näätänen et al., 2005). In this regard, roving-standard paradigms are optimal for studying memory-trace formation since they can exclude the effect of preceding regularities when assessing memory effects that are dependent on the number of stimuli, and allow the assessment of repetition effects on both deviant and standards. Overall, an MMN increase with repetitions has been found at frontal or mastoid electrodes in several RP studies (Baldeweg et al., 2004, 2006; Haenschel et al., 2005; Cooper et al., 2013), arguing in favor for a progressive strengthening of the memory trace (Näätänen, 1992). However, results from all three studies, and findings by Costa-Faidella and colleagues (2011a), suggest that MMN increase with repetitions is mainly caused by a stronger N1 stimulus-specific adaptation of the response to repetitive standard stimulation, as compared to smaller increases for the deviant tones. Our results are in strict agreement with the above-mentioned studies. At the time interval of the N1m, overlapping that of the MMN, we found a significant amplitude decrease with repetition, thus mimicking RP findings. On the other hand, repetition effects on deviant responses were smaller. Whole-brain analysis revealed a big cluster showing sub-threshold effects when comparing deviant responses after 3 and 24 repetitions. Similarly, ROI analysis showed an effect of repetition in the right HG and precuneus. Given that the predictability of the deviant occurrence might be high when using roving presentation designs with a small number of train lengths, one could assume strong expectations to hamper deviant increase as a function of the preceding repetitions (Chennu et al., 2013). Overall, our data suggests that memory-trace encoding is mainly mediated by stimulus-specific adaptation to repetitive stimulation, in consonance with animal findings (Ulanovsky et al. 2003), but enhancement of deviant stimuli suggests that a memory-based comparison process cannot be discarded.

Conclusions

Our spatio-temporal analysis shows that two separate mechanisms are involved during auditory memory-trace formation, as reflected by the repetition-related modulation effects observed to stimuli presented in a roving-standard paradigm. First, repetition suppression occurs at 95 - 140 ms after repetition onset in a widely distributed network involving temporal and parietal brain regions. This finding is in agreement with the suppression of the N1 component during

the time course of the "repetition positivity", previously reported. Even though enhancement of the earlier P50 and later P2 components of the ERP was not observed in our data, we describe a second mechanism that might be engaged during regularity encoding. A late repetition enhancement effect between 230 and 270 ms indexed as a sustained field was localized in more anterior temporo-insular regions, and overlapping frontal and parietal cortices. Our findings show that different regions, both auditory and non-auditory, participate from auditory memory-trace formation at different time scales. Thus, suggesting that predictive signals might be passed through hierarchically organized regions, according to predictive coding notions.

Acknowledgements

This work was supported by the National Program for Fundamental Research (reference number PSI2012-37174), and the FPI grant (BES-2010-030160) of the Spanish Ministry of Economy and Competitiveness; the 2014SGR177 grant of the Generalitat de Catalunya, and the ICREA Academia Distinguished Professorship awarded to Carles Escera. The authors want to thank Dr. Piia Astikainen for her advice during the analysis.

References

Alain, C., Arnott, S.R., Hevenor, S., Graham, S., Grady, C.L. (2001) "What" and "where" in the human auditory system. Proc. Natl. Acad. Sci. USA 98, 12301–12306.

Althen, H., Grimm, S., Escera, C. (2013) Simple and complex acoustic regularities are encoded at different levels of the auditory hierarchy. Eur. J. Neurosci. 38, 3448–3455.

Antunes, F.M., Malmierca, M.S. (2011) Effect of auditory cortex deactivation on stimulus-specific adaptation in the medial geniculate body. J. Neurosci. 31, 17306–17316.

Antunes, F.M., Nelken, I., Covey, E., Malmierca, M.S. (2010) Stimulus-Specific Adaptation in the Auditory Thalamus of the Anesthetized Rat. PLoS One 5, e14071.

Atienza, M., Cantero, J.L., Dominguez-Marin, E. (2002) The time course of neural changes underlying auditory perceptual learning. Learn. Mem. 9, 138–150.

Ayala, Y., Malmierca, M.S. (2013) Stimulus-specific adaptation and deviance detection in the inferior colliculus. Front. Neural Circuits 6, 89.

Baldeweg, T. (2006) Repetition effects to sounds: evidence for predictive coding in the auditory system. Trends Cogn. Sci. 10, 93–94.

Baldeweg, T. (2007) ERP repetition effects and mismatch negativity generation - A predictive coding perspective. J. Psychophysiol. 21, 204.

Baldeweg, T., Klugman, A., Gruzelier, J., Hirsch, S.R. (2004) Mismatch negativity potentials and cognitive impairment in schizophrenia. Schizophr. Res. 69, 203–217.

Baldeweg, T., Williams, J.D., Gruzelier, J.H. (1999) Differential changes in frontal and sub-temporal components of mismatch negativity. Int. J. Psychophysiol. 33, 143–148.

Baldeweg, T., Wong, D., Stephan, K.E. (2006) Nicotinic modulation of human auditory sensory memory: Evidence from mismatch negativity potentials. Int. J. Psychophysiol. 59, 49–58.

Bendixen, A., Roeber, U., Schröger, E. (2007) Regularity extraction and application in dynamic auditory stimulus sequences. J. Cogn. Neurosci. 19, 1664–1677.

Boutros, N.N., Gjini, K., Urbach, H., Pflieger, M.E. (2011) Mapping repetition suppression of the N100 evoked response to the human cerebral cortex. Biol. Psychiatry 69, 883–889.

Brainard, D.H. (1997) The Psychophysics Toolbox. Spat. Vis. 10, 433–436.

Budd, T.W., Barry, R.J., Gordon, E., Rennie, C., Michie, P.T. (1998) Decrement of the N1 auditory event-related potential with stimulus repetition: habituation vs. refractoriness. Int. J. Psychophysiol. 31, 51–68.

Chennu, S., Noreika, V., Gueorguiev, D., Blenkmann, A., Kochen, S., Ibáñez, A., Owen, A.M., Bekinschtein, T.A. (2013) Expectation and attention in hierarchical auditory prediction. J. Neurosci. 33, 11194–11205.

Cooper, R.J., Atkinson, R.J., Clark, R.A., Michie, P.T. (2013) Event-related potentials reveal modelling of auditory repetition in the brain. Int. J. Psychophysiol. 88, 74–81.

Cornella, M., Leung, S., Grimm, S., Escera, C. (2012) Detection of simple and pattern regularity violations occurs at different levels of the auditory hierarchy. PLoS One 7, e43604.

Costa-Faidella, J., Baldeweg, T., Grimm, S., Escera, C. (2011a) Interactions between "what" and "when" in the auditory system: temporal predictability enhances repetition suppression. J. Neurosci. 31, 18590–18597.

Costa-Faidella, J., Grimm, S., Slabu, L., Díaz-Santaella, F., Escera, C. (2011b) Multiple time scales of adaptation in the auditory system as revealed by human evoked potentials. Psychophysiology 48, 774–783.

Cowan, N., Winkler, I., Teder, W., Näätänen, R. (1993) Memory prerequisites of mismatch negativity in the auditory event-related potential (ERP). J. Exp. Psychol. Learn. Mem. Cogn. 19, 909–921.

Dale, A.M., Fischl, B., Sereno, M.I. (1999) Cortical surface-based analysis. I. Segmentation and surface reconstruction. Neuroimage 9, 179–194.

Dale, A.M., Liu, A.K., Fischl, B.R., Buckner, R.L., Belliveau, J.W., Lewine, J.D., Halgren, E. (2000) Dynamic statistical parametric mapping: combining fMRI and MEG for high-resolution imaging of cortical activity. Neuron 26, 55–67.

Dammers, J., Schiek, M., Boers, F., Silex, C., Zvyagintsev, M., Pietrzyk, U., Mathiak, K. (2008) Integration of amplitude and phase statistics for complete artifact removal in independent components of neuromagnetic recordings. IEEE Trans. Biomed. Eng. 55, 2353–2362.

Desikan, R.S., Ségonne, F., Fischl, B., Quinn, B.T., Dickerson, B.C., Blacker, D., Buckner, R.L., Dale, A.M., Maguire, R.P., Hyman, B.T., Albert, M.S., Killiany, R.J. (2006) An automated labeling system for subdividing the human cerebral cortex on MRI scans into gyral based regions of interest. Neuroimage 31, 968–980.

Desimone, R. (1996) Neural mechanisms for visual memory and their role in attention. Proc. Natl. Acad. Sci. USA 93, 13494–13499.

Dittmann-Balçar, A., Jüptner, M., Jentzen, W., Schall, U. (2001) Dorsolateral prefrontal cortex activation during automatic auditory duration-mismatch processing in humans: a positron emission tomography study. Neurosci. Lett. 308, 119–122.

Duque, D., Malmierca, M.S. (2014) Stimulus-specific adaptation in the inferior colliculus of the mouse: anesthesia and spontaneous activity effects. Brain. Struct. Funct. (in press)

Eliades, S.J., Crone, N.E., Anderson, W.S., Ramadoss, D., Lenz, F.A., Boatman-Reich, D. (2014) Adaptation of High-Gamma Responses in Human Auditory Association Cortex. J. Neurophysiol. (in press)

Escera, C., Leung, S., Grimm, S. (2014) Deviance detection based on regularity encoding along the auditory hierarchy: electrophysiological evidence in humans. Brain Topogr. 27, 527–538.

Escera, C., Malmierca, M.S. (2014) The auditory novelty system: an attempt to integrate human and animal research. Psychophysiology 51, 111–123.

Fischl, B., Sereno, M.I., Dale, A.M. (1999a) Cortical surface-based analysis. II: Inflation, flattening, and a surface-based coordinate system. Neuroimage 9, 195–207.

Fischl, B., Sereno, M.I., Tootell, R.B., Dale, A.M. (1999b) High-resolution intersubject averaging and a coordinate system for the cortical surface. Hum. Brain Mapp. 8, 272–284.

Friston, K. (2005) A theory of cortical responses. Philos. Trans. R. Soc. B. Biol. Sci. 360, 815–836.

Garrido, M.I., Friston, K.J., Kiebel, S.J., Stephan, K.E., Baldeweg, T., Kilner, J.M. (2008) The functional anatomy of the MMN: A DCM study of the roving paradigm. Neuroimage 42, 936–944.

Garrido, M.I., Kilner, J.M., Stephan, K.E., Friston, K.J. (2009) The mismatch negativity: A review of underlying mechanisms. Clin. Neurophysiol. 120, 453–463.

Giard, M.H., Perrin, F., Pernier, J., Bouchet, P. (1990) Brain generators implicated in the processing of auditory stimulus deviance: a topographic event-related potential study. Psychophysiology 27, 627–640.

Grill-Spector, K., Henson, R., Martin, A. (2006) Repetition and the brain: neural models of stimulus-specific effects. Trends Cogn. Sci. 10, 14–23.

Grimm, S., Escera, C., Slabu, L., Costa Faidella, J. (2011) Electrophysiological evidence for the hierarchical organization of auditory change detection in the human brain. Psychophysiology 48, 377–384.

Grimm, S., Recasens, M., Althen, H., Escera, C. (2012) Ultrafast tracking of sound location changes as revealed by human auditory evoked potentials. Biol. Psychol. 89, 232–239.

Haenschel, C., Vernon, D.J., Dwivedi, P., Gruzelier, J.H., Baldeweg, T. (2005) Event-related brain potential correlates of human auditory sensory memory-trace formation. J. Neurosci. 25, 10494–10501.

Hari, R., Kaila, K., Katila, T., Tuomisto, T., Varpula, T. (1982) Interstimulus interval dependence of the auditory vertex response and its magnetic counterpart: implications for their neural generation. Electroencephalogr. Clin. Neurophysiol. 54, 561–569.

Heinemann, L. V, Kaiser, J., Altmann, C.F. (2011) Auditory repetition enhancement at short interstimulus intervals for frequency-modulated tones. Brain Res. 1411, 65–75.

Heinemann, L. V, Rahm, B., Kaiser, J., Gaese, B.H., Altmann, C.F. (2010) Repetition enhancement for frequency-modulated but not unmodulated sounds: a human MEG study. PLoS One 5, e15548.

Huang, M.X., Edgar, J.C., Thoma, R.J., Hanlon, F.M., Moses, S.N., Lee, R.R., Paulson, K.M., Weisend, M.P., Irwin, J.., Bustillo, J.R., Adler, L.E., Miller, G.A., Canive, J.M. (2003) Predicting EEG responses using MEG sources in superior temporal gyrus reveals source asynchrony in patients with schizophrenia. Clin. Neurophysiol. 114, 835–850.

Huotilainen, M., Winkler, I., Alho, K., Escera, C., Virtanen, J., Ilmoniemi, R.J., Jaaskelainen, I.P., Pekkonen, E., Näätänen, R. (1998) Combined mapping of human auditory EEG and MEG responses . Electroencephalogr. Clin. Neurophysiol. 108, 370–379.

Imada, T., Hari, R., Loveless, N., McEvoy, L., Sams, M. (1993) Determinants of the auditory mismatch response. Electroencephalogr. Clin. Neurophysiol. 87, 144–153.

Jääskeläinen, I.P., Ahveninen, J., Bonmassar, G., Dale, A.M., Ilmoniemi, R.J., Levänen, S., Lin, F.H., May, P., Melcher, J., Stufflebeam, S.M., Tiitinen, H., Belliveau, J.W. (2004) Human posterior auditory cortex gates novel sounds to consciousness. Proc. Natl. Acad. Sci. USA 101, 6809–6814.

James, T.W., Humphrey, G.K., Gati, J.S., Menon, R.S., Goodale, M.A. (2000) The effects of visual object priming on brain activation before and after recognition. Curr. Biol. 10, 1017–1024.

Jaramillo, S., Zador, A.M. (2011) The auditory cortex mediates the perceptual effects of acoustic temporal expectation. Nat. Neurosci. 14, 246–251.

Javitt, D.C., Grochowski, S., Shelley, A.M., Ritter, W. (1998) Impaired mismatch negativity (MMN) generation in schizophrenia as a function of stimulus deviance, probability, and interstimulus/interdeviant interval. Electroencephalogr. Clin. Neurophysiol. 108, 143–153.

Josef Golubic, S., Aine, C.J., Stephen, J.M., Adair, J.C., Knoefel, J.E., Supek, S. (2014) Modulatory role of the prefrontal generator within the auditory M50 network. Neuroimage 92, 120–131.

Korzyukov, O., Pflieger, M.E., Wagner, M., Bowyer, S.M., Rosburg, T., Sundaresan, K., Elger, C.E., Boutros, N.N. (2007) Generators of the intracranial P50 response in auditory sensory gating. Neuroimage 35, 814–826.

Laufer, I., Negishi, M., Constable, R.T. (2009) Comparator and non-comparator mechanisms of change detection in the context of speech--an ERP study. Neuroimage 44, 546–562.

Liegeois-Chauvel, C., Musolino, A., Badier, J.M., Marquis, P., Chauvel, P. (1994) Evoked potentials recorded from the auditory cortex in man: evaluation and topography of the middle latency components. Electroencephalogr. Clin. Neurophysiol. 92, 204–214.

Loveless, N., Hari, R., Hämäläinen, M., Tiihonen, J. (1989) Evoked responses of human auditory cortex may be enhanced by preceding stimuli. Electroencephalogr. Clin. Neurophysiol. 74, 217–227.

Marinkovic, K., Baldwin, S., Courtney, M.G., Witzel, T., Dale, A.M., Halgren, E. (2011) Right hemisphere has the last laugh: neural dynamics of joke appreciation. Cogn. Affect. Behav. Neurosci. 11, 113–130.

Marinkovic, K., Dhond, R.P., Dale, A.M., Glessner, M., Carr, V., Halgren, E. (2003) Spatiotemporal dynamics of modality-specific and supramodal word processing. Neuron 38, 487–497.

May, P.J.C., Tiitinen, H. (2010) Mismatch negativity (MMN), the deviance-elicited auditory deflection, explained. Psychophysiology 47, 66–122.

Molholm, S., Martinez, A., Ritter, W., Javitt, D.C., Foxe, J.J. (2005) The neural circuitry of pre-attentive auditory change-detection: an fMRI study of pitch and duration mismatch negativity generators. Cereb. Cortex 15, 545–551.

Näätänen, R. (1992) Attention and Brain Function. Hillsdale, NJ: Erlbaum.

Näätänen, R., Gaillard, A.W., Mantysalo, S. (1978) Early selective-attention effect on evoked potential reinterpreted. Acta. Psychol. (Amst.) 42, 313–329.

Näätänen, R., Jacobsen, T., Winkler, I. (2005) Memory-based or afferent processes in mismatch negativity (MMN): a review of the evidence. Psychophysiology 42, 25–32.

Näätänen, R., Paavilainen, P., Rinne, T., Alho, K. (2007) The mismatch negativity (MMN) in basic research of central auditory processing: a review. Clin. Neurophysiol. 118, 2544–2590.

Näätänen, R., Picton, T. (1987) The N1 Wave of the Human Electric and Magnetic Response to Sound: A Review and an Analysis of the Component Structure. Psychophysiology 24, 375–425.

Näätänen, R., Rinne, T. (2002) Electric brain response to sound repetition in humans: an index of long-term-memory - trace formation? Neurosci. Lett. 318, 49–51.

Näätänen, R., Tervaniemi, M., Sussman, E., Paavilainen, P., Winkler, I. (2001) “Primitive intelligence” in the auditory cortex. Trends. Neurosci. 24, 283–288.

Nousak, J.M., Deacon, D., Ritter, W., Vaughan, H.G. (1996) Storage of information in transient auditory memory. Brain Res. Cogn. Brain. Res. 4, 305–317.

Oostenveld, R., Fries, P., Maris, E., Schoffelen, J.M. (2011) FieldTrip: Open source software for advanced analysis of MEG, EEG, and invasive electrophysiological data. Comput. Intell. Neurosci. 2011, 156869.

Opitz, B., Schröger, E., von Cramon, D. (2005) Sensory and cognitive mechanisms for preattentive change detection in auditory cortex. Eur. J. Neurosci. 21, 531-535.

Pérez-González, D., Malmierca, M.S., Covey, E. (2005) Novelty detector neurons in the mammalian auditory midbrain. Eur. J. Neurosci. 22, 2879–2885.

Recasens, M., Grimm, S., Capilla, A., Nowak, R., Escera, C. (2014a) Two sequential processes of change detection in hierarchically ordered areas of the human auditory cortex. Cereb. Cortex 24, 143–153.

Recasens, M., Grimm, S., Wollbrink, A., Pantev, C., Escera, C. (2014b) Encoding of nested levels of acoustic regularity in hierarchically organized areas of the human auditory cortex. Hum. Brain Mapp. (in press)

Rinne, T., Alho, K., Ilmoniemi, R.J., Virtanen, J., Näätänen, R. (2000) Separate time behaviors of the temporal and frontal mismatch negativity sources. Neuroimage 12, 14–19.

Roeber, U., Widmann, A., Schröger, E. (2003) Auditory distraction by duration and location deviants: a behavioral and event-related potential study. Cogn. Brain Res. 17, 347–357.

Romanski, L.M., Tian, B., Fritz, J., Mishkin, M., Goldman-Rakic, P.S., Rauschecker, J.P. (1999) Dual streams of auditory afferents target multiple domains in the primate prefrontal cortex. Nat. Neurosci. 2, 1131–1136.

Sams, M., Alho, K., Näätänen, R. (1984) Short-term habituation and dishabituation of the mismatch negativity of the ERP. Psychophysiology 21, 434–441.

Schacter, D.L., Dobbins, I.G., Schnyer, D.M. (2004) Specificity of priming: a cognitive neuroscience perspective. Nat. Rev. Neurosci. 5, 853–862.

Schönwiesner, M., Novitski, N., Pakarinen, S., Carlson, S., Tervaniemi, M., Näätänen, R. (2007) Heschl's gyrus, posterior superior temporal gyrus, and mid-ventrolateral prefrontal cortex have different roles in the detection of acoustic changes. J. Neurophysiol. 97, 2075–2082.

Segaert, K., Weber, K., de Lange, F.P., Petersson, K.M., Hagoort, P. (2013) The suppression of repetition enhancement: a review of fMRI studies. Neuropsychologia 51, 59–66.

Shahin, A.J., Roberts, L.E., Miller, L.M., McDonald, K.L., Alain, C. (2007) Sensitivity of EEG and MEG to the N1 and P2 auditory evoked responses modulated by spectral complexity of sounds. Brain Topogr. 20, 55–61.

Slabu, L., Escera, C., Grimm, S., Costa-Faidella, J. (2010) Early change detection in humans as revealed by auditory brainstem and middle-latency evoked potentials. Eur. J. Neurosci. 32, 859–865.

Tadel, F., Baillet, S., Mosher, J.C., Pantazis, D., Leahy, R.M. (2011) Brainstorm: a user-friendly application for MEG/EEG analysis. Comput. Intell. Neurosci. 2011, 879716.

Travis, K.E., Leonard, M.K., Brown, T.T., Hagler, D.J., Curran, M., Dale, A.M., Elman, J.L., Halgren, E. (2011) Spatiotemporal neural dynamics of word understanding in 12- to 18-month-old-infants. Cereb. Cortex 21, 1832–1839.

Ulanovsky, N., Las, L., Farkas, D., Nelken, I. (2004) Multiple time scales of adaptation in auditory cortex neurons. J. Neurosci. 24, 10440–10453.

Ulanovsky, N., Las, L., Nelken, I. (2003) Processing of low-probability sounds by cortical neurons. Nat. Neurosci. 6, 391–398.

Wang, A.L., Mouraux, A., Liang, M., Iannetti, G.D. (2008) The enhancement of the N1 wave elicited by sensory stimuli presented at very short inter-stimulus intervals is a general feature across sensory systems. PLoS One 3, e3929.

Weisser, R., Weisbrod, M., Roehrig, M., Rupp, A., Schroeder, J., Scherg, M. (2001) Is frontal lobe involved in the generation of auditory evoked P50? . Neuroreport 12, 3303–3307.

Yago, E., Escera, C., Alho, K., Giard, M.H. (2001) Cerebral mechanisms underlying orienting of attention towards auditory frequency changes. Neuroreport 12, 2583–2587.

Ylinen, S., Huotilainen, M. (2007) Is there a direct neural correlate for memory-trace formation in audition? Neuroreport 18, 1281–1284.

Yvert, B., Crouzeix, A., Bertrand, O., Seither-Preisler, A., Pantev, C. (2001) Multiple supratemporal sources of magnetic and electric auditory evoked middle latency components in humans . Cereb. cortex 11, 411–423.

Yvert, B., Fischer, C., Bertrand, O., Pernier, J. (2005) Localization of human supratemporal auditory areas from intracerebral auditory evoked potentials using distributed source models. Neuroimage 28, 140–153.

Summary of results and discussion

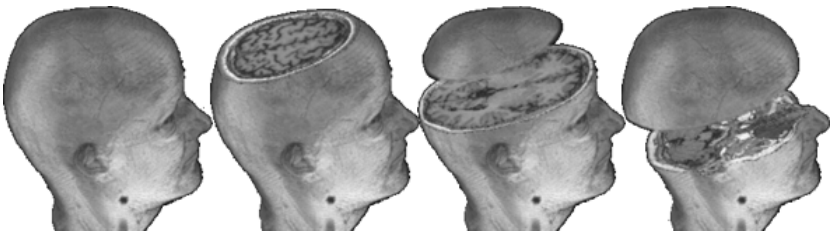

SUMMARY OF RESULTS AND DISCUSSION

In the present PhD thesis three MEG experiments were conducted in order to explore the underlying neuronal generators of acoustic regularity encoding and deviance detection in the auditory system of healthy humans. We recorded ERFs to repetitive and deviant stimuli presented in "oddball" and "roving-stimulus" sequences, and estimated the brain sources by means of inverse solution procedures using MEG.

In the first study we aimed to find separated anatomical areas underlying deviance-related MLR and MMNm sources. Deviance-related effects were obtained by subtracting the ERF to infrequent deviant tones from the activity evoked by repeated standard tones presented in a frequency oddball paradigm at two different time intervals, the Nbm (~43 ms) and MMNm (~115 ms). Neuronal generators of deviance-related Nbm enhancement were located in more anterior and medial sites than those of the MMNm.

In the second study we assessed whether simple (local) and complex (global) levels of acoustic regularity were encoded at the early time range of the MLR or at later processing stages, as reflected by the MMNm. In addition, we estimated brain generators at both latencies in order to find anatomical evidence of a functional separation between deviance detection at MLR and MMNm time ranges. Our results indicate that local frequency changes elicited MLR modulations in components Nbm (~50 ms) and Pbm (~65 ms), in addition to a frequency-MMN (~140 ms). Global sequence violations elicited by improbable tone repetitions evoked a late MMN (~180 ms). Sources of the global MMN were localized in posterior and secondary regions of the STG. Enhanced activity to local changes, instead, was localized near primary auditory areas at different latencies.

In the third study we aimed to find neuromagnetic correlates of acoustic regularity encoding at the anatomical level. By employing a roving-standard paradigm, neuronal populations underlying repetitive frequency tones at different positions were estimated. We observed that repetition suppression at the N1m time range (95-150 ms), and repetition enhancement in the time interval of a sustained field (SF: 230-270 ms) underlied memory-trace formation. Source reconstruction revealed that suppression spanned through posterior regions of the auditory

cortex and the precuneus. Enhanced responses at later time intervals overlapped anterior areas of the auditory cortex, spanning towards more frontal regions.
In studies I and II, deviance-related effects were assessed (deviant minus standard activity). In study III, the modulation of deviant and standard activity with repetition was tested, but no direct assessment of deviance-related effects was conducted. We did not specifically analyze MLR components in study III either. MEG was used as recording technique and source estimation of event-related fields was carried out in all three studies. That said, a discussion of the results from the present PhD thesis will be presented here under the light of previous and related findings.

EARLY DEVIANCE DETECTION IN THE MLR RANGE

As mentioned in the introduction, deviance detection has been investigated by means of the MMN ERP. Recent human studies (Grimm and Escera, 2012; Escera et al., 2014) and parallel findings in animals (Pérez-González and Malmierca, 2014) showed that correlates of deviance detection exist in earlier time intervals than the MMN. Findings presented in Studies I and II corroborate this notion. In both studies, frequency violations elicited enhanced activity at different time intervals, the MLR and MMNm time ranges. In study I we designed a frequency oddball paradigm with very similar characteristics to that employed by Grimm and colleagues (2011) using EEG. Pure tones were presented at fast stimulus-onset-asynchrony (SOA) and rare frequency deviations (probability = 0.2) elicited an MMNm response around 115 ms, in addition to an amplitude enhancement of the Nb component of the MLR at about 40 ms post deviant onset, when compared to standard stimuli. MMN elicitation by infrequent frequency changes is the best-established finding in the MMN literature (Sams et al., 1985; Paavilainen et al., 1993; Jacobsen and Schröger, 2001). With regard to MLR effects, several studies suggest that the Nb deviance-related enhancement is a consistent finding when employing pure tone deviations (Grimm et al., 2011; Alho et al., 2012; Leung et al., 2012; Althen et al., 2013). Alho et al. (2012) reported an Nb enhancement for both pure tones and missing-fundamental tones in an oddball design. Their findings rule-out the possibility that early activity enhancement reflected the processing of harmonic-related information, but rather indicate that Nb is related to pitch

processing in the primary auditory cortex (PAC). Leung and colleagues (2012) used a multi-feature paradigm with four types of deviation: frequency, duration, intensity, and interaural time differences. In the MLR time range, only frequency changes elicited an Nb amplitude increase, suggesting that Nb response might be related to frequency-specific neural activity throughout the ascending auditory pathway. Their findings, in addition, suggest that very early memory traces can be created despite of certain levels of variability in the repetitive stimulation. So far, such notion had been observed only in later time intervals (Gomes et al., 1995). Further evidence pointing to a link between Nb and pre-attentive pitch processing is provided by Puschmann and colleagues (2013), who showed that both detected and undetected band-pass filtered noise changes embedded in complex auditory scenes elicited an Nb enhancement. In spite of the fact that converging evidence shows that amplitude modulations of the Nb component of the MLR is related to pitch processing, Slabu and colleagues (2010) reported an enhancement of the Pa component, at about 30 ms post deviant onset, for changes in band-pass filtered noises. Similarly, Cornella et al. (2013) observed an early amplitude modulation of the Pa component of the MLR when presenting frequency-modulated tones in an oddball paradigm. The authors observed that the Pa component was larger for standard as compared to deviant sweeps. Notably, the direction of the effects was the opposite of what had been expected according to previous findings (a deviant increase), and it was suggested that deviations from the encoded memory trace might require higher-order mechanisms in the case of complex stimuli (Cornella et al., 2013). Similarly, results presented in the study II of the present thesis, show a clear modulation of the Pb/P50 component, in addition to an Nb enhancement, to highly predictable frequency changes. Amplitude modulation of the P50 component has been reported previously as indexing sensory "gating", that is, a dishabituation ("gating-in") to salient rare stimuli, or habituation ("gating-out) to redundant stimulation (Boutros and Belger, 1999; Paraskevopoulos et al., 2012).

While early deviance-related effects seem to emerge in the time range of the Nb component for frequency or pitch changes (except for: Slabu et al., 2010; Cornella et al., 2013), changes in other simple acoustic features like location seem to be processed preferentially in distinct intervals of the MLR. That is the case of sound location changes. Sonnadara et al. (2006) reported an early enhanced negativity at

25 ms (Na component of the MLR) after occasional changes in perceived sound location that was accompanied by a later MMN. Such first indication of deviance-related processing in the MLR interval was confirmed in a subsequent study where clicks in free-field stimulation were presented in either the left or right hemifields during oddball (rare 30°-shifts in location) conditions (Grimm et al., 2012). Again, Cornella et al. (2012) showed enhanced Na responses to occasional feature changes in interaural time difference of stimuli presented through headphones. Enhanced responses in the transition from the Na-Pa components have been observed for intensity deviants too, suggesting that common brain sources might be involved in intensity and location information encoding (Althen et al., 2011). Finally, temporal regularity violations elicited by infrequent decrements in the SOA led to enhanced Pa and Nb responses (Leung et al., 2013). Overall, results presented above suggest that MLR components showing deviance-related effects for different features reflect the activity of neural populations encoding specific acoustic features. That is, deviance-related Nb effects might reflect spectral information processing (Alho et al., 2012; Escera et al., 2014). However, this suggestion is only empirically supported in the case of frequency, for which early feature-specific responses have been obtained (Leung et al., 2012). To sum up, studies I and II strengthen the idea that deviance detection, and hence regularity encoding, is a basic principle of the human auditory processing acting on multiple levels (for a recent review see: Escera and Malmierca, 2014).

BRAIN SOURCES OF MLR AND DEVIANCE-RELATED MLR

Evidence for early deviance detection provided by EEG studies is based on the fast timing of MLR modulation before the MMN interval. Studies discussed so far did not directly investigate whether change detection in the MLR range is elicited in hierarchically inferior auditory structures than those of the MMN. Nevertheless, a large body of evidence indicates that transient MLR (not deviance-related) has its origins in both subcortical and cortical structures, spanning from primary to secondary regions (Deiber et al., 1988; Liégeois-Chauvel et al., 1994). Specifically, the Nam component (~20 ms) is suggested to reflect thalamo-cortical activity (Deiber et al., 1988), with origins in both subcortical (Kraus and McGee, 1988), and cortical generators in the postero-medial HG, as revealed using intracranial

recordings (Yvert et al., 2005). The transition between Na and Pa (~30 ms) has been regarded as the first activity generated in the primary cortex (Lütkenhöner et al., 2003). Actually, Pantev and colleagues (1995) reported that Pam component mirrored the tonotopic organization of N1m. Surprisingly, oddball studies indicate that location and intensity deviations are processed in those particular time ranges (20-30 ms), instead of frequency deviations, as would be expected according to the tonotopic organization of the PAC (Saenz and Langers, 2014). Also Leung and colleagues (2013) showed that temporal violations were processed at the level of the Pa and Nb responses. Pa modulations have been observed using complex sounds like pitched noises (Slabu et al., 2010) or frequency modulated tones (Cornella et al., 2013), which is difficult to accommodate with the notion that spectrally complex sounds are processed beyond core regions in the PAC (Wessinger et al., 2001). Relevant with regard to studies I and II, later components like Nb (~40 ms) and Pb/P50 (~60 ms) might have their origins in more lateral aspects of the HG (Liégeois-Chauvel et al., 1994; Godey et al., 2001) or even lateral portions of the STG (Yvert et al., 2001; Inui et al., 2006). Overall, the assumption stated in EEG studies that MLR modulations support an origin in or near the PAC and that deviance-related MLR reflect a hierarchically lower stage of processing is supported by above-mentioned findings. This might be particularly true given that generators of subsequent auditory activity like the N1 have been descrived in secondary areas like the planum temporale (PT), in intracranial (Liégeois-Chauvel et al., 1994) and MEG studies (Pantev et al., 1995).

Still, anatomical evidence showing hierarchically inferior source generators of deviance-related MLR is crucial to conclude that ultra-fast responses represent a different mechanism than the well-studied MMN. Studies I and II clearly addressed this topic for the first time by estimating the location of neuronal populations involved in early deviance detection. In those studies MEG data was acquired. MEG provides excellent temporal resolution capable of tracking ultra-fast activity occurring in the human brain, and allows for a reasonably high spatial resolution, given the high number of sensors and the incorruptibility of magnetic fields when crossing tissues above the cortex (Vrba and Robinson, 2001; Hari and Salmelin, 2012). Even though a detailed review of the characteristics, advantages and disadvantages of MEG is beyond the scope of the present thesis (for a detailed

introduction to MEG, readers are suggested to read: Hämäläinen et al., 1993; Hansen et al., 2010), important caveats need to be made regarding the spatial accuracy of source estimation in MEG. First, magnetic fields generated by cortical populations are extremely small, typically ranging between 50 and 500 fT (Hämäläinen et al., 1993). The activity of a large number of neurons, similarly oriented, needs to be synchronous in order to be detected by MEG sensors. "To reach a MEG signal with the magnitude of 10 nAm it is necessary that 50,000 pyramidal neurons are synchronously active" (Hansen et al., 2010). Second: Given that MEG signal is recorded from the scalp, an infinite number of possible source configurations can exist. This is known as "inverse problem". Therefore, source reconstruction is subject to computational models of the biophysical sources. That is, accurate source estimation depends on the models' assumptions, which may introduce constrains to achieve a source configuration able to explain the recorded signals. Third: magnetic fields decrease with distance to a higher degree than electric signals. Thus, small activity generated in deep areas of the brain like the thalamus or the brainstem will hardly be detected. That might explain why the detectability of the early Nam component of the MLR has yielded conflicting results (Mäkelä et al., 1994; Kuriki et al., 1995; Borgmann et al., 2001; Godey et al., 2001; Yvert et al., 2001). In view of the noted caveats, source estimates from studies I and II should now be discussed. The main finding from study I revealed that early deviance-related Nbm and MMNm sources were spatially separated. It is also relevant that in both time intervals neuronal generators were estimated in the right hemisphere. The right lateralization of MMN sources is a well-established finding (Paavilainen et al., 1991; Grimm et al., 2006), especially when it comes to frequency or pitch deviations (Doeller et al., 2003; Molholm et al., 2005). This lateralization of pitch MMN is consistent with the notion that the right hemisphere is engaged in tonal information processing, whereas the left hemisphere processes temporal information (Zatorre and Belin, 2001), and speaks in favor of a feature dependence of MMN generators. Similarly in the Nbm time range, Leung and colleagues (2012) observed more prominent Nbm responses to frequency deviants in the right hemisphere, again arguing in favor for a feature-dependent processing at the level of MLR. Similar hemispheric asymmetries were observed in study II in response to local frequency violations. However, in the MMNm interval a bilateral

activation was observed, and deviance-related Nbm activity was stronger on the left hemisphere, though no statistical differences existed between hemispheres. In this regard, results from study III show that suppression of the N1m component to repeated tone presentations is greater in the right hemisphere (see HG ROI), in line with previous findings (Boutros et al., 2011). Such finding suggests that right hemisphere's preference for spectral information is already developed in the regularity-encoding phase, prior to deviance detection, and in very early cortical stations.

Study I showed that deviance-related effects in the MLR time range were localized in anterior and medial regions of the auditory cortex, as compared to source generators of MMNm. Nbm deviance-related generators were located in the anterior and medial portion of the HG, and the strongest signal appeared in the medial aspect of the HG. Similarly in study II, enhanced activity to local violations in the time range of MLR was localized in the vicinity of HG, bilaterally. HG, or transverse gyrus, in humans is a rough marker of the tonotopically organized PAC. Even though anatomical differences between the human and the monkey temporal plane do not allow for a precise correlation between well-defined areas in animals, and human structures with high inter-individual variability (Hackett et al., 2001), analogous regions of the monkey's PAC have been identified along the medio-lateral axis of the human HG by means of cytoarchitectonic analysis (Morosan et al., 2001). Postero-medial regions of the HG are thought to represent the core of the PAC, which is surrounded by belt and parabelt regions, like the antero-lateral HG, the planum polare, the planum temporale (PT), and lateral surface of the STG (Hackett, 2011). Therefore, findings from study I suggest that anatomical sources of deviance detection at the Nbm interval correspond to PAC (Brodmann area 41), specifically to Te1 cytoarchitectonical subdivisions (Morosan et al., 2001). On the other hand, MMNm sources were located in right hemispheric regions of the STG, the middle temporal gyrus, and in the superior temporal sulcus, in line with previous findings (Opitz et al., 1999, 2002; Tervaniemi et al., 2000, 2006; Doeller et al., 2003; Schall et al., 2003; Rinne et al., 2005; Schönwiesner et al., 2007). Architectonic maps in humans have identified these regions as Te2.2 and Te3 subdivisions of the auditory cortex (Brodmann area 42 and 22) (Morosan et al., 2005), thought to correspond to secondary auditory areas. To the authors

knowledge, this is the first evidence showing that two mechanisms of deviance detection exist in anatomically distinct regions of the auditory cortex, and establish a link between human deviance detection and single-neuron stimulus specific adaptation in animals occurring at the level of PAC (Ulanovsky et al., 2003, 2004). Regarding MLR and MMN spatial separation, source localization of deviance-related MLR effects and MMNm to frequency changes in study II yielded somewhat different locations as compared to study I. MMNm generators to local frequency changes were obtained in a more anterior and slightly more medial location than Nbm sources. In the left hemisphere, frequency MMNm sources were located more anterior than Pbm, and more inferior than Nbm and Pbm sources. Such differences might be explained for by differences in the stimulus sequence employed. In study II SOA was faster, local deviant probability was higher, and the occurrence of frequency violations was fixed and thus highly predictable. Though parsimonious, one explanation for the discrepancy in the results could be that MMNm was driven by differential refractoriness states, thus leading to more anterior MMNm generators (Jääskeläinen et al., 2004) in study II. In line with the results observed in study I, global changes in study II revealed a much more posterior source of MMNm as compared to deviance-related MLR sources. As will be discussed below, global MMNm could not be accounted by adaptation effects. To summarize briefly, our findings are consistent with the notion that two separated brain regions in the cortex underlie change detection at two distinct time intervals. While MMNm generators lie in secondary regions mainly, earlier deviance-related processes occur at the level of the PAC, a hierarchically inferior region of the auditory cortex.

FUNCTIONAL ROLE OF EARLY AND LATE DEVIANCE DETECTION MECHANISMS

One of the aims of the current PhD thesis was to examine whether early and late deviance detection mechanisms reflect recurrent or functionally different processes. Given the spatiotemporal separation previously described for early and late deviance detection mechanisms, we advocate for the latter. Beyond cytoarchitechtonical differences, Howard and colleagues (2000) observed that intracranially recorded auditory evoked responses in the HG and the posterior STG differed in their sensitivities to stimulation rate. Further evidence confirmed that the HG and postero-lateral superior temporal areas are highly interconnected

(Brugge et al., 2003, 2008), and established a functional separation between mesial core regions in HG, the posterior STG, and the antero-lateral portion of the HG (Liégeois-Chauvel et al., 1991; Brugge et al., 2008, 2009). Such findings, corroborate previous anatomical evidence suggesting that the auditory cortex contains multiple and interconnected regions to provide hierarchical processing of acoustic information (Wessinger et al., 2001; Hackett, 2011). In a similar line, Schönwiesner and colleagues (2007) suggested different functional roles for mismatch responses obtained at the mesial HG, lateral HG, the STG, and prefrontal areas. Study II aimed to show that the hierarchically earlier deviance-detection mechanism in the vicinity of the PAC is functionally different from the one indexed by the later MMNm. We designed a sophisticated version of the oddball paradigm where simple local frequency deviations were embedded in fixed sound sequences. Global violations in the form of additional tone repetitions occurred infrequently in the sound sequences, thus violating higher-order pattern-like regularities. Corroborating previous findings from our research group, complex or global changes elicited and MMNm response, but no deviance-related MLR modulations (Cornella et al., 2012; Althen et al., 2013). Althen et al. (2013) used feature combinations as complex stimuli, and Cornella et al. (2012) employed infrequent tone repetitions in a tone-alternating sequence. In none of the cases complex deviations elicited MLR modulations, thus suggesting that hypercomplex and pattern invariance in not yet encoded at the level of the MLR (Escera et al., 2014). Instead, simple changes in location (Cornella et al., 2012) and frequency (Althen et al., 2013) elicited both an MMN response and an early MLR modulation in components Na and Nb, respectively. Using similar global-local sequences, MMN to simple pitch violations accompanied by global MMN has been observed previously under passive conditions (Horvath et al., 2001; Herholz et al., 2009, 2011). When introducing active task demands, MMN to local changes is elicited in the STG and PAC, whereas global violations are indexed by a P3b response distributed over a large brain-network (Bekinschtein et al., 2009; Wacongne et al., 2011). Though these latter results suggest that conscious awareness is necessary to detect high-order regularities, our data is consistent with previous findings showing that pattern changes can be detected pre-attentively without overt attention (Horvath et al., 2001; Herholz et al., 2009, 2011; Cornella et al., 2012; Althen et al., 2013).

Our data showed that source generators of local deviations are located in anterior regions of the auditory cortex, overlapping both primary and secondary areas (Bekinschtein et al., 2009). Recent fMRI findings suggested that a more distributed cortical network underlied the detection of frequency violations in the monkey brain (Uhrig et al., 2014). Such network involved subcortical structures, which might be related to the deviance-related MLR modulations observed in study II. With regard to the source localization of the global MMNm, our data agree with previous findings suggesting that physical dimensions-like frequency and more complex regularities are encoded in distinct auditory areas (Alho et al., 1996; Levänen et al., 1996; Alain et al., 1999). More precisely, global MMNm sources were generated in the PT, an area within the STG lying posterior to the HG. The PT represents a high-order processing stage in the auditory hierarchy (Zheng, 2009) that has been related to sensoriomotor processes like rhythm (Chen et al., 2009), and speech production (Hickok and Poeppel, 2007; Pa and Hickok, 2008; Zheng et al., 2013). In line, Griffiths and Warren (2002) suggested that PT contains mechanisms for parsing the different types of auditory information included in complex sounds, which work in a template-matching fashion (Näätänen et al., 2005; Winkler et al., 2009). Overall, findings from study II suggest that acoustic regularities of different complexity are processed by separated spatiotemporal brain mechanisms. These results indicate that different auditory features of a single stimulus percept might be concurrently maintained by hierarchically different structures at different time intervals.

COGNITIVE AND SENSORY MECHANISMS OF DEVIANCE DETECTION

As presented in the introduction, a long debate exists around the issue of MMN reflecting memory-related activity (Näätänen et al., 2005, 2011; May and Tiitinen, 2010). This debate is not irrelevant to early deviance detection mechanisms. Whether early novelty detection involves memory-related neuronal activity or, in contrast, is accounted for by the differential states of refractoriness of afferent neural populations is key to understand the functional role of widespread and hierarchically organized deviance detection in the auditory system. In order to rule out adaptation effects occurring in oddball paradigms control conditions have been designed where random stimuli are presented with equal probability

(Schröger and Wolff, 1996; Jacobsen and Schröger, 2001; Jacobsen et al., 2003). Using such conditions, physically identical control and deviant tones with the same probability are compared, thus canceling out effects caused by the mere rareness of the deviant tone, and keeping memory-based effects caused by the presentation of infrequent stimuli in an otherwise constant presentation. In addition, studies investigating early deviance detection (for a review see: Grimm and Escera, 2012) employ a "reversed" condition that allows for the comparison between physically identical deviant and standard tones, in substitution for the traditional "deviance minus standard" comparison conducted in most MMN studies. That alleviates possible confounding effects caused by the comparison of two levels of the same features (e.g., 1000 – 1223 Hz), known to exert a strong influence on MLR and ABR (for example see: Althen et al., 2011). Both types of control condition were introduced in study I, and only a reversed condition was included in study II for the comparison of local effects. In study I, we observed that Nb activity was higher for deviant tones as compared to control stimuli; however that difference did not reach statistical significance. Using a very similar design, Grimm et al. (2011) did find a significant difference between deviant and control tones, thus arguing in favor for memory-related processing in very early latencies. Similar "genuine" effects at the level of MLR were reported by Slabu et al. (2010) and Grimm et al. (2012). In fact, recent evidence indicates that the human auditory brainstem is capable to encode acoustic regularities and detect acoustic changes based on memory-related processes rather than on sensory-based adaptation (Slabu et al., 2012). Slabu and colleagues (2012) recorded FFR from syllables presented in an oddball fashion and observed that the second and fourth harmonics of syllables presented in the role of deviant were smaller as compared to standard and control harmonics. Again, using a control condition Cacciaglia and colleagues (2014) obtained the first direct fMRI evidence for the involvement of subcortical structures like the medial geniculate body (MGB) and inferior colliculi (IC) during deviance detection. One reason for the inconsistencies between study I and previous findings where control conditions have been used could be that responses to control tones were less adapted than deviants, given that lateral inhibition caused by proximal neurons responding to the standard frequency in the oddball block was greater than that affecting responses in the control condition

(Kujala et al., 2007; Schröger, 2007; Taaseh et al., 2011; Ruhnau et al., 2012). Supporting this "overcontrol" argument, the frequency difference between deviant and standard tones was smaller in our study than in the design of Grimm et al., (2011), thus leading to stronger lateral inhibition. Given the lack of genuine effects in both time intervals, our data from study I and II do not allow us to make a strong claim in favor of the existence of memory-based processes in the early interval of the MLR. In view of the previously reported findings, we suggest that both sensory and cognitive mechanisms interplay during early deviance detection. In the time range of the MMN, however, we observed that source activation for transient standard and deviant stimulation occurred in separated locations. The difference between neural generators for N1m to deviant and standards in the anterior–posterior axis is consistent with previous MEG studies arguing for the involvement of separate change-specific neural populations underlying MMNm (Tiitinen et al., 1993; Korzyukov et al., 1999). In study II, the location of MMNm sources to global deviations in secondary areas also supports the notion that higher-order, or cognitive, processes underlie MMN generation. Moreover, elicitation of MMNm to global changes in study II cannot be accounted for by a release from refractoriness, as supported by the adaptation hypothesis (May and Tiitinen, 2010). According to this interpretation, additional adaptation should have occurred to a repeated tone, disregarding its role as deviant or standard. Instead we observed an enhanced response in the MMNm range indicating that standard sequences had been encoded and its deviations detected. Overall, our data does not allow concluding that early deviance detection reflected a memory-based comparison process. Still, our results fit well with the idea that deviance detection system is composed of separate mechanisms playing different roles during the extraction of acoustic regularities. Using a comparable interpretation, Schönwiesner et al. (2007) observed that only secondary areas on the posterior STG were sensitive to the different magnitudes of deviation, thus suggesting a "cognitive" mechanisms. Medial HG activation, in primary auditory areas, reflected a "sensory" mechanism of simple change detection possibly accounted for by stimulus-specific adaptation mechanisms (Ulanovsky et al., 2003; Opitz et al., 2005).

REGULARITY ENCODING AND UNDERLYING BRAIN SOURCES

Until now, we have discussed the timing, location and role of the deviance detection mechanisms as highlighted in studies I and II. Rather than focusing on early latencies, study III aimed to explore the mechanisms preceding deviance detection, that is, the encoding of acoustic features or regularities. Surprisingly, this topic has received much less attention than the processes involved in human change detection. Single-cell, multi-unit, and local field potential recordings in animal studies show that certain acoustic features like frequency (Ulanovsky et al., 2003, 2004), and intensity (Ulanovsky et al., 2003; Farley et al., 2010) are encoded in the PAC after a very short onset interval around 20-40 ms. Such studies report that repeated stimulation leads to stimulus-specific adaptation (SSA), that is, the suppression of neurons responding to specific stimulus features. SSA has been regarded as a neuronal correlate of sensory-memory formation (Ulanovsky et al., 2003, 2004), and recent human studies indicate that human correlates of SSA can be recorded at the scalp level. Such ERP correlate has been termed repetition positivity (RP), since it is reflected by a positive slow drift of the EEG signal recorded at frontal sites spanning from 50 to 250 ms (Baldeweg, 2006, 2007). The RP is modulated by both bottom-up stimulation characteristics like timing regularity (Costa-Faidella et al., 2011a), and top-down modulations like attentional demands (Haenschel et al., 2005), suggesting influences from both parietal and frontal cortices (Baldeweg, 2006). Both SSA and RP occur without overt attention, are stimulus-specific and develop rapidly, which suggest that the two might be counterparts of the same mechanisms of short-term memory formation (Haenschel et al., 2005; Baldeweg, 2007; Nelken and Ulanovsky, 2007). In study III we employed a roving-standard paradigm, frequently used to elicit the RP. Notably we did not obtain an early modulation of the P50 component with stimulus repetition, which is at odds with previous findings (Baldeweg et al., 2004, 2006; Haenschel et al., 2005; Costa-Faidella et al., 2011a; Cooper et al., 2013). Given that differences in results can hardly be accounted for by a low number of stimulus repetitions used in our study, our suggestion is that MEG might be less sensitive to small differences produced by stimulus repetition than EEG. On the other hand, we did obtain a characteristic repetition suppression (RS) of the N1m component. In human MEG studies, the adaptation time constant of auditory cortex N1m

response has been found to closely correlate with the duration of behaviorally measured auditory sensory memory (Lu et al., 1992). Time constants of adaptation are not uniform (Ulanovsky et al., 2004; Costa-Faidella et al., 2011b) but rather reflect a continuum that could form the basis of sensory memory representations (Jääskeläinen et al., 2007, 2011). Instead of the repetition enhancement (RE) occurring at the P2 component usually reported in RP studies, our findings indicate that a late sustained field (SF), around 250 ms, emerged after few repetitions and showed a clear RE. Such direct index of regularity encoding has been reported previously (Näätänen and Rinne, 2002; Bendixen et al., 2007; Ylinen and Huotilainen, 2007). Bendixen et al. (2007) showed that such an effect of RE was mirrored by decreases in reaction time, therefore suggesting that RE gradually strengthened memory-based rules. Bigelow and colleagues (2014) recorded single-unit and multi-unit activity from neurons located in the PAC of two monkeys performing an auditory short-term memory task. The authors observed that early suppression of PAC neurons occurred during the matching sound interval. Instead, during the later portion of the sound presentation, firing rates increased for match trials. Similar findings had been reported in the planum polare, the most-rostral area of the STG, and the prefrontal cortex (Ng et al., 2014). Such findings, paralleling our RE for the SF, were interpreted as reflecting top-down feedback from prefrontal to primary and secondary auditory areas. In spite of clear methodological differences between study III and latter reported findings, the similar pattern of electrophysiological activity suggest that rather than two separated mechanisms of regularity encoding, RS and RE at different time scales might reflect the encoding of bottom-up information and the prediction error suppression feedback from high-order regions respectively (Baldeweg, 2006). In support for this notion, source reconstruction in study III revealed that both auditory and non-auditory areas are involved during the encoding of acoustic regularities.

Source estimates of brain areas showing RS during the N1m interval were localized in both primary and secondary areas of the auditory cortex bilaterally, corroborating previous results (Hari et al., 1982; Näätänen and Picton, 1987; Näätänen et al., 1992; Budd et al., 1998). Notably, medial areas of the posterior wall of the parietal cortex like the precuneus showed a marked suppression with

stimulus repetition. Likewise, sources of RE occurring in the latency of the SF were modeled in anterior auditory regions, spanning anteriorly towards the insula, inferior to the prefrontal cortex. Though a clear neuromagnetic correlate of RP was not found in study III, these results corroborate the notion that memory-trace formation represents a non-unitary phenomenon composed of different processing stages of regularity encoding (Haenschel et al., 2005; Costa-Faidella et al., 2011a). Suppression of early posterior N1 sources has been related to the temporal ("when"), and location ("where") aspect of sound stimulation, as temporal predictability and location lead to N1 suppression. Instead, later and anterior sources probably underlying SF and P2 enhancement have been related to sound identity ("what") aspects (Ahveninen et al., 2006; Costa-Faidella et al., 2011a). In line with findings presented in study III, previous fMRI studies have found MMN sources in parietal regions, in the vicinity of the precuneus (Alain et al., 2001; Molholm et al., 2005; Laufer et al., 2009), and Boutros et al., (2011), using electrodes placed on the cortical mantle, registered a strong RS in prefrontal, cingulate and medial parietal regions that exceeded the suppression observed in typically auditory perceptual regions. All together, discussed studies suggest that the encoding of acoustic regularities takes place in both auditory and non-auditory regions, and suggest that top-down modulations from parietal and frontal cortices are involved in RS and RE as indices of acoustic memory-trace formation.

Conclusions

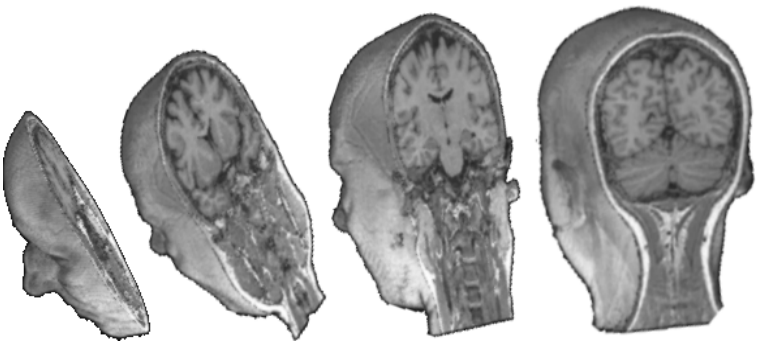

COCLUSIONS

The goal of the present PhD thesis was to investigate the mechanisms of deviance detection in early and late time intervals, reveal a functional dissociation between both mechanisms, and localize the neuronal generators involved in auditory deviance detection and regularity encoding to show that deviance detection and regularity encoding mechanisms are organized in a hierarchical fashion in the human auditory cortex.

1. In a regular acoustic context, frequency deviations are processed in two different time intervals and anatomical locations. First, deviance detection occurs around 40 ms after change onset, as indexed by an amplitude modulation of the Nbm component of the MLR, in areas close to primary auditory cortices. Around 115 ms, an MMNm evoked potential is generated near secondary areas. A "genuine" memory-based processing at early latencies could not be confirmed.

2. Complex of global acoustic deviations are not tracked at the early time interval of the MLR but in the later latency of the MMNm, generated in clearly differentiated secondary cortices. Complex auditory regularities require high-order mechanisms, beyond MLR latencies and areas, to be integrated. Local or simple levels of acoustic regularity are processed recursively in different areas and intervals. This suggests that hierarchically distinct auditory areas underlie the maintenance of different aspects auditory object formation.

3. Encoding of invariances like frequency, giving rise to predictive models of our acoustic environment, are processed in both auditory regions like the Heschl's gyrus and superior temporal gyrus and in higher-order areas like the medial parietal lobe and frontal cortices. Regularity encoding in the human brain is reflected by both a suppression of early N1m activity and an enhancement of a sustained field that emerges with repetition.

References

REFERENCES

Ahveninen, J., Jääskeläinen, I.P., Raij, T., Bonmassar, G., Devore, S., Hämäläinen, M., Levänen, S., Lin, F.-H., Sams, M., Shinn-Cunningham, B.G., Witzel, T., Belliveau, J.W. (2006). Task-modulated "what" and "where" pathways in human auditory cortex. *Proc Natl Acad Sci U S A*, 103(39), 14608–14613.

Alain, C., Achim, a, Woods, D.L. (1999). Separate memory-related processing for auditory frequency and patterns. *Psychophysiology*, 36(6), 737–744.

Alain, C., Arnott, S.R., Hevenor, S., Graham, S., Grady, C.L. (2001). "What" and "where" in the human auditory system. *Proc Natl Acad Sci U S A*, 98(21), 12301–12306.

Alho, K., Grimm, S., Mateo-León, S., Costa-Faidella, J., Escera, C. (2012). Early processing of pitch in the human auditory system. *Eur J Neurosci*, 36(7), 2972–2978.

Alho, K., Huotilainen, M., Näätänen, R. (1995). Are memory traces for simple and complex sounds located in different regions of auditory cortex? Recent MEG studies. *Electroencephalogr Clin Neurophysiol Suppl*, 44, 197–203.

Alho, K., Tervaniemi, M., Huotilainen, M., Lavikainen, J., Tiitinen, H., Ilmoniemi, R., Knuutila, J., Näätänen, R. (1996). Processing of complex sounds in the human auditory cortex as revealed by magnetic brain responses. *Psychophysiology*, 33, 369–375.

Alho, K., Winkler, I., Escera, C., Huotilainen, M., Virtanen, J., Jääskeläinen, I.P., Pekkonen, E., Ilmoniemi, R.J. (1998). Processing of novel sounds and frequency changes in the human auditory cortex: magnetoencephalographic recordings. *Psychophysiology*, 35(2), 211–224.

Althen, H., Grimm, S., Escera, C. (2011). Fast detection of unexpected sound intensity decrements as revealed by human evoked potentials. *PLoS One*, 6(12), e28522.

Althen, H., Grimm, S., Escera, C. (2013). Simple and complex acoustic regularities are encoded at different levels of the auditory hierarchy. *Eur J Neurosci*, 38(10), 3448–3455.

Antunes, F.M., Malmierca, M.S. (2011). Effect of auditory cortex deactivation on stimulus-specific adaptation in the medial geniculate body. *J Neurosci*, 31(47), 17306–17316.

Antunes, F.M., Nelken, I., Covey, E., Malmierca, M.S. (2010). Stimulus-specific adaptation in the auditory thalamus of the anesthetized rat. *PLoS One*, 5(11), e14071.

Ayala, Y.A., Malmierca, M.S. (2013). Stimulus-specific adaptation and deviance detection in the inferior colliculus. *Front Neural Circuits*, 6, 89.

Baess, P., Widmann, A., Roye, A., Schröger, E., Jacobsen, T. (2009). Attenuated human auditory middle latency response and evoked 40-Hz response to self-initiated sounds. *Eur J Neurosci*, 29(7), 1514–1521.

Baldeweg, T. (2006). Repetition effects to sounds: evidence for predictive coding in the auditory system. *Trends Cogn Sci*, 10(3), 93–94.

Baldeweg, T. (2007). ERP repetition effects and mismatch negativity generation - A predictive coding perspective. *J Psychophysiol*, 21(3-4), 204.

Baldeweg, T., Klugman, A., Gruzelier, J., Hirsch, S.R. (2004). Mismatch negativity potentials and cognitive impairment in schizophrenia. *Schizophr Res*, 69(2-3), 203–217.

Baldeweg, T., Klugman, A., Gruzelier, J.H., Hirsch, S.R. (2002). Impairment in frontal but not temporal components of mismatch negativity in schizophrenia. *Int J Psychophysiol*, 43(2), 111–122.

Baldeweg, T., Williams, J.D., Gruzelier, J.H. (1999). Differential changes in frontal and sub-temporal components of mismatch negativity. *Int J Psychophysiol*, 33(2), 143–148.

Baldeweg, T., Wong, D., Stephan, K.E. (2006). Nicotinic modulation of human auditory sensory memory: Evidence from mismatch negativity potentials. *Int J Psychophysiol*, 59(1), 49–58.

Bekinschtein, T.A., Dehaene, S., Rohaut, B., Tadel, F., Cohen, L., Naccache, L. (2009). Neural signature of the conscious processing of auditory regularities. *Proc Natl Acad Sci U S A*, 106(5), 1672–1677.

Bendixen, A., Prinz, W., Horváth, J., Trujillo-Barreto, N.J., Schröger, E. (2008). Rapid extraction of auditory feature contingencies. *Neuroimage*, 41(3), 1111–1119.

Bendixen, A., Roeber, U., Schröger, E. (2007). Regularity extraction and application in dynamic auditory stimulus sequences. *J Cogn Neurosci*, 19(10), 1664–1677.

Bendixen, A., SanMiguel, I., Schröger, E. (2012). Early electrophysiological indicators for predictive processing in audition: a review. *Int J Psychophysiol*, 83(2), 120–131.

Bendixen, A., Scharinger, M., Strauß, A., Obleser, J. (2014). Prediction in the service of comprehension: Modulated early brain responses to omitted speech segments. *Cortex*, 53, 9–26.

Bigelow, J., Rossi, B., Poremba, A. (2014). Neural correlates of short-term memory in primate auditory cortex. *Front Neurosci*, 8, 250.

Borgmann, C., Ross, B., Draganova, R., Pantev, C. (2001). Human auditory middle latency responses: influence of stimulus type and intensity. *Hear Res*, 158(1-2), 57–64.

Boutros, N.N., Belger, A. (1999). Midlatency evoked potentials attenuation and augmentation reflect different aspects of sensory gating. *Biol Psychiatry*, 45(7), 917–922.

Boutros, N.N., Gjini, K., Urbach, H., Pflieger, M.E. (2011). Mapping repetition suppression of the N100 evoked response to the human cerebral cortex. *Biol Psychiatry*, 69(9), 883–889.

Bregman, A.S. (1990). *Auditory Scene Analysis: The Perceptual Organization of Sound*. Cambridge: The MIT Press.

Brugge, J.F., Nourski, K.V., Oya, H., Reale, R.A., Kawasaki, H., Steinschneider, M., Howard 3rd, M.A. (2009). Coding of repetitive transients by auditory cortex on Heschl's gyrus. *J Neurophysiol*, 102(4), 2358–2374.

Brugge, J.F., Volkov, I.O., Garell, P.C., Reale, R.A., Howard 3rd, M.A. (2003). Functional connections between auditory cortex on Heschl's gyrus and on the lateral superior temporal gyrus in humans. *J Neurophysiol*, 90(6), 3750–3763.

Brugge, J.F., Volkov, I.O., Oya, H., Kawasaki, H., Reale, R.A., Fenoy, A., Steinschneider, M., Howard 3rd, M.A. (2008). Functional localization of auditory cortical fields of human: click-train stimulation. *Hear Res*, 238(1-2), 12–24.

Budd, T.W., Barry, R.J., Gordon, E., Rennie, C., Michie, P.T. (1998). Decrement of the N1 auditory event-related potential with stimulus repetition: habituation vs. refractoriness. *Int J Psychophysiol*, 31(1), 51–68.

Cacciaglia, R., Escera, C., Slabu, L., Grimm, S., Sanjuán, A., Ventura-Campos, N., Ávila, C. (2014). Involvement of the human midbrain and thalamus in auditory deviance detection. *Neuropsychologia*, (submitted).

Celesia, G.G. (1976). Organization of auditory cortical areas in man. *Brain*, 99(3), 403–414.

Chandrasekaran, B., Hornickel, J., Skoe, E., Nicol, T., Kraus, N. (2009). Context-dependent encoding in the human auditory brainstem relates to hearing speech in noise: implications for developmental dyslexia. *Neuron*, 64(3), 311–319.

Chandrasekaran, B., Kraus, N. (2010). The scalp-recorded brainstem response to speech: neural origins and plasticity. *Psychophysiology*, 47(2), 236–246.

Chandrasekaran, B., Skoe, E., Kraus, N. (2014). An integrative model of subcortical auditory plasticity. *Brain Topogr*, 27(4), 539–552.

Chen, J.L., Penhune, V.B., Zatorre, R.J. (2009). The role of auditory and premotor cortex in sensorimotor transformations. *Ann N Y Acad Sci*, 1169, 15–34.

Cooper, R.J., Atkinson, R.J., Clark, R.A., Michie, P.T. (2013). Event-related potentials reveal modelling of auditory repetition in the brain. *Int J Psychophysiol*, 88(1), 74–81.

Cornella, M., Leung, S., Grimm, S., Escera, C. (2012). Detection of simple and pattern regularity violations occurs at different levels of the auditory hierarchy. *PLoS One*, 7(8), e43604.

Cornella, M., Leung, S., Grimm, S., Escera, C. (2013). Regularity encoding and deviance detection of frequency modulated sweeps: human middle- and long-latency auditory evoked potentials. *Psychophysiology*, 50(12), 1275–1281.

Costa-Faidella, J., Baldeweg, T., Grimm, S., Escera, C. (2011a). Interactions between "what" and "when" in the auditory system: temporal predictability enhances repetition suppression. *J Neurosci*, 31(50), 18590–18597.

Costa-Faidella, J., Grimm, S., Slabu, L., Díaz-Santaella, F., Escera, C. (2011b). Multiple time scales of adaptation in the auditory system as revealed by human evoked potentials. *Psychophysiology*, 48(6), 774–783.

Cowan, N., Winkler, I., Teder, W., Näätänen, R. (1993). Memory prerequisites of mismatch negativity in the auditory event-related potential (ERP). *J Exp Psychol Learn Mem Cogn*, 19(4), 909–921.

Csépe, V. (1995). On the origin and development of the mismatch negativity. *Ear Hear*, 16(1), 91–104.

Csépe, V., Pantev, C., Hoke, M., Hampson, S., Ross, B. (1992). Evoked magnetic responses of the human auditory cortex to minor pitch changes: localization of the mismatch field. *Electroencephalogr Clin Neurophysiol*, 84(6), 538–548.

Deiber, M.P., Iba, V., Fischer, C., Perrin, F., Mauguirre, F., Ibanez, V., Mauguiere, F. (1988). Sequential mapping favours the hypothesis of distinct generators for Na and Pa middle latency auditory evoked potentials. *Electroencephalogr Clin Neurophysiol*, 71(3), 187–197.

Deouell, L.Y. (2007). The frontal generator of the mismatch negativity revisited. *J Psychophysiol*, 21(3-4), 188.

Doeller, C., Opitz, B., Mecklinger, A., Krick, C., Reith, W., Schröger, E. (2003). Prefrontal cortex involvement in preattentive auditory deviance detection: neuroimaging and electrophysiological evidence. *Neuroimage*, 20(2), 1270–1282.

Downar, J., Crawley, a P., Mikulis, D.J., Davis, K.D. (2001). The effect of task relevance on the cortical response to changes in visual and auditory stimuli: an event-related fMRI study. *Neuroimage*, 14(6), 1256–1267.

Downar, J., Crawley, A.P., Mikulis, D.J., Davis, K.D. (2002). A cortical network sensitive to stimulus salience in a neutral behavioral context across multiple sensory modalities. *J Neurophysiol*, 87(1), 615–620.

Duque, D., Malmierca, M.S., Caspary, D.M. (2014). Modulation of stimulus-specific adaptation by GABA(A) receptor activation or blockade in the medial geniculate body of the anaesthetized rat. *J Physiol*, 592(4), 729–743.

Dyson, B.J., Alain, C. (2004). Representation of concurrent acoustic objects in primary auditory cortex. *J Acoust Soc Am*, 115(1), 280.

Escera, C., Leung, S., Grimm, S. (2014). Deviance detection based on regularity encoding along the auditory hierarchy: electrophysiological evidence in humans. *Brain Topogr*, 27(4), 527–538.

Escera, C., Malmierca, M.S. (2014). The auditory novelty system: an attempt to integrate human and animal research. *Psychophysiology*, 51(2), 111–123.

Farley, B.J., Quirk, M.C., Doherty, J.J., Christian, E.P. (2010). Stimulus-specific adaptation in auditory cortex is an NMDA-independent process distinct from

the sensory novelty encoded by the mismatch negativity. *J Neurosci*, 30(49), 16475–16484.

Friston, K. (2005). A theory of cortical responses. *Philos Trans R Soc B Biol Sci*, 360(1456), 815–836.

Giard, M.H., Per, F., Bertrand, O. (1995). Separate representation of stimulus frequency , intensity , and duration in auditory sensory memory: an event-related potential and dipole-model analysis. *J Cogn Neurosci*, 7(2), 133-143.

Giard, M.H., Perrin, F., Pernier, J., Bouchet, P. (1990). Brain generators implicated in the processing of auditory stimulus deviance: a topographic event-related potential study. *Psychophysiology*, 27(6), 627–640.

Godey, B., Schwartz, D., de Graaf, J.B., Chauvel, P., Liégeois-Chauvel, C. (2001). Neuromagnetic source localization of auditory evoked fields and intracerebral evoked potentials: a comparison of data in the same patients. *Clin Neurophysiol*, 112(10), 1850–1859.

Gomes, H., Ritter, W., Vaughan, H.G. (1995). The nature of preattentive storage in the auditory system. *J Cogn Neurosci*, 7(1), 81–94.

Griffiths, T.D., Warren, J.D. (2002). The planum temporale as a computational hub. *Trends Neurosci*, 25(7), 348–353.

Griffiths, T.D., Warren, J.D. (2004). What is an auditory object?. *Nat Rev*, 5(11), 887–892.

Grimm, S., Escera, C. (2012). Auditory deviance detection revisited: evidence for a hierarchical novelty system. *Int J Psychophysiol*, 85(1), 88–92.

Grimm, S., Escera, C., Slabu, L., Costa-Faidella, J., Costa Faidella, J. (2011). Electrophysiological evidence for the hierarchical organization of auditory change detection in the human brain. *Psychophysiology*, 48(3), 377–384.

Grimm, S., Recasens, M., Althen, H., Escera, C. (2012). Ultrafast tracking of sound location changes as revealed by human auditory evoked potentials. *Biol Psychol*, 89(1), 232–239.

Grimm, S., Roeber, U., Trujillo Barreto, N., Schröger, E. (2006). Mechanisms for detecting auditory temporal and spectral deviations operate over similar time windows but are divided differently between the two hemispheres. *Neuroimage*, 32(1), 275–282.

Gutschalk, A., Mase, R., Roth, R., Ille, N., Rupp, A., Hähnel, S., Picton, T.W., Scherg, M., Hahnel, S. (1999). Deconvolution of 40 Hz steady-state fields reveals two overlapping source activities of the human auditory cortex. *Clin Neurophysiol*, 110(5), 856–868.

Hackett, T.A. (2011). Information flow in the auditory cortical network. *Hear Res*, 271(1-2), 133–146.

Hackett, T.A., Preuss, T.M., Kaas, J.H. (2001). Architectonic identification of the core region in auditory cortex of macaques, chimpanzees, and humans. *J Comp Neurol*, 441(3), 197–222.

Haenschel, C., Vernon, D.J., Dwivedi, P., Gruzelier, J.H., Baldeweg, T. (2005). Event-related brain potential correlates of human auditory sensory memory-trace formation. *J Neurosci*, 25(45), 10494–10501.

Hämäläinen, M., Hari, R., Ilmoniemi, R.J., Knuutila, J., Lounasmaa, O. (1993). Magnetoencephalography - Theory, instrumentation, and applications to noninvasive studies of the working human brain. *Rev Mod Phys*, 65(2), 413.

Hari, R., Hämäläinen, M., Ilmoniemi, R., Kaukoranta, E., Reinikainen, K., Salminen, J., Alho, K., Näätänen, R., Sams, M. (1984). Responses of the primary auditory cortex to pitch changes in a sequence of tone pips: neuromagnetic recordings in man. *Neurosci Lett*, 50(1-3), 127–132.

Hari, R., Kaila, K., Katila, T., Tuomisto, T., Varpula, T. (1982). Interstimulus interval dependence of the auditory vertex response and its magnetic counterpart: implications for their neural generation. *Electroencephalogr Clin Neurophysiol*, 54(5), 561–569.

Hari, R., Salmelin, R. (2012). Magnetoencephalography: From SQUIDs to neuroscience. Neuroimage 20th anniversary special edition. *Neuroimage*, 61(2), 386–396.

Herholz, S.C., Boh, B., Pantev, C. (2011). Musical training modulates encoding of higher-order regularities in the auditory cortex. *Eur J Neurosci*, 34(3), 524–529.

Herholz, S.C., Lappe, C., Pantev, C. (2009). Looking for a pattern: an MEG study on the abstract mismatch negativity in musicians and nonmusicians. *BMC Neurosci*, 10, 42.

Hickok, G., Poeppel, D. (2007). The cortical organization of speech processing. *Nat Rev Neurosci*, 8(5), 393–402.

Horváth, J., Czigler, I., Sussman, E., Winkler, I. (2001). Simultaneously active pre-attentive representations of local and global rules for sound sequences in the human brain. *Brain Res Cogn Brain Res*, 12(1), 131–144.

Howard, M.A., Volkov, I.O., Mirsky, R., Garell, P.C., Noh, M.D., Granner, M., Damasio, H., Steinschneider, M., Reale, R.A., Hind, J.E., Brugge, J.F. (2000). Auditory cortex on the human posterior superior temporal gyrus. *J Comp Neurol*, 416(1), 79–92.

Inui, K., Okamoto, H., Miki, K., Gunji, A., Kakigi, R. (2006). Serial and parallel processing in the human auditory cortex: a magnetoencephalographic study. *Cereb Cortex*, 16(1), 18–30.

Jääskeläinen, I.P., Ahveninen, J., Andermann, M.L., Belliveau, J.W., Raij, T., Sams, M. (2011). Short-term plasticity as a neural mechanism supporting memory and attentional functions. *Brain Res*, 1422, 66–81.

Jääskeläinen, I.P., Ahveninen, J., Belliveau, J.W., Raij, T., Sams, M. (2007). Short-term plasticity in auditory cognition. *Trends Neurosci*, 30(12), 653–661.

Jääskeläinen, I.P., Ahveninen, J., Bonmassar, G., Dale, A.M., Ilmoniemi, R.J., Levänen, S., Lin, F.-H.H., May, P., Melcher, J., Stufflebeam, S.M., Tiitinen, H., Belliveau, J.W. (2004). Human posterior auditory cortex gates novel sounds. *Proc Natl Acad Sci U S A*, 101(17), 6809–6814.

Jacobsen, T., Horenkamp, T., Schröger, E. (2003). Preattentive memory-based comparison of sound intensity. *Audiol Neurootol*, 8(6), 338–346.

Jacobsen, T., Schröger, E. (2001). Is there pre-attentive memory-based comparison of pitch? *Psychophysiology*, 38(4), 723.

Javitt, D.C., Schroeder, C.E., Steinschneider, M., Arezzo, J.C., Vaughan, H.G. (1992). Demonstration of mismatch negativity in the monkey. *Electroencephalogr Clin Neurophysiol*, 83(1), 87–90.

Javitt, D.C., Steinschneider, M., Schroeder, C.E., Arezzo, J.C. (1996). Role of cortical N-methyl-D-aspartate receptors in auditory sensory memory and mismatch negativity generation: implications for schizophrenia. *Proc Natl Acad Sci U S A*, 93, 11962–11967.

Kaas, J.H., Hackett, T.A., Tramo, M. (1999). Auditory processing in primate cerebral cortex. *Curr Opin Neurobiol*, 9(2), 164–170.

Kappenman, E.S., Luck, S.J. (2012). ERP components: the ups and downs of brainwave recordings. In: *The Oxford handbook of event-related potential components* (Luck, S.J., Kappenman, E.S., eds), pp 3–30. New York: Oxford University Press.

Korzyukov, O., Alho, K., Kujala, A., Gumenyuk, V., Ilmoniemi, R.J., Virtanen, J., Kropotov, J., Näätänen, R. (1999). Electromagnetic responses of the human auditory cortex generated by sensory-memory based processing of tone-frequency changes. *Neurosci Lett*, 276(3), 169–172.

Kraus, N., McGee, T. (1988). Color imaging of the human middle latency response. *Ear Hear*, 9(4), 159–167.

Kraus, N., McGee, T., Littman, T., Nicol, T., King, C. (1994). Nonprimary auditory thalamic representation of acoustic change. *J Neurophysiol*, 72(3), 1270–1277.

Kropotov, J.D., Näätnen, R., Sevostianov, A.V., Alho, K., Reinikainen, K., Kropotova, O.V. (1995). Mismatch negativity to auditory stimulus change recorded directly from the human temporal cortex. *Psychophysiology*, 32(4), 418–422.

Kujala, T., Tervaniemi, M., Schröger, E. (2007). The mismatch negativity in cognitive and clinical neuroscience: theoretical and methodological considerations. *Biol Psychol*, 74(1), 1–19.

Kuriki, S., Nogai, T., Hirata, Y. (1995). Cortical sources of middle latency responses of auditory evoked magnetic field. *Hear Res*, 92(1-2), 47–51.

Laufer, I., Negishi, M., Constable, R.T. (2009). Comparator and non-comparator mechanisms of change detection in the context of speech - an ERP study. *Neuroimage*, 44(2), 546–562.

Leung, S., Cornella, M., Grimm, S., Escera, C. (2012). Is fast auditory change detection feature specific? An electrophysiological study in humans. *Psychophysiology*, 49(7), 933–942.

Leung, S., Recasens, M., Grimm, S., Escera, C. (2013). Electrophysiological index of acoustic temporal regularity violation in the middle latency range. *Clin Neurophysiol*, 124(12), 2395-2405.

Levänen, S., Ahonen, A., Hari, R., McEvoy, L., Sams, M. (1996). Deviant auditory stimuli activate human left and right auditory cortex differently. *Cereb Cortex*, 6(2), 288–296.

Liégeois-Chauvel, C., Musolino, A., Badier, J.M., Marquis, P., Chauvel, P. (1994). Evoked potentials recorded from the auditory cortex in man: evaluation and topography of the middle latency components. *Electroencephalogr Clin Neurophysiol*, 92(3), 204–214.

Liégeois-Chauvel, C., Musolino, A., Chauvel, P. (1991). Localization of the primary auditory area in man. *Brain*, 114 (Pt 1A), 139–151.

Light, G.A., Näätänen, R. (2013). Mismatch negativity is a breakthrough biomarker for understanding and treating psychotic disorders. *Proc Natl Acad Sci U S A*, 110(38), 15175–15176.

Lopes da Silva, F.H. (2010). Electrophysiological basis of MEG signals. In: *MEG: An Introduction to Methods* (Hansen, P., Kringelbach, M.L., Salmelin, R., eds), pp 1-23. New York: Oxford University Press.

Loveless, N., Levänen, S., Jousmäki, V., Sams, M., Hari, R. (1996). Temporal integration in auditory sensory memory: neuromagnetic evidence. *Electroencephalogr Clin Neurophysiol Potentials Sect*, 100(3), 220–228.

Lu, Z.L., Williamson, S.J., Kaufman, L. (1992). Behavioral lifetime of human auditory sensory memory predicted by physiological measures. *Science*, 258(5088), 1668–1670.

Lütkenhöner, B., Krumbholz, K., Lammertmann, C., Seither-Preisler, A., Steinsträter, O., Patterson, R.D. (2003). Localization of primary auditory cortex in humans by magnetoencephalography. *Neuroimage*, 18(1), 58–66.

Maess, B., Jacobsen, T., Schröger, E., Friederici, A.D. (2007). Localizing pre-attentive auditory memory-based comparison: magnetic mismatch negativity to pitch change. *Neuroimage*, 37(2), 561–571.

Mäkelä, J., Hämäläinen, M., Hari, R., McEvoy, L. (1994). Whole-head mapping of middle-latency auditory-evoked magnetic-fields. *Electroencephalogr Clin Neurophysiol*, 92(5), 414–421.

Malmierca, M.S., Cristaudo, S., Pérez-González, D., Covey, E. (2009). Stimulus-specific adaptation in the inferior colliculus of the anesthetized rat. *J Neurosci*, 29(17), 5483–5493.

Malmierca, M.S., Sanchez-Vives, M. V, Escera, C., Bendixen, A. (2014). Neuronal adaptation, novelty detection and regularity encoding in audition. *Front Syst Neurosci*, 8, 111.

Mathiak, K., Hertrich, I., Lutzenberger, W., Ackermann, H. (2002). Functional cerebral asymmetries of pitch processing during dichotic stimulus application: a whole-head magnetoencephalography study. *Neuropsychologia*, 40(6), 585–593.

May, P., Tiitinen, H. (2010). Mismatch negativity (MMN), the deviance-elicited auditory deflection, explained. *Psychophysiology*, 47(1), 66–122.

McGee, T., Kraus, N., Littman, T., Nicol, T. (1992). Contributions of medial geniculate body subdivisions to the middle latency response. *Hear Res*, 61(1-2), 147–154.

Molholm, S., Martinez, A., Ritter, W., Javitt, D.C., Foxe, J.J. (2005). The neural circuitry of pre-attentive auditory change-detection: an fMRI study of pitch and duration mismatch negativity generators. *Cereb Cortex*, 15(5), 545–551.

Møller, A.R. (2006). *Hearing: Anatomy, Physiology, and Disorders of the Auditory System*. Amsterdam: Academic Press.

Morosan, P., Rademacher, J., Schleicher, A., Amunts, K., Schormann, T., Zilles, K. (2001). Human primary auditory cortex: Cytoarchitectonic subdivisions and mapping into a spatial reference system. *Neuroimage*, 13(4), 684–701.

Morosan, P., Schleicher, A., Amunts, K., Zilles, K. (2005). Multimodal architectonic mapping of human superior temporal gyrus. *Anat Embryol (Berl)*, 210(5-6), 401–406.

Müller, B.W., Jüptner, M., Jentzen, W., Müller, S.P. (2002). Cortical activation to auditory mismatch elicited by frequency deviant and complex novel sounds: A PET study. *Neuroimage*, 17(1), 231–239.

Müller, M.M., Keil, A., Kissler, J., Gruber, T. (2001). Suppression of the auditory middle-latency response and evoked gamma-band response in a paired-click paradigm. *Exp Brain Res*, 136(4), 474–479.

Näätänen, R. (1992). *Attention and Brain Function*. Hillsdale: L. Erlbaum.

Näätänen, R., Jacobsen, T., Winkler, I. (2005). Memory-based or afferent processes in mismatch negativity (MMN): a review of the evidence. *Psychophysiology*, 42(1), 25–32.

Näätänen, R., Kujala, T., Winkler, I. (2011). Auditory processing that leads to conscious perception: a unique window to central auditory processing opened

by the mismatch negativity and related responses. *Psychophysiology*, 48(1), 4–22.

Näätänen, R., Lehtokoski, A., Lennes, M., Cheour, M., Huotilainen, M., Iivonen, A., Vainio, M., Alku, P., Ilmoniemi, R.J., Luuk, A., Allik, J., Sinkkonen, J., Alho, K. (1997). Language-specific phoneme representations revealed by electric and magnetic brain responses. *Nature*, 385(6615), 432-434.

Näätänen, R., Picton, T. (1987). The N1 wave of the human electric and magnetic response to sound: a review and an analysis of the component structure. *Psychophysiology*, 24(4), 375–425.

Näätänen, R., Rinne, T. (2002). Electric brain response to sound repetition in humans: an index of long-term-memory - trace formation? *Neurosci Lett*, 318(1), 49–51.

Näätänen, R., Teder, W., Alho, K., Lavikainen, J. (1992). Auditory attention and selective input modulation: a topographical ERP study. *Neuroreport*, 3(6), 493–496.

Näätänen, R., Winkler, I. (1999). The concept of auditory stimulus representation in cognitive neuroscience. *Psychol Bull*, 125(6), 826–859.

Näätänen, R., Winkler, I. (2007). Interpreting the mismatch negativity. *J Psychophysiol*, 21(3), 147.

Nelken, I. (2008). Processing of complex sounds in the auditory system. *Curr Opin Neurobiol*, 18(4), 413–417.

Nelken, I., Ulanovsky, N. (2007). Mismatch negativity and stimulus-specific adaptation in animal models. *J Psychophysiol*, 21(3-4), 214.

Ng, C.W., Plakke, B., Poremba, A. (2014). Neural correlates of auditory recognition memory in the primate dorsal temporal pole. *J Neurophysiol*, 111(3), 455–469.

Oostenveld, R., Fries, P., Maris, E., Schoffelen, J.M. (2011). FieldTrip: Open source software for advanced analysis of MEG, EEG, and invasive electrophysiological data. *Comput Intell Neurosci*, 2011, 156869.

Opitz, B., Mecklinger, A., von Cramon, D.Y., Kruggel, F. (1999). Combining electrophysiological and hemodynamic measures of the auditory oddball. *Psychophysiology*, 36(1), 142–147.

Opitz, B., Rinne, T., Mecklinger, A., von Cramon, D.Y., Schröger, E. (2002). Differential contribution of frontal and temporal cortices to auditory change detection: fMRI and ERP results. *Neuroimage*, 15(1), 167–174.

Opitz, B., Schröger, E., von Cramon, D. (2005). Sensory and cognitive mechanisms for preattentive change detection in auditory cortex. *Eur J Neurosci*, 21(2), 531.

Pa, J., Hickok, G. (2008). A parietal-temporal sensory-motor integration area for the human vocal tract: evidence from an fMRI study of skilled musicians. *Neuropsychologia*, 46(1), 362–368.

Paavilainen, P. (2013). The mismatch-negativity (MMN) component of the auditory event-related potential to violations of abstract regularities: A review. *Int J Psychophysiol*, 88, 109–123.

Paavilainen, P., Alho, K., Reinikainen, K., Sams, M., Näätänen, R. (1991). Right-hemisphere dominance of different mismatch negativities. *Electroencephalogr Clin Neurophysiol*, 78(6), 466–479.

Paavilainen, P., Arajärvi, P., Takegata, R. (2007). Preattentive detection of nonsalient contingencies between auditory features. *Neuroreport*, 18(2), 159–163.

Paavilainen, P., Tiitinen, H., Alho, K., Näätänen, R. (1993). Mismatch negativity to slight pitch changes outside strong attentional focus. *Biol Psychol*, 37(1), 23–41.

Pantev, C., Bertrand, O., Eulitz, C., Verkindt, C., Hampson, S., Schuierer, G., Elbert, T. (1995). Specific tonotopic organizations of different areas of the human auditory cortex revealed by simultaneous magnetic and electric recordings. *Electroencephalogr Clin Neurophysiol*, 94(1), 26–40.

Pantev, C., Elbert, T., Makeig, S., Hampson, S., Eulitz, C., Hoke, M. (1993). Relationship of transient and steady-state auditory evoked fields. *Electroencephalogr Clin Neurophysiol*, 88(5), 389–396.

Paraskevopoulos, E., Kuchenbuch, A., Herholz, S.C., Pantev, C. (2012). Statistical learning effects in musicians and non-musicians: an MEG study. *Neuropsychologia*, 50(2), 341–349.

Pelizzone, M., Hari, R., Mäkelä, J.P., Huttunen, J., Ahlfors, S., Hämäläinen, M. (1987). Cortical origin of middle-latency auditory evoked responses in man. *Neurosci Lett*, 82(3), 303–307.

Pérez-González, D., Malmierca, M.S. (2014). Adaptation in the auditory system: an overview. *Front Integr Neurosci*, 8, 19.

Pérez-González, D., Malmierca, M.S., Covey, E. (2005). Novelty detector neurons in the mammalian auditory midbrain. *Eur J Neurosci*, 22(11), 2879–2885.

Pincze, Z., Lakatos, P., Rajkai, C., Ulbert, I., Karmos, G. (2001). Separation of mismatch negativity and the N1 wave in the auditory cortex of the cat: a topographic study. *Clin Neurophysiol*, 112(5), 778–784.

Pratt, H. (2012). Sensory ERP Components. In: *The Oxford handbook of event-related potential components* (Luck, S.J., Kappenman, E.S., eds), pp 89–114. New York: Oxford University Press.

Puschmann, S., Sandmann, P., Ahrens, J., Thorne, J., Weerda, R., Klump, G., Debener, S., Thiel, C.M. (2013). Electrophysiological correlates of auditory change detection and change deafness in complex auditory scenes. *Neuroimage*, 75, 155–164.

Rinne, T., Alho, K., Alku, P., Holi, M., Sinkkonen, J., Virtanen, J., Bertrand, O., Näätänen, R. (1999a). Analysis of speech sounds is left-hemisphere predominant at 100-150ms after sound onset. *Neuroreport*, 10(5), 1113–1117.

Rinne, T., Alho, K., Ilmoniemi, R.J., Virtanen, J., Näätänen, R. (2000). Separate time behaviors of the temporal and frontal mismatch negativity sources. *Neuroimage*, 12(1), 14–19.

Rinne, T., Degerman, A., Alho, K. (2005). Superior temporal and inferior frontal cortices are activated by infrequent sound duration decrements: An fMRI study. *Neuroimage*, 26(1), 66–72.

Rinne, T., Gratton, G., Fabiani, M., Cowan, N., Maclin, E., Stinard, a, Sinkkonen, J., Alho, K., Näätänen, R. (1999b). Scalp-recorded optical signals make sound processing in the auditory cortex visible? *Neuroimage*, 10(5), 620–624.

Rinne, T., Kirjavainen, S., Salonen, O., Degerman, A., Kang, X., Woods, D.L., Alho, K. (2007). Distributed cortical networks for focused auditory attention and distraction. *Neurosci Lett*, 416(3), 247–251.

Ruhnau, P., Herrmann, B., Schröger, E. (2012). Finding the right control: the mismatch negativity under investigation. *Clin Neurophysiol*, 123(3), 507–512.

Saenz, M., Langers, D.R. (2014). Tonotopic mapping of human auditory cortex. *Hear Res*, 307, 42–52.

Sams, M., Hämäläinen, M., Antervo, A., Kaukoranta, E., Reinikainen, K., Hari, R. (1985). Cerebral neuromagnetic responses evoked by short auditory stimuli. *Electroencephalogr Clin Neurophysiol*, 61(4), 254–266.

Sams, M., Kaukoranta, E., Hämäläinen, M., Näätänen, R. (1991). Cortical activity elicited by changes in auditory stimuli: different sources for the magnetic N100m and mismatch responses. *Psychophysiology*, 28(1), 21–29.

Schall, U., Johnston, P., Todd, J., Ward, P., Michie, P. (2003). Functional neuroanatomy of auditory mismatch processing: an event-related fMRI study of duration-deviant oddballs. *Neuroimage*, 20(2), 729–736.

Schönwiesner, M., Novitski, N., Pakarinen, S., Carlson, S., Tervaniemi, M., Näätänen, R. (2007). Heschl's gyrus, posterior superior temporal gyrus, and mid-ventrolateral prefrontal cortex have different roles in the detection of acoustic changes. *J Neurophysiol*, 97(3), 2075–2082.

Schröger, E. (2007). Mismatch negativity - A microphone into auditory memory. *J Psychophysiol*, 21(3-4), 138.

Schröger, E., Bendixen, A., Trujillo-Barreto, N.J., Roeber, U. (2007). Processing of abstract rule violations in audition. *PLoS One*, 2(11), e1131.

Schröger, E., Wolff, C. (1996). Mismatch response of the human brain to changes in sound location. *Neuroreport*, 7(18), 3005–3008.

Shtyrov, Y., Osswald, K., Pulvermüller, F. (2008). Memory traces for spoken words in the brain as revealed by the hemodynamic correlate of the mismatch negativity. *Cereb Cortex*, 18(1), 29–37.

Slabu, L., Escera, C., Grimm, S., Costa-Faidella, J. (2010). Early change detection in humans as revealed by auditory brainstem and middle-latency evoked potentials. *Eur J Neurosci*, 32(5), 859–865.

Slabu, L., Grimm, S., Escera, C. (2012). Novelty detection in the human auditory brainstem. *J Neurosci*, 32(4), 1447–1452.

Sonnadara, R.R., Alain, C., Trainor, L.J. (2006). Occasional changes in sound location enhance middle latency evoked responses. *Brain Res*, 1076(1), 187–192.

Sussman, E., Ritter, W., Vaughan, H.G., Vaughan Jr, H.G. (1998). Predictability of stimulus deviance and the mismatch negativity. *Neuroreport*, 9(18), 4167–4170.

Sussman, E.S., Gumenyuk, V. (2005). Organization of sequential sounds in auditory memory. *Neuroreport*, 16(13), 1519–1523.

Sussman, E.S., Shafer, V.L. (2014). New perspectives on the mismatch negativity (MMN) component: an evolving tool in cognitive neuroscience. *Brain Topogr*, 27(4), 425–427.

Szycik, G.R., Stadler, J., Brechmann, A., Münte, T.F. (2013). Preattentive mechanisms of change detection in early auditory cortex: a 7 Tesla fMRI study. *Neuroscience*, 253, 100–109.

Taaseh, N., Yaron, A., Nelken, I. (2011). Stimulus-specific adaptation and deviance detection in the rat auditory cortex. *PLoS One*, 6(8), e23369.

Tadel, F., Baillet, S., Moscher, J.C., Pantazis, D., Leahy, R.M. (2011). Brainstorm: a user-friendly application for MEG/EEG analysis. *Comput Intell Neurosci*, 2011, 879716.

Tervaniemi, M., Jacobsen, T., Röttger, S., Kujala, T., Widmann, A, Vainio, M., Näätänen, R., Schröger, E. (2006). Selective tuning of cortical sound-feature processing by language experience. *Eur J Neurosci*, 23(9), 2538–2541.

Tervaniemi, M., Medvedev, S. V, Alho, K., Pakhomov, S. V, Roudas, M.S., Van Zuijen, T.L., Näätänen, R. (2000). Lateralized automatic auditory processing of phonetic versus musical information: A PET study. *Hum Brain Mapp*, 10(2), 74–79.

Tervaniemi, M., Saarinen, J., Paavilainen, P., Danilova, N., Näätänen, R. (1994). Temporal integration of auditory information in sensory memory as reflected by the mismatch negativity. *Biol Psychol*, 38(2-3), 157–167.

Tiitinen, H., Alho, K., Huotilainen, M., Ilmoniemi, R.J., Simola, J., Näätänen, R. (1993). Tonotopic auditory cortex and the magnetoencephalographic (MEG) equivalent of the mismatch negativity. *Psychophysiology*, 30(5), 537–540.

Tikhonravov, D., Neuvonen, T., Pertovaara, A., Savioja, K., Ruusuvirta, T., Näätänen, R., Carlson, S. (2008). Effects of an NMDA-receptor antagonist MK-801 on an MMN-like response recorded in anesthetized rats. *Brain Res*, 1203, 97–102.

Uhrig, L., Dehaene, S., Jarraya, B. (2014). A hierarchy of responses to auditory regularities in the macaque brain. *J Neurosci*, 34(4), 1127–1132.

Ulanovsky, N., Las, L., Farkas, D., Nelken, I. (2004). Multiple time scales of adaptation in auditory cortex neurons. *J Neurosci*, 24(46), 10440–10453.

Ulanovsky, N., Las, L., Nelken, I. (2003). Processing of low-probability sounds by cortical neurons. *Nat Neurosci*, 6(4), 391–398.

Umbricht, D., Schmid, L., Koller, R., Vollenweider, F.X., Hell, D., Javitt, D.C. (2000). Ketamine-induced deficits in auditory and visual context-dependent processing in healthy volunteers: implications for models of cognitive deficits in schizophrenia. *Arch Gen Psychiatry*, 57, 1139–1147.

Vrba, J., Robinson, S.E. (2001). Signal processing in magnetoencephalography. *Methods*, 25(2), 249–271.

Wacongne, C., Labyt, E., van Wassenhove, V., Bekinschtein, T., Naccache, L., Dehaene, S. (2011). Evidence for a hierarchy of predictions and prediction errors in human cortex. *Proc Natl Acad Sci U S A*, 108(51), 20754–20759.

Wessinger, C.M., VanMeter, J., Tian, B., Van Lare, J., Pekar, J., Rauschecker, J.P. (2001). Hierarchical organization of the human auditory cortex revealed by functional magnetic resonance imaging. *J Cogn Neurosci*, 13(1), 1–7.

Winkler, I., Czigler, I. (2012). Evidence from auditory and visual event-related potential (ERP) studies of deviance detection (MMN and vMMN) linking predictive coding theories and perceptual object representations. *Int J Psychophysiol*, 83, 132–143.

Winkler, I., Denham, S.L., Nelken, I. (2009). Modeling the auditory scene: predictive regularity representations and perceptual objects. *Trends Cogn Sci*, 13(12), 532–540.

Winkler, I., Karmos, G., Näätänen, R. (1996). Adaptive modeling of the unattended acoustic environment reflected in the mismatch negativity event-related potential. *Brain Res*, 742(1-2), 239–252.

Woldorff, M.G., Hillyard, S.A. (1991). Modulation of early auditory processing during selective listening to rapidly presented tones. *Electroencephalogr Clin Neurophysiol*, 79(3), 170–191.

Woods, D.L. (1995). The component structure of the N1 wave of the human auditory evoked potential. *Electroencephalogr Clin Neurophysiol Suppl*, 44, 102–109.

Yabe, H., Tervaniemi, M., Reinikainen, K., Näätänen, R. (1997). Temporal window of integration revealed by MMN to sound omission. *Neuroreport*, 8(8), 1971–1974.

Yabe, H., Tervaniemi, M., Sinkkonen, J., Huotilainen, M., Ilmoniemi, R.J., Näätänen, R. (1998). Temporal window of integration of auditory information in the human brain. *Psychophysiology*, 35(5), 615–619.

Yago, E., Escera, C., Alho, K., Giard, M.H. (2001). Cerebral mechanisms underlying orienting of attention towards auditory frequency changes. *Neuroreport*, 12(11), 2583–2587.

Ylinen, S., Huotilainen, M. (2007). Is there a direct neural correlate for memory-trace formation in audition? *Neuroreport*, 18(12), 1281–1284.

Yoshiura, T., Ueno, S., Iramina, K., Masuda, K. (1995). Source localization of middle latency auditory evoked magnetic fields. *Brain Res*, 703(1-2), 139–144.

Yvert, B., Crouzeix, A., Bertrand, O., Seither-Preisler, A., Pantev, C. (2001). Multiple supratemporal sources of magnetic and electric auditory evoked middle latency components in humans. *Cereb Cortex*, 11(5), 411–423.

Yvert, B., Fischer, C., Bertrand, O., Pernier, J. (2005). Localization of human supratemporal auditory areas from intracerebral auditory evoked potentials using distributed source models. *Neuroimage*, 28(1), 140–153.

Zatorre, R., Belin, P. (2001). Spectral and temporal processing in human auditory cortex. *Cereb Cortex*, 11(10), 946–953.

Zatorre, R., Belin, P., Penhune, V. (2002). Structure and function of auditory cortex: music and speech. *Trends Cogn Sci*, 6(1), 37–46.

Zheng, Z.Z. (2009). The functional specialization of the planum temporale. *J Neurophysiol*, 102(6), 3079–3081.

Zheng, Z.Z., Vicente-Grabovetsky, A., MacDonald, E.N., Munhall, K.G., Cusack, R., Johnsrude, I.S. (2013). Multivoxel patterns reveal functionally differentiated networks underlying auditory feedback processing of speech. *J Neurosci*, 33(10), 4339–4348.

Annex

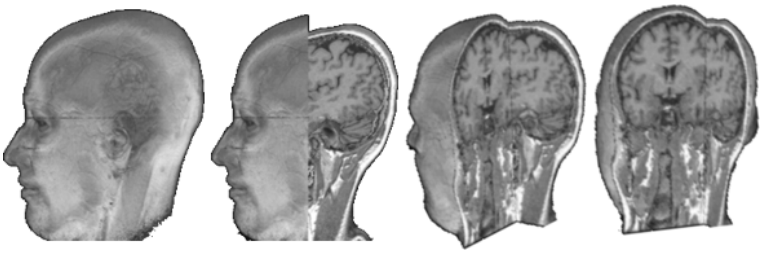

ANNEX: SUMMARIES (CATALAN VERSION)

RESUM GENERAL

El nostre entorn auditiu és ric en informació contínuament canviant. De tot el repertori d'estímuls auditius que arriben als nostres sistemes sensorials, el nostre cervell ha de crear una representació mental fidedigna del món. Per fer-ho, el nostre sistema auditiu codifica les característiques acústiques regulars, les emmagatzema en la memòria sensorial en forma d'objectes auditius, i contínuament compara aquestes regularitats amb els inputs sensorials entrants. Donat que els esdeveniments sonors discordants poden contenir informació extremadament rellevant per l'assoliment dels nostres objectius, els canvis o sons nous han de ser detectats de forma ràpida, automàtica i inconscientment. Permetent, per tant, l'assignació de recursos atencionals i un ajustament òptim del nostre comportament. Els canvis sobtats en el nostre entorn acústic evoquen el potencial de disparitat (*mismatch negativity*, MMN), un potencial evocat auditiu (PEA) generat entre els 100 i 250 ms després de l'inici d'un so en l'escorça supratemporal i prefrontal. El MMN s'obté de manera experimental en un paradigma "*oddball*", en el que estímuls nous o infreqüents (*deviants*) s'intercalen en una seqüència regular de sons repetitius (*standards*) caracteritzats per un tret auditiu particular (freqüència, intensitat, localització, ritme), o per regularitats auditives més complexes com patrons, regles abstractes o la combinació de trets. A nivell operacional, el MMN s'obté per mitjà de la sostracció de l'activitat evocada per *standards* d'aquella evocada pels *deviants*. Tot i això, estudis recents han desafiat la idea que el MMN és l'únic indicador electrofisiològic de la detecció de sons dispars en humans. La desviació de trets auditius simples en el rang de les respostes de latència mitja (*middle-latency responses,* MLR), generades entre els 20 i els 50 ms després de l'aparició d'un so, produeixen modulacions d'amplitud que reflecteixen l'existència d'un mecanisme molt primerenc de codificació de regularitat i detecció de sons dispars.

L'objectiu d'aquesta tesi doctoral és examinar les fonts neuronals subjacents a la codificació de regularitats auditives, i la conseqüent detecció d'estímuls que trenquen amb la regularitat, en rangs temporals primerencs (MLR) i tardans (MMN). Específicament, l'estudi I té com a objectiu mostrar una separació entre les

fonts generadores de la detecció de novetat en el rang de les MLR i el MMN. Emprant un paradigma *oddball*, canvis de freqüència van provocar una resposta augmentada tant en el rang de les MLR com en el del MMN. El modelatge de fonts cerebrals amb magnetoencefalografia (MEG) va revelar que les fonts neuronals de les MLR relacionades amb la novetat tenien un origen en àrees auditives primàries, mentre que els generadors del MMN estaven localitzats en regions secundàries. L'objectiu de l'estudi II era demostrar que les MLR i el mecanisme de detecció de novetat MMN, més tardà, estan involucrats en el processament de nivells diferents de regularitat acústica. Fent ús d'un disseny *oddball* més sofisticat que incloïa canvis locals i globals es va observar que regularitats complexes es codificaven només en el rang del MMN i es generaven en regions secundàries. Els mecanismes de detecció de novetat més primerencs no varen mostrar respostes augmentades al trencament de regularitats complexes, així doncs suggerint que mecanismes primerencs i tardans estan involucrats en el processament de nivells diferents de regularitat. Finalment, el tercer estudi tenia com a objectiu mostrar les fonts generadores involucrades en la codificació de trets acústics. Es va emprar un paradigma *roving-standard* en el que es presenten trens de tons repetitius. Els resultats van indicar que tant processos de decrement per repetició com d'increment per repetició intervenen en la formació de traces de memòria auditiva. I que les fonts generadores d'aquests processos estan situades tant en regions típicament auditives com en regions no auditives d'ordre superior.

En conclusió, els resultats de la present tesi indiquen que els mecanismes de detecció primerenca de novetat existeixen en intervals de temps anteriors als del MMN i són generats en l'escorça auditiva primària, en consonància amb resultats previs en animals que mostren adaptació específica a trets auditius en regions primàries. A més, els resultats suggereixen que la codificació de la regularitat no només és un fenomen omnipresent, sinó que també està organitzat de forma jeràrquica, on mecanismes inferiors estan involucrats en la codificació de trets simples i regions d'ordre superior es dediquen a la codificació de regularitats complexes. Donant suport a una organització jeràrquica de la codificació de regularitats, els resultats suggereixen que regions no auditives d'alt ordre del cervell humà participen en la formació de noves traces de memòria ecoica. Aquestes troballes estan en consonància amb la idea que la percepció auditiva es

basa en sistemes sensorials organitzats jeràrquicament, l'objectiu dels quals és predir esdeveniments futurs basant-se en la codificació prèvia de regularitats. Per fer-ho, senyals d'error i senyals predictives són enviades a través d'estadis organitzats de processament.

RESUM ESTUDI I (*Abstract*)

La detecció de novetat auditiva ocorre al voltant dels 150 ms després del inici d'un so dispar. Estudis recents en animals i humans han descrit processos relacionats amb el canvi que ocorren durant els primers 50 ms després del inici d'un so. Tot i això, encara no és clar que aquests processos primerencs i tardans de detecció de novetat estiguin organitzats jeràrquicament en l'escorça auditiva humana. Es va implementar una reconstrucció de fonts coneguda com *beamformer* per tal d'estimar les fonts cerebrals associades a 2 marcadors temporals diferents de detecció de novetat. Els resultats van mostrar que canvis de freqüència inusuals provoquen un augment del component Nbm de les respostes de latència mitja (MLR), amb un màxim als 43 ms; a més del potencial de disparitat (MMNm), amb un pic als 115 ms. Les fonts del MMNm, localitzades en el gir temporal superior dret, estaven localitzades de manera més lateral i més posterior que l'activitat relacionada amb el canvi en el rang de les MLR, localitzada en l'escorça auditiva primària dreta. La reconstrucció de fonts va revelar que la detecció de canvis en l'entorn auditiu és un procés portat a terme en dos rangs temporals diferents, i per regions auditives separades a nivell espaial. Corroborant estudis en animals, els nostres resultats suggereixen que àrees primàries i secundàries estan involucrades en estadis successius de detecció de novetat, així doncs, donant suport a l'existència d'una xarxa jeràrquica dedicada a la detecció de canvis auditius.

RESUM ESTUDI II (*Abstract*)

El nostre sistema auditiu és capaç de codificar regularitats acústiques de nivells creixents de complexitat per tal de modelar i predir esdeveniments sonors futurs. Evidències recents suggereixen que els indicadors primerencs de detecció de canvi en el rang de les respostes de latència mitja (MLR) precedeixen el potencial de disparitat (MMN), una "resposta d'error" ben establerta que està associada amb la detecció de la novetat. Estudis també suggereixen que només el MMN està

involucrat en el processament de nivells de regularitat complexa, però no les respostes primerenques MLR relacionades amb el canvi. Tot i això, no és clar si aquests dos mecanismes interaccionen durant l'anàlisi de l'escena auditiva mitjançant la codificació de nivells de regularitat interrelacionats, o si les fonts neuronals implicades en la detecció de canvis locals i globals estan organitzades jeràrquicament. Vàrem enregistrar els camps evocats magnetoencefalogràfics generats al presentar, de forma ràpida, seqüències locals de quatre tons que contenien un canvi de freqüència. La integració temporal d'aquest mateixos estímuls locals definia, al seu torn, una regularitat global. Aquestes últimes regularitats globals eren violades de manera infreqüent per la repetició d'un to. Es va obtenir un potencial MMNm global als 140-220 ms quan es violava una regularitat global, però no es van observar efectes relacionats amb la disparitat en latències primerenques. A la inversa, modulacions en els components Nbm (45-55 ms) i Pbm (60-75) de les MLR, i una resposta MMN precoç als 120-160 ms varen aparèixer en resposta a violacions locals. Diferents generadors neuronals de l'escorça auditiva estaven involucrats en el processament de violacions de regularitats locals i globals; suggerint per tant que, nivells interrelacionats de complexitat en la representació d'objectes auditius estan representats mentalment en àrees corticals diferents. Els nostres resultats suggereixen que diferents estadis de processament i àrees anatòmiques involucrades en la codificació i posterior detecció de violacions, estan organitzades de manera jeràrquica en l'escorça auditiva humana.

RESUM ESTUDI III (*Abstract*)

Tradicionalment, la formació de traces de memòria ecoica ha estat inferida a partir de la resposta incrementada a la violació d'aquestes. El potencial de disparitat (MMN), un potencial evocat auditiu (PEA) generat entre els 100 i els 250 ms després del inici d'un so dispar és un indicador indirecte de codificació de regularitat que reflecteix un procés de comparació basat en la memòria. Recentment, la positivitat per repetició (RP) ha estat descrit com un PEA candidat a correlacionar amb la formació directa de traces de memòria. La RP consisteix en efectes de supressió i d'increment que ocorren en diferents components auditius entre els 50 i els 250 ms després del inici d'un so. Tot i això, la localització dels

generadors neuronals involucrats en la codificació de nous trets acústics ha rebut poc interès. Aquest estudi té com a objectiu investigar les fonts neuronals que intervenen en la formació i enfortiment de noves traces de memòria, mitjançant l'ús d'un paradigma *roving-standard,* en el que trens de freqüències i duracions diferents són presentats de forma aleatòria. Les fonts generadores de l'activitat incrementada per repetició (*repetition enhancement*, RE) i de l'activitat suprimida per repetició (*repetition suppression*, RS) van ser modelades mitjançant l'ús de magnetoencefalografia (MEG) en subjectes sans. Els nostres resultats mostren que, en consonància amb les troballes del potencial RP, l'activitat N1m (~95-150 ms) es suprimeix amb la repetició d'estímuls. A més, vàrem observar l'aparició d'un camp sostingut (*sustained field*, SF; ~230-270 ms) que mostrava RE. L'anàlisi de fonts va revelar generadors neuronals de RS i RE situats tant en àrees auditives com no auditives, com l'escorça parietal medial i àrees frontals. El moment temporal i la localització dels generadors neuronals involucrats en la RS i la RE indiquen la existència de mecanismes funcionals separats dedicats a la formació de traces de memòria acústica en estadis de processament auditiu diferents del cervell humà.